

**ENGINEERING PROPERTIES OF POFA-GGBS-BASED
FIBRE REINFORCED STRUCTURAL LIGHTWEIGHT
GEOPOLYMER CONCRETE**

AZIZUL ISLAM

**FACULTY OF ENGINEERING
UNIVERSITY OF MALAYA
KUALA LUMPUR
2014**

ENGINEERING PROPERTIES OF POFA-GGBS-BASED
FIBRE REINFORCED STRUCTURAL LIGHTWEIGHT
GEOPOLYMER CONCRETE

AZIZUL ISLAM

DISSERTATION SUBMITTED IN FULFILMENT OF THE
REQUIREMENT FOR THE DEGREE OF MASTER OF
ENGINEERING SCIENCE

FACULTY OF ENGINEERING
UNIVERSITY OF MALAYA
KUALA LUMPUR

2014

University of Malaya

ORIGINAL LITERARY WORK DECLARATION

Name of the Candidate: **Azizul Islam**

Passport No:

Registration /Metric No: **KGA120024**

Name of the degree: **Master of Engineering Science**

Title of Dissertation:

**ENGINEERING PROPERTIES OF POFA-GGBS-BASED FIBRE REINFORCED
STRUCTURAL LIGHTWEIGHT GEOPOLYMER CONCRETE**

Field of study: **Structural Engineering and Materials**

I do solemnly and sincerely declare that:

1. I am the sole author/writer of this work;
2. This work is original;
3. Any use of any work in which copy exists was done by way of fair dealing and for permitted purposes and any excerpt or extract from, or reference to or reproduction of any copyright work has been disclosed expressly and sufficiently and the title of the work and its authorship have been acknowledged;
4. I do not have any actual knowledge nor do I ought reasonably to know that the making of this work constitutes an infringement of any copyright work;
5. I hereby assign all and every rights in the copyright to this work to the University of Malaya (UM), who henceforth shall be owner of the copyright of this work and that any reproduction or use in any form or by any means whatsoever is prohibited without the written consent of UM having been first had and obtained;
6. I am fully aware that if in the course of making this work I have infringed any copyright whether intentionally or otherwise, I may be subject to legal action or any other action as may be determined by UM.

Candidate's Signature

Date:

Subscribed and solemnly declared before,

Witness's Signature

Date:

Name:

Designation:

ABSTRACT

The use of ordinary Portland cement (OPC) in concrete construction is under critical review due to the release of high amount of carbon dioxide (CO₂) gas in to the atmosphere. Geopolymer concrete (GC) is a novel green material that uses waste materials as the binder instead of OPC. This research focuses on utilizing locally available waste materials – palm oil fuel ash (POFA), ground granulated blast furnace slag (GGBS) and fly ash (FA) – as the binder, manufactured sand (MS) and quarry dust (QD) as replacement materials for the fine aggregate, and oil palm shell (OPS) as the coarse aggregate, which were activated by alkaline liquids to produce sustainable concrete, hereafter called OPSGC (oil palm shell geopolymer concrete).

This investigation reports the development of mix design, effect of steel fibre to the impact resistance of POFA-GGBS-based lightweight geopolymer concrete. The engineering properties of OPSGC – compressive, flexural and splitting tensile strength, modulus of elasticity and Poisson's ratio – were investigated; in addition, the quantity of OPS in impact resistance of steel fibre reinforced geopolymer concrete were studied and reported.

Initially, three binders – POFA, GGBS and FA were used to develop an appropriate geopolymer mortar mix. Eleven mixes were prepared with varying binder contents. The other constituent materials such as fine aggregate and water were kept constant. After obtaining the appropriate mix proportion of mortar, nine concrete mixes were prepared for structural grade geopolymer concrete using OPS, crushed granite, MS, QD and

conventional sand (NS). The impact behaviour of GC was investigated based on fourteen concrete mixes prepared with and without fibre using different OPS contents. The other constituent materials – fine aggregate (MS), activator and water were kept constant.

All the specimens of geopolymer mortar were cured in oven for 24 h at 65 °C and thereafter kept in room temperature (about 26–29 °C) before testing for the compressive strength. However, for the structural grade concrete two curing conditions, oven-dry and ambient curing were observed. Since the ambient curing produced better results than oven cured specimens, the specimens of impact resistance test were cured using ambient condition.

The highest compressive strength of about 66 MPa was achieved for the mortar containing 30% of POFA and 70% of GGBS with a total binder content of 460 kg/m³. For structural grade concrete with 40% of POFA and 60% of GGBS, the highest compressive strength of about 33 MPa and 42 MPa for OPSGC and NWGC (normal weight geopolymer concrete), respectively; the binder contents in these mixes were 425 kg/m³ and 220 kg/m³ respectively. The tensile strength of OPSGC was found satisfactorily as the splitting tensile strength of 2.74 MPa fulfilled the minimum requirement of 2 MPa. Its flexural strength of 3.19 MPa was comparable to that of NWGC. In addition, the Young's modulus of elasticity of 11.12 GPa was obtained for OPSGC.

Finally, after adding steel fibre the impact behaviour also investigated. Result shows that the highest compressive strength of about 28 MPa was achieved for the OPSGC containing 50% of POFA and 50% of GGBS with a total binder content of 454 kg/m³

with the lowest OPS content of 181 kg/m^3 . In contrast, about 40 MPa was achieved for NWGC with a total binder content of 308 kg/m^3 . The impact energy of 5,945 J for OPSGC specimens with 0.5% steel fibres was found. The tensile strength of OPSGC increases significantly after adding 0.5% of steel fibre as well. The highest splitting tensile strength of 2.72 MPa and flexural strength of 4.11 MPa was found, which was 19% and 39% higher than its control mix.

The research shows that POFA could be used as an ideal binder in the development of geopolymer concrete (GC) with GGBS. The development of structural grade OPSGC and its comparable mechanical properties as that of NWGC shows that the former could be used for structural purpose. In addition, the fibre enhanced the impact resistance and other mechanical properties of the OPSGC.

ABSTRAK

Penggunaan simen Portland biasa (OPC) dalam sektor pembinaan diberi tumpuan yang hebat akibat jumlah pembebasan gas karbon dioksida (CO₂) yang tinggi ke atmosfera. Konkrit Geopolimer (GC) adalah bahan mesra-alam yang terdiri daripada bahan-bahan buangan sebagai pengikat untuk menggantikan OPC. Kajian ini memberi tumpuan kepada penggunaan bahan-bahan buangan tempatan yang sedia ada – abu bahan api kelapa sawit (POFA), tanah pasir sanga relau bagas (GGBS) dan abu terbang (FA) – sebagai pengikat, pasir buatan (MS) dan debu kuari (QD) sebagai pengganti agregat halus, dan tempurung kelapa sawit (OPS) sebagai pengganti agregat kasar, yang diaktifkan oleh alkali untuk menghasilkan konkrit yang mesra-alam, dan diberikan nama OPSGC.

Kajian ini melaporkan reka bentuk campuran, kesan gentian keluli terhadap daya tahan hentaman bagi konkrit ringan geopolimer POFA-GGBS. Sifat-sifat kejuruteraan OPSGC – daya mampatan, lenturan dan tegangan membelah kekuatan, modulus keanjalan dan nisbah Poisson – telah disiasat; di samping itu, kesan kuantiti OPS terhadap daya tahan hentaman konkrit geopolimer yang diikat dengan gentian keluli telah dikaji dan dilaporkan.

Pada mulanya, tiga pengikat – POFA, GGBS dan FA telah digunakan untuk membentuk campuran mortar geopolimer yang sesuai. Sebanyak sebelas campuran telah disediakan dengan pelbagai kandungan pengikat. Bahan-bahan jujuk yang lain seperti agregat halus dan air telah dimalarkan. Selepas mendapat bahagian campuran yang sesuai bagi mortar, sebanyak sembilan campuran konkrit telah disediakan untuk konkrit gred struktur geopolimer yang menggunakan OPS, granit yang dihancurkan, MS, QD dan pasir biasa (NS). Kesan terhadap daya tahan GC telah disiasat berdasarkan empat belas campuran

konkrit yang disediakan dengan kandungan OPS berbeza yang diikat dengan gentian berserta yang tanpa gentian keluli. Bahan-bahan lain jujuk – agregat halus (MS), pengaktif dan air telah dimalarkan.

Semua spesimen mortar geopolimer telah dirawat dalam ketuhar selama 24 jam pada suhu 65°C dan selepas itu dikekalkan dalam suhu bilik (kira-kira 26–29°C) sebelum ujian kekuatan mampatan dijalankan. Walau bagaimanapun, bagi konkrit gred struktur konkrit, dua kaedah rawatan iaitu kaedah pengeringan dalam ketuhar dan pengeringan dalam suhu bilik telah diberikan perhatian. Oleh sebab kaedah pengeringan dalam suhu bilik menghasilkan keputusan yang lebih baik daripada kaedah pengeringan dalam ketuhar, specimen konkrit untuk ujian daya tahan hentaman dirawat dengan kaedah pengeringan dalam suhu bilik.

Daya tahan mampatan yang paling tinggi iaitu kira-kira 66 MPa telah dicapai bagi mortar yang mengandungi 30% POFA dan 70% GGBS dan jumlah kandungan pengikat sebanyak 460 kg/m³. Bagi konkrit gred struktur yang terdiri daripada 40% POFA dan 60% GGBS, daya tahan mampatan yang paling tinggi sebanyak kira-kira 33 MPa dan 42 MPa telah dilaporkan untuk OPSGC dan NWGC (konkrit biasa geopolimer) masing-masing; kandungan pengikat dalam campuran ini adalah sebanyak 425 kg/m³ dan 220 kg/m³ masing-masing. Daya tahan tegangan OPSGC didapati memuaskan dengan daya tahan tegangan pembelahan setinggi 2.74 MPa, lantas memenuhi syarat minimum sebanyak 2 MPa. Daya tahan lenturan sebanyak 3.19 MPa adalah setanding dengan NWGC. Di samping itu, modulus Young keanjalan 11.12 GPa telah diperolehi bagi OPSGC.

Akhirnya, selepas menambah gentian keluli, ciri-ciri hentaman juga disiasat. Keputusan menunjukkan bahawa daya tahan mampatan yang paling tinggi kira-kira 28 MPa telah dicapai untuk OPSGC yang mengandungi 50% POFA dan 50% GGBS dengan jumlah kandungan pengikat sebanyak 454 kg/m^3 dengan kandungan OPS yang paling rendah 181 kg/m^3 . Sebaliknya, kira-kira 40 MPa telah dicapai untuk NWGC dengan jumlah kandungan pengikat sebanyak 308 kg/m^3 . Tenaga hentaman setinggi 5,945 J didapati untuk specimen OPSGC dengan 0.5% gentian keluli. Daya tahan tegangan OPSGC menunjukkan peningkatan yang ketara selepas menambah 0.5% gentian keluli juga. Daya tahan tegangan pembelahan sebanyak 2.72 MPa dan daya tahan lenturan 4.11 MPa telah diperolehi dan ia adalah 19% dan 39% lebih tinggi daripada campuran kawalannya.

Kajian ini menunjukkan bahawa POFA sesuai digunakan sebagai pengikat dalam pembentukan konkrit geopolimer (GC) dengan GGBS. OPSGC gred struktur dan sifat-sifat mekanikalnya yang setanding dengan NWGC menunjukkan bahawa OPSGC boleh digunakan untuk tujuan struktur. Di samping itu, gentian keluli didapati meningkatkan daya tahan hentaman dan sifat-sifat mekanikal OPSGC.

ACKNOWLEDGEMENT

I would like to thank Almighty Allah (SWT) for providing me the opportunity to pursue my studies as well as instilling the patience and persistence during my research work.

I wish to express my sincere thanks and profound appreciation to my supervisor, Dr. Ubagaram Johnson Alengaram for his guidance, encouragement and valuable time spent on the fruitful discussion throughout the work, which was extremely valuable in conducting this research work.

I would also like to express my gratefulness to my co-supervisor Prof. Ir. Dr. Mohd Zamin Bin Jumaat for his treasured and relevant advice throughout the study.

I would like to acknowledge the grant (UMRG) provided by the University of Malaya to fulfil the study as well as the research works.

Finally, I would like to thank the most important people in my life, my parents, brothers, my wife and my daughter Tanisha Tabassum who have provided their endless support and patience throughout the years.

TABLE OF CONTENTS

Original literary work declaration.....	ii
Abstract.....	iii
Abstrak.....	vi
Acknowledgement.....	ix
Table of contents.....	x
List of figures.....	xv
List of tables.....	xix
List of symbols and abbreviations.....	xxi
CHAPTER 1 : INTRODUCTION.....	1
1.1 Background.....	1
1.2 Geopolymers.....	2
1.3 Usage of local waste materials in geopolymer concrete.....	3
1.3.1 Binders from industrial by-products.....	3
1.3.2 Wastes from palm oil factories.....	4
1.3.3 Fine aggregates.....	5
1.3.4 Oil palm shell as coarse aggregate.....	5
1.4 Problem statement.....	6
1.5 Research objectives.....	7
1.6 Scope of study.....	8
1.7 Structure of the dissertation.....	9
CHAPTER 2 : LITERATURE REVIEW.....	11
2.1 General.....	11
2.2 Geopolymers.....	12
2.3 Properties of geopolymer.....	13
2.4 Source materials.....	14

2.5	Mixture proportions of geopolymer concrete	18
2.6	Mortar for geopolymer	20
2.7	Effect of water-to-geopolymer solids ratio	21
2.8	Curing of geopolymer concrete	22
2.9	Lightweight concrete	23
2.10	Development of new LWC and OPS used as a coarse aggregate.....	24
2.11	Fibre reinforced geopolymer concrete.....	24
2.12	Impact Test	26
2.13	Application of geopolymer concrete	27
2.14	Research gap addressed in this research.....	30
CHAPTER 3 : MATERIALS AND METHODS.....		32
3.1	Introduction.....	32
3.2	Materials used to develop geopolymer mortar and concrete	33
3.2.1	Characterisation of materials.....	33
3.2.2	Ground granulated blastfurnace slag.....	33
3.2.3	Palm oil fuel ash.....	34
3.2.4	Fly ash	36
3.2.5	Fine aggregates.....	37
3.2.6	Coarse aggregates.....	38
3.3	Activator solution	40
3.4	Water.....	41
3.5	Fibres	41
3.6	Mix proportion and casting of specimens.....	41
3.6.1	Preparation of fresh geopolymer mortar and casting	42
3.6.2	Mix proportions of geopolymer concrete.....	44
3.6.3	Mix proportions of geopolymer concrete with and without fibre	47

3.7	Workability and oven-dry density tests	50
3.8	Curing regime	50
3.8.1	Curing of 50-mm cube specimens for geopolymer mortar	50
3.8.2	Curing of geopolymer concrete specimens	51
3.8.3	Curing of geopolymer concrete with and without fibre	51
3.9	Specimen moulding and testing.....	52
3.9.1	Compressive strength test of mortar.....	52
3.9.2	Mechanical properties tests of geopolymer concrete	52
3.9.3	Mechanical properties tests of geopolymer concrete with and without fibre 53	
3.9.4	Ultrasonic pulse velocity (UPV)	53
3.9.5	Poisson's ratio	54
3.9.6	Drop hammer impact test of fibre reinforced oil palm shell geopolymer concrete (FROPSGC).....	54
3.10	Data collection and analysis	56
3.11	Carbon footprint.....	57
CHAPTER 4 : RESULTS AND DISCUSSION		58
4.1	Introduction.....	58
4.2	Density of the source materials of geopolymer mortar mix	58
4.2.1	Effect of specific gravity and fineness on the density.....	58
4.2.2	Density reduction	59
4.3	Development of compressive strength in geopolymer mortar.....	59
4.4	Effect of GGBS on the compressive strength of the mortar	62
4.5	Effect of POFA on the compressive strength of the mortar	64
4.6	Analysis of chemical composition.....	65
4.7	Properties of geopolymer concrete with OPS as coarse aggregate.....	68

4.7.1	Workability.....	68
4.7.2	Density	69
4.8	Mechanical properties of geopolymer concrete.....	69
4.8.1	Development of compressive strength in geopolymer concrete	69
4.8.2	Ultrasonic pulse velocity (UPV)	81
4.8.3	Splitting Tensile Strength (STS)	82
4.8.4	Flexural Strength	89
4.8.5	Modulus of elasticity (E- value).....	94
4.8.6	Poisson's ratio	100
4.9	Mechanical properties of OPSGC with and without fibre.....	101
4.9.1	Density	101
4.9.2	Development of compressive strength in steel fibre reinforced OPSGC...	104
4.9.3	Splitting tensile strength.....	108
4.9.4	Flexural strength.....	110
4.9.5	Modulus of elasticity (E- value) for OPSGC with and without steel fibres	
	112	
4.10	Impact energy	112
4.10.1	First crack impact energy	113
4.10.2	Ultimate impact energy	115
4.10.3	Failure mode.....	117
4.10.4	Crack development resistance	118
CHAPTER 5	: CONCLUSIONS AND RECOMMENDATIONS	120
5.1	Introduction.....	120
5.2	Summary of Conclusions.....	120
5.3	Recommendations for the future works.....	125
REFERENCES	126

LIST OF PUBLICATIONS AND PAPERS PRESENTED	135
APPENDICES	136

LIST OF FIGURES

Figure 2.1: Structural models of geopolymer concrete-Davidovits (Davidovits, 2011).	13
Figure 2.2: The slag floats above the pig iron at the bottom of the blast furnace (Davidovits, 2011).....	16
Figure 2.3: Order of tamping in moulding of test specimens [ASTM:C109/C109M-12]	21
Figure 2.4: Effect of water-to-geopolymer solids ratio by mass on compressive strength of geopolymer concrete (Hardjito & Rangan, 2005).....	22
Figure 2.5: Finite element model of impact test (Nia et al., 2012)	26
Figure 2.6: (a) Queensland’s University GCI building with 3 suspended floors made from structural geopolymer concrete, (b) precast slag/fly ash - based geopolymer concrete floor parts, Australia (Aldred & Day, 2012).....	28
Figure 2.7: Composite pultruded girder and Grade 40 geopolymer deck bridge in Brisbane (Aldred & Day, 2012)	28
Figure 3.1: Source materials used in the present study	35
Figure 3.2: Particle size distribution of GGBS, POFA and FA	36
Figure 3.3: Fineness of POFA with different grinding periods	36
Figure 3.4: Particle size distribution of NS, MS and QD.....	38
Figure 3.5: Coarse fraction of fine aggregate (a) Mining sand (NS); (b) Manufactured sand (MS) and (c) Quarry dust (QD)	38
Figure 3.6: Coarse aggregate (a) uncrushed OPS; (b) crushed OPS; and (c) crushed granite	39
Figure 3.7: Steel fibres used to reinforced geopolymer concrete.....	41
Figure 3.8: Preparation of geopolymer mortar.....	43
Figure 3.9: Graphical representation of fresh concrete mix ratio by volume (a) OPSGC; (b) NWGC	46

Figure 3.10: Casting specimens for compressive strength, splitting tensile strength, flexural strength and Young's modulus test.....	46
Figure 3.11: Casting specimens for impact test, compressive strength, splitting tensile strength, flexural strength and Young's modulus test.....	48
Figure 3.12: Graphical representation of fresh concrete mix ratio by volume (a) 1:2.5:0.4 (OPSGC); (b) 1:2.5:0.6 (OPSGC); (c) 1:2.5:0.8 (OPSGC); and (d) NWGC	49
Figure 3.13: Slump test	50
Figure 3.14: Test specimens covered with plastic film and specimens in air drying condition.....	51
Figure 3.15: Compression testing machine and failure mode of cubes	52
Figure 3.16: Measurement of UPV	53
Figure 3.17: Poisson's ratio	54
Figure 3.18: Impact test arrangement.....	55
Figure 3.19: Crack width measurement (a) microscope, (b) laptop, and (c) impact test specimen.....	56
Figure 4.1: Reduction in density of mortar specimen.....	59
Figure 4.2: Development of compressive strength of mortar with varying binder content ratio.....	61
Figure 4.3: The effect of GGBS on the compressive strength of mortar mixed with POFA and FA at 28-day	63
Figure 4.4: The effect of POFA on the compressive strength of mortar mixed with GGBS and FA at 28-day	65
Figure 4.5: The comparison between major chemical composition and compressive strength of mortar	67
Figure 4.6: Development of compressive strength at initial 24 h oven-dry curing.....	72

Figure 4.7: Development of compressive strength at ambient curing	72
Figure 4.8: Failure mode of 100-mm cube (a) satisfactory failure (BS EN 12390-3, 2009); and (b) experimental specimen failure.	73
Figure 4.9: Compressive strength at 28 days of age of geopolymer concrete subjected to initial 24 h OD in relative to those of AD curing.....	75
Figure 4.10: Relationship between 28-day compressive strength of NWGC and OPSGC under AD and OD curing conditions.....	78
Figure 4.11. 28-day compressive strength of OPSGC (initial 24 h OD curing)	80
Figure 4.12. 28-day compressive strength of OPSGC (ambient curing)	80
Figure 4.13. Relationship between splitting tensile and compressive strength of NWGC at 28-day.....	85
Figure 4.14: (a) Splitting tensile testing; (b) placement of cylinder specimen; (c) specimen after testing.....	87
Figure 4.15. Relationship between splitting tensile and compressive strength of OPSGC at 28-day.....	88
Figure 4.16: (a) Flexural strength testing and (b) specimen after testing	91
Figure 4.17: Relationship between flexural strength and compressive strength of OPSGC	93
Figure 4.18. The relationship of MOE and compressive strength at 28-day	95
Figure 4.19. Stress-strain curve.....	99
Figure 4.20: Relationship of density and compressive strength of steel fibre reinforced OPSGC.....	103
Figure 4.21: Compressive strength with respect to density and OPS contents.....	103
Figure 4.22: Relationship of compressive strength and OPS contents of non and steel fibre reinforced OPSGC.....	106
Figure 4.23: Development of compressive strength of OPSGC with 0.0% steel fibre.	107

Figure 4.24: Development of compressive strength of OPSGC with 0.5% steel fibre.	107
Figure 4.25: Relationship between splitting tensile, flexural and compressive strength of OPSGC with and without fibres at 28-day	109
Figure 4.26: Flexural and splitting tensile strength with respect to compressive strength and OPS contents	111
Figure 4.27. The relationship between MOE and compressive strength (at 28-day) of OPSGC with and without steel fibres	112
Figure 4.28: Relationship between OPS content and blow number to cause first crack under impact test	114
Figure 4.29: Relationship between OPS content and blow number to cause specimen failure under impact test	116
Figure 4.30. Origination process of crack through OPS aggregates at late age (Teo et al., 2006)	117
Figure 4.31: (a) Primary cracks in OPSGC panel; and (b) primary and secondary cracks in FROPSGC panel	119

LIST OF TABLES

Table 1.1: Summary of mixes	9
Table 2.1: Summary of mix proportion (by weight) of geopolymer concrete	20
Table 2.2: Minimum strength for structural lightweight concrete (Clarke, 2005).....	24
Table 3.1: Specimen details and test conducted with code of practice	32
Table 3.2: Chemical compositions of source materials as determined by X-ray fluorescence (XRF) analysis (wt. %)	34
Table 3.3: Physical properties of source materials.....	35
Table 3.4: Physical properties of mining sand, manufactured sand and quarry dust.....	37
Table 3.5: Physical properties of OPS and crushed granite	39
Table 3.6: Mixture proportion of geopolymer mortar (kg/m ³)	43
Table 3.7: Experimental parameters for geopolymer mortar	44
Table 3.8: Mixture proportion of geopolymer concrete (kg/m ³).....	45
Table 3.9: Experimental parameters of geopolymer concrete	45
Table 3.10: Mixture proportion of geopolymer concrete with and without fibre (kg/m ³)	47
Table 3.11: Experimental parameters of geopolymer concrete with and without fibre..	48
Table 4.1: Average oven-dry density (ODD) (kg/m ³) of geopolymer mortar at 3-day ..	59
Table 4.2: Development of the compressive strength (MPa) and standard deviation of 3 mortar cubes at different ages	61
Table 4.3: The comparison of increase in the compressive strength (%) with respect to that of 28 days	62
Table 4.4: Oxide-mole ratios of the reactant mixture (Khale & Chaudhary, 2007; Davidovits, 2011).....	65
Table 4.5: Major chemical composition of mortar and 28-day compressive strength....	67
Table 4.6: SiO ₂ /Al ₂ O ₃ and CaO/Al ₂ O ₃ ratios of mortar mixes	68

Table 4.7: Chemical composition of binder based on 60% of GGBS and 40% of POFA	70
Table 4.8: Comparison of oxide-mole ratio proposed by Davidovits (2011) and those obtained from experimental	71
Table 4.9: Workability, oven-dry density (ODD) and compressive strength of NWGC and OPSGC	76
Table 4.10: Development of ultrasonic pulse velocity (UPV) of NWGC and OPSGC at 28-day.....	81
Table 4.11: Splitting tensile strength of NWGC.....	84
Table 4.12: Splitting tensile strength of OPSGC	88
Table 4.13: Comparison of compressive strength, splitting tensile strength, flexural strength and elastic modulus	90
Table 4.14: Flexural strength of OPSGC	93
Table 4.15: Elastic moduli and Poisson's ratios of concrete at 28-day	96
Table 4.16: Density and compressive strength of OPSGC and NWGC with 0% and 0.5% steel fibre.....	102
Table 4.17: Comparison of compressive strength, splitting tensile strength, flexural strength and elastic modulus at 28-day for OPSGC with and without steel fibres.....	109
Table 4.18: Impact test results tested on OPSGC with and without steel fibre	114
Table 4.19: Crack widths and number of secondary cracks prior to failure of all mixes	118

LIST OF SYMBOLS AND ABBREVIATIONS

Symbols	Descriptions
f_c'	compressive strength
f_t'	splitting tensile strength
f_r'	flexural strength
E	modulus of elasticity (Young's modulus)
μ_i	Impact ductile index
\emptyset	diameter
ρ	Density of the fresh specimen
ρ_{odd}	Oven-dry density
F	Maximum load at failure
P	Maximum applied load indicated by the testing machine

Abbreviations	Descriptions
FA	fly ash
GGBS	ground granulated blast furnace slag
POFA	palm oil fuel ash
RHA	rice husk ash
LWC	lightweight concrete
LWA	lightweight aggregate
OPS	oil palm shell
NS	conventional mining sand (normal sand)
MS	manufactured sand (MS)
QD	quarry dust (Q-dust)
OPSGC	oil palm shell geopolymer concrete
NWGC	normal weight geopolymer concrete
OPSC	oil palm shell concrete

FRC	fibre reinforced concrete
AD	air-dry
OD	oven-dry
ODD	oven-dry density
FROPSGC	fibre reinforced oil palm shell geopolymer concrete
M	molarity
MOE	modulus of elasticity
CSH	calcium-silicate-hydrates
NaOH	sodium hydroxide
OPC	ordinary Portland cement
PKS	palm kernel shell
PP	polypropylene
SP	superplasticizer
SSD	saturated surface dry
XRF	X-ray fluorescence
Al	aluminium
Al ₂ O ₃	aluminium oxide (Alumina)
Ca	calcium
CaO	calcium oxide
Ca (OH) ₂	calcium hydroxide
CO ₂	carbon dioxide
Fe ₂ O ₃	ferric oxide
H ₂ O	water
KOH	potassium hydroxide
K ₂ O	potassium oxide
LOI	loss on ignition

Na	sodium
Na ₂ SiO ₃	sodium silicate
Si	silicon
SiO ₂	silica or quartz
SO ₃	sulphuric anhydride

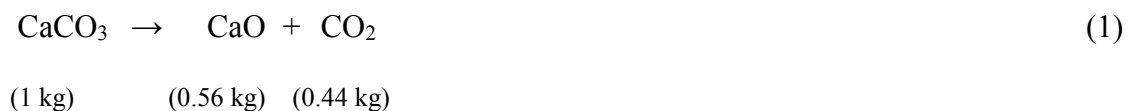
CHAPTER 1 : INTRODUCTION

1.1 Background

Rapid industrialization during the last 100 years caused tremendous changes in the construction; over 11 billion tonnes of concrete is being used annually (Mehta & Monteiro, 2006), thus leading it to one of the most widely used construction materials. However, the developmental activities were accompanied by exploitation of natural resources in the production of concrete. The realization of overuse of construction materials in concrete had alarmed the entire world to minimize the natural materials and this also led to search for alternate construction materials to achieve sustainability. One of the major constituent materials in concrete is cement and its production and energy demand are well established.

The huge demand for concrete using Ordinary Portland Cement (OPC) has resulted in high volume of CO₂ emission, and lead to ecological imbalance due to continuous depletion of natural resources. The reality of air pollution through carbon dioxide (CO₂) emission into the atmosphere from the production of cement has been told innumerable times. The carbon di-oxide (CO₂) emissions from the production of OPC is approximately 5–7% of global anthropogenic emissions (Huntzinger & Eatmon, 2009; Meyer, 2009). It was reported (Davidovits, 1994) that 1 tonne of cement produces 1 tonne of CO₂.

The process of formation of CO₂ by calcining can be expressed by the following equation:



The share of CaO in clinker amounts varies from 64%–67%. The remainder consists of silicon oxides, iron oxides, and aluminium oxides. Therefore, CO₂ emission from clinker production amounts to about 0.5 kg/kg. The CO₂ emission per tonne of cement depends on the ratio of clinker to cement. This ratio varies normally from 0.5 to 0.95 (Ernst Worrell et al., 2001)

In addition, the depletion of natural sand due to quarrying activities has already caused flooding in many parts of the world; the need for alternate materials for natural sand through the use of recycling of old mortar (Meyer, 2009; Kou & Poon, 2013) has also been investigated; however there have been efforts to utilize the manufactured sand, commonly known as MS from the waste of crushed granite aggregates as a replacement for conventional sand.

One of the main goals in achieving sustainable construction materials is to reduce the overuse of virgin materials used to produce cement, coarse and fine aggregates. The utilization of industrial by-products such as fly ash (FA), silica fume and ground granulated blast furnace slag (GGBS) as the cement replacement or as the additional cementitious materials has had a constructive effect in minimizing greenhouse gas emissions. In order to achieve an environmentally friendly concrete the alternate material like geopolymer concrete through the use of industrial waste materials could be an ideal solution.

1.2 Geopolymers

Geopolymers are new materials for coatings and adhesives, new binders for fibre composites, waste encapsulation and new cementing material for concrete. The

geopolymer technology proposed by Davidovits (Davidovits, 2002), illustrates considerable promise for application in concrete industry as an alternative binder to the Portland cement. In terms of global warming the geopolymer technology could reduce the CO₂ emission to the atmosphere caused by cement industries. The wide variety of geopolymer concrete's potential applications includes: fire resistant materials, decorative stone artefacts, thermal insulation, low-tech building materials, low energy ceramic tiles, refractory items, thermal shock refractories, bio-technologies (materials for medicinal applications) (Davidovits, 2011).

1.3 Usage of local waste materials in geopolymer concrete

1.3.1 Binders from industrial by-products

Every year millions of tons of industrial wastes are generated and most of these wastes are unutilized or underutilized. These wastes cause environmental issues due to storage problem and pollution to the surrounding field. Increasing concern about the environmental consequences of waste disposal has led researchers to investigate the utilization of the wastes as potential construction materials (Khale & Chaudhary, 2007). Inspired by the geopolymer technology and the fact that the palm oil fuel ash (POFA) is a waste material, rich in silica abundantly available in Malaysia, could be used as a pozzolanic material as an alternative to Portland cement.

The other waste material that is abundant in Malaysia is Ground granulated blast furnace slag (GGBS), a by-product of the production of iron in a blast furnace and it is composed chiefly of calcium and magnesium silicates and aluminosilicate. GGBS is a low performance cementitious material, which can achieve high compression strength when an alkaline activator is used. FA is a fine powder of mainly spherical glass particles

having pozzolanic properties which shall consist essentially of reactive silicon dioxide (SiO_2) and aluminium oxide (Al_2O_3). The government of Malaysia decided that by 2010 the share of coal in the fuel mix for electricity generation would rise to about 40% (Kupaei et al., 2013). The increased use of coal burning in thermal power plants has increased the production of FA to an estimated 3 million tons per annum. The abundance of FA in Malaysia could pave way for the development of geopolymer concrete.

1.3.2 Wastes from palm oil factories

Malaysia is currently producing more than half of the world's total output of palm oil, planted over 5 million hectares of land, yielding about 18.89 tonnes/hectare of fresh fruit bunch (FEB) (MPOB, 2012). The wastes produced from the palm oil factories include empty fruit bunches (EFB), oil palm shell (OPS), palm oil clinker (POC) and palm oil fuel ash (POFA). OPS and POC have been used as coarse aggregates in the development of lightweight concrete (Mohammed et al., 2011; Shafiq et al., 2011a; Nazari & Khalaj, 2012; Alengaram et al., 2013; Kupaei et al., 2013; Mohammed et al., 2013; Kanadasan & Razak, 2014; Mo et al., 2014b; Mohammed et al., 2014). The empty fruit bunches (EFB), have traditionally been burnt and their ash commonly known as palm oil fuel ash (POFA) recycled into the plantation as fertilizer, which is about 5% of solid waste product. This ash have the potentiality to be used as pozzolanic materials in concrete industry (Sata et al., 2010). POFA has been used as cement replacement material in concrete and it has pozzolanic properties that not only enables the replacement of cement but also plays an important role in making strong and durable concrete.

1.3.3 Fine aggregates

Quarrying of natural sand has a great irreversible environment impact (Short & Kinniburgh, 1978) as it causes reduction in the ground water that affects the moisture content of the soil. During the year 2010, Malaysia consumed 2.76 billion metric tons of natural aggregate of this amount 1.17 billion metric tons or 42.4%, was sand (Ashraf et al., 2011). In many regions of the world, the extraction of sand and gravel is heavily taxed or banned completely to try to preserve remaining deposits (Sreenivasa, 2012). Thus, it is imperative for the construction industries should find alternatives to meet the growing demand for fine aggregates.

One of the options is to utilize the waste materials from the crushing of granite aggregates (Celik & Marar, 1996), commonly known as manufactured sand (MS) as the fine aggregates. Generally, the quarry dust (QD) obtained during the crushing of granite aggregate is considered waste and sometime used in land filling; however, recently there is a renewed interest to reuse the QD. Thus, the QD is processed through centrifuge action to smoothen the angular edges and the resulting particles are rounded and it is used to replace for natural sand. The processed QD is christened as MS and widely used in Singapore, India and some other countries to replace conventional sand where the demand for sand is high/not available in abundance.

1.3.4 Oil palm shell as coarse aggregate

Malaysia is currently producing more than half of the world's total output of palm oil, planted over 5 million hectares of land, yielding about 18.89 tonnes/hectare of fresh fruit bunch (FEB) (MPOB, 2012). The wastes produced from the palm oil factories include

empty fruit bunches (EFB), oil palm shells (OPS), palm oil clinker (POC) and palm oil fuel ash (POFA). OPS and POC have been used as coarse aggregates in the development of lightweight concrete (Mohammed et al., 2011; Shafiqh et al., 2011a; Nazari & Khalaj, 2012; Alengaram et al., 2013; Kupaei et al., 2013; Mohammed et al., 2013; Kanadasan & Razak, 2014; Mo et al., 2014b; Mohammed et al., 2014). OPS is hard in nature and does not deteriorate easily once bound in concrete and therefore, it does not contaminate or leach to produce toxic substances (Basri et al., 1999). The density of OPS concrete is around 20 - 25% lower than normal weight concrete and it could be used to develop lightweight concrete.

1.4 Problem statement

Throughout the world, much research is being conducted on the use of industrial by-products such as fly ash (FA), silica fume, ground granulated blast furnace slag (GGBS), and rice husk ash, as the cement replacement or as the additional cementitious materials has had a constructive effect in minimizing greenhouse gas emissions or to streamline present waste disposal techniques by making them more affordable. The greatest problem faced by industries, as far as waste disposal is concerned in the safe and effective disposal of its effluent, sludge and by-products such as large quantities of fly ash that are produced during the combustion of coal used for electricity generation. Most of this ash is disposed in landfills at suitable sites (Woolard et al., 2000).

The increasing load of toxic metals in the landfill potentially increases the threat to ground water contamination. On the other hand, Malaysia is currently producing more than half of the world's total output of palm oil and palm oil fuel ash is commonly known as POFA,

which is about 5% of solid waste product, have the potentiality to be used as pozzolanic materials in concrete industry (Sata et al., 2010). A large area is required to dispose these waste materials. But there are very few research have been conducted on the utilization of POFA as a source material to produce environmentally friendly concrete and MS in the replacement of normal sand. Another waste material produced from the palm oil industry, OPS, that could be an alternative to the conventional coarse aggregate other than landfilling and can reduce the cost of construction. Hence, in this research have designed some objectives to figure out different aspects to investigate the performance of these waste materials to produce structural grade concrete.

1.5 Research objectives

1. To develop appropriate mixture design for geopolymer mortar using ground granulated blastfurnace slag (GGBS), palm oil fuel ash (POFA) and fly ash (FA) as binder.
2. To study the effect of crushed and uncrushed oil palm shell (OPS) as a coarse aggregate and three types of sand (mining sand, manufactured sand and quarry dust) in the geopolymer structural concrete.
3. To investigate the effect of curing on the mechanical properties of geopolymer concrete.
4. To investigate the effect of variation in OPS contents and steel fibre on the mechanical properties of geopolymer concrete.
5. To study the impact behaviour of the fibre reinforced geopolymer concrete panels with varying crushed and uncrushed OPS contents.

1.6 Scope of study

The scope of the research is based on the objectives set above and it is given below:

The chemical and physical properties (particle size distribution) tests for palm oil fuel ash (POFA), ground granulated Blastfurnace slag (GGBS) and fly ash (FA) were conducted using X-Ray Fluorescence (XRF) and particle size analyser, respectively.

A total of eleven mixes were performed for POFA-GGBS-FA based mortar to obtain the optimum mix proportion. The variables were the contents of local waste materials (POFA/GGBS/FA). Manufactured sand (MS) was used instead of conventional mining sand (NS). NaOH and Na₂SiO₃ were used as alkaline activator for geopolymerization.

After obtaining the optimum mix from the mortar, another nine more mixes were prepared using POFA and GGBS as source materials. The variables were 3 types of sand – mining sand (NS), manufactured sand (MS), quarry dust (QD) and coarse aggregate – crushed and uncrushed OPS. A control mix using normal weight aggregate (NWA) was also prepared.

Another fourteen mixes were prepared using the following:

- Binder/MS ratio: 1:2.5
- OPS/binder ratio: 0.4, 0.6, 0.8 (for both in crushed and uncrushed OPS)
- A control mix of with and without fibre

- Panels of 600×600×50 mm were prepared for impact test

The salient feature of this group of mixes (step 3 in Table 1.1) is to include the steel fibre to investigate the effect of fibre under impact test.

Table 1.1: Summary of mixes

No. of mixes	Variables	Non-variables
Step 1: 11 mixes	POFA, GGBS, FA	MS
Step 2: 9 mixes	NS, MS, QD uncrushed OPS, crushed OPS, NWA	POFA, GGBS
Step 3: 14 mixes	uncrushed OPS, crushed OPS	POFA, GGBS, MS, NWA, steel fibre

Tests included:

- Mechanical properties – cube compressive strength, splitting tensile strength, flexural strength, Young’s modulus and Poisson’s ratio.
- Panels were subjected to impact test using drop hammer test.

1.7 Structure of the dissertation

Chapter 1 provides a brief background and discussion of geopolymer concrete, the problem statement, and objectives of present study and scope of work.

Chapter 2 presents background and literature review to justify the research gaps found for the research work in this thesis. Literature review on geopolymer, lightweight concrete

(LWC), oil palm shell concrete (OPSC), fibre reinforced concrete (FRC), their mechanical properties and impact resistant characteristics are presented. Materials used in this research such as POFA, GGBS, FA, NS, MS, QD, OPS, crushed granite and steel fibre are discussed. The available published literature on geopolymer technology is also briefly reviewed.

Chapter 3 describes the methodology of developing mix design and the structural lightweight geopolymer concrete. This chapter also outlines a number of series of specimens and variables adopted.

Chapter 4 reports the results and discussion of the study, comparison of different results with crushed and uncrushed OPS along with three different fine aggregate – NS, MS, QD.

Chapter 5 outlines the conclusions and recommendations for future works.

CHAPTER 2 : LITERATURE REVIEW

2.1 General

The discovery of a new class of inorganic materials, geopolymer resins, binders, cements and concretes, resulted in wide scientific interest and kaleidoscopic development of its applications. From the first industrial research efforts in 1972 at the Cordi-Géopolymère private research laboratory, Saint-Quentin, France, until the end of 2006, hundreds of papers and patents were published dealing with geopolymer science and technology (Davidovits, 2011). Today, people are more concerned about the environment than any other issues that face us, including the economy. The industrialized countries of Latin America and Asia are experiencing very quickly economic and social development that is bringing modern civilization environmental problems, as well as water, air pollution and decay problems, to over-all the world (UNEP, 2012). Malaysia is one of the rapid economical and civilization growth countries. In the long term, "progress" works opposite to us if it continues to be disturbing to nature. This realization will find increasing acceptance. In the 21st century environmental protection will act a fundamental role and politicians and scientists will be face a major challenge (UNEP, 2012).

In this chapter, background and literature review has been presented to justify the research gaps found for the research work in this thesis. Literature review on geopolymer, lightweight concrete (LWC), oil palm shell concrete (OPSC), fibre reinforced concrete (FRC), their mechanical properties and impact resistant characteristics are presented. Materials used in this research such as POFA, GGBS, FA, NS, MS, QD, OPS, crushed granite and steel fibre are discussed. The available published literature on geopolymer technology is also briefly reviewed.

2.2 Geopolymers

In order to achieve an environmentally friendly concrete, several studies (Wallah & Rangan, 2006; Alengaram et al., 2011; Johari et al., 2012; Kupaei et al., 2013; Islam et al., 2014; Yusuf et al., 2014b) are on-going on the utilization of waste materials to produce green concrete. Among the researches, the successful one was through the development of geopolymer concrete to eliminate the use of cement. The term “GEOPOLYMER” was first applied by Prof. Dr. Joseph Davidovits in 1979 (Davidovits, 2002). The method of production of geopolymer concrete is similar to that of conventional concrete. Geopolymerisation involves a chemical reaction in which Si-O-Al-O bonds are formed as a result of the reaction between an alkaline and a source of Alumina-Silicate oxides. Geopolymer compositions are similar to natural Zeolites; however, their structures are amorphous to semi-crystalline. This is due to the faster reaction time of geopolymers compared with Zeolites that yield crystalline structures. Geopolymer concrete is well-suited to manufacture precast concrete products that can be used in infrastructure developments (Lloyd & Rangan, 2010). A number of researchers (Hardjito et al., 2004; Bakharev, 2005a, 2005c, 2005b, 2006; Lloyd & Rangan, 2010) have published articles on the use of FA as source material in the development of geopolymer concrete. The significant research in geopolymer includes thermal behaviour (Bakharev, 2006), durability in sodium and magnesium sulfate solutions (Bakharev, 2005a), and resistance to acid attack (Bakharev, 2005c) of geopolymeric materials.

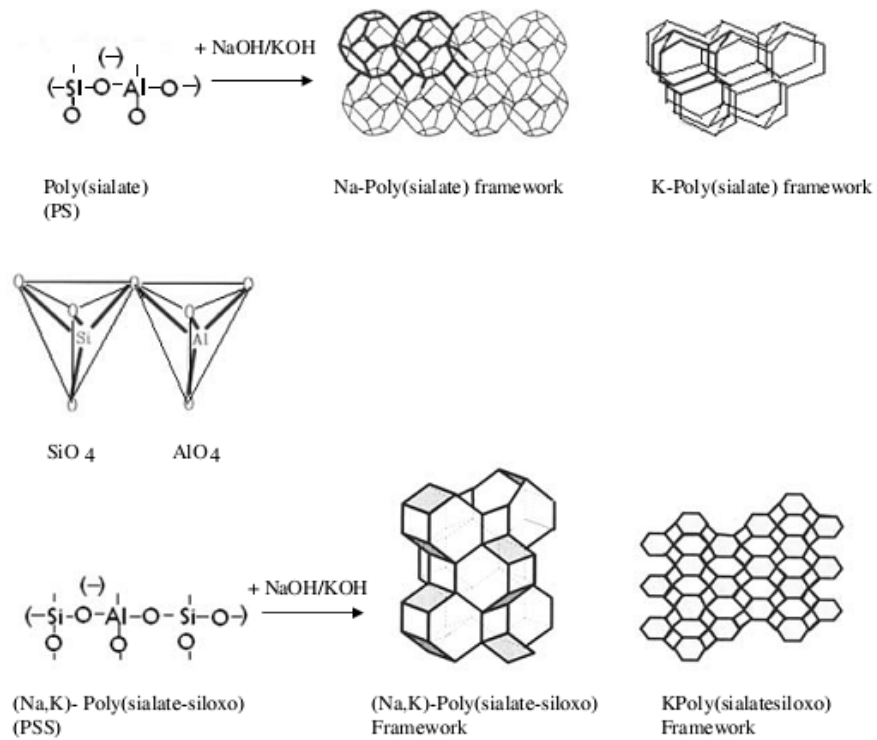


Figure 2.1: Structural models of geopolymer concrete-Davidovits (Davidovits, 2011)

Geopolymer is an inorganic alumino-hydroxide polymer synthesized from predominantly silicon and aluminium materials of geological origin and industrial by-product material such as FA (with low calcium) as shown in Figure 2.1.

2.3 Properties of geopolymer

Earlier researchers reported that geopolymer enables high early strength, low shrinkage, freeze-thaw resistance, sulphate resistance, corrosion resistance, acid resistance, fire resistance, and no dangerous alkali-aggregate reaction (Hardjito & Rangan, 2005; Wallah & Rangan, 2006).

Dangerous alkali-aggregate-reaction could be produced due to the addition of alkalis in the normal Portland cement or concrete. But the geopolymeric system even with higher alkali content is safer from that criteria (Wallah & Rangan, 2006). Davidovits (2011) opined that bar expansion test in accordance with ASTM:C227-10 (2010) shows geopolymer cements with higher alkali content did not produce any dangerous alkali-aggregate reaction compared to Portland cement.

As the human population of the world increases so does the need for housing and infrastructure increase and consequently so does the use of cement.

2.4 Source materials

Geopolymer concrete consists of two main parts defined as the source materials and the alkaline liquids.

1. Geopolymers' source materials are based on aluminosilicate should be rich in silicon (Si) and aluminium (Al). Any material which is rich in amorphous shape of Si and Al can be used as the source material to produce geopolymer. This source material can be both natural minerals such as kaolinite and clays or industrial by-products such as slag, rice-husk ash, red mud, fly ash and silica fume. The source material used for the production of geopolymers can be an individual material or a combination of several types of them (Xu & Van Deventer, 2002). In this study, GGBS, POFA and FA have been used as source materials.

Among the waste or by-product materials, fly ash and slag are the most potential source of geopolymers. Several studies have been reported related to the use of these source materials. The recent research works (Ariffin et al., 2013; Islam et al., 2014; Mijarsh et al., 2014) on the use of palm oil fuel ash (POFA) as the source material opens new avenue in the development of geopolymer concrete as well as normal concrete (Aldahdooh et al., 2013; Lim et al., 2013). Aldahdooh et al. (2013) reported that POFA can be used to produce high strength fibre reinforced concrete of about 158 MPa at 90-days. Mijarsh et al. (2014) developed geopolymer mortar using 65 wt% of POFA and found the compressive strength of 47 MPa after 7-days of curing. Kupaei et al. (Kupaei et al., 2013) developed fly ash (FA) based lightweight geopolymer concrete using OPS as lightweight coarse aggregate.

Blastfurnace slag is the by-product produced simultaneously with iron in the Blastfurnace and is composed chiefly of calcium and magnesium silicates and aluminosilicate. It is granulated by rapid quenching of the molten material. The resulting granules, which are mainly glassy in composition, are subsequently dried and ground to a fine powder (BS 6699, 1992).

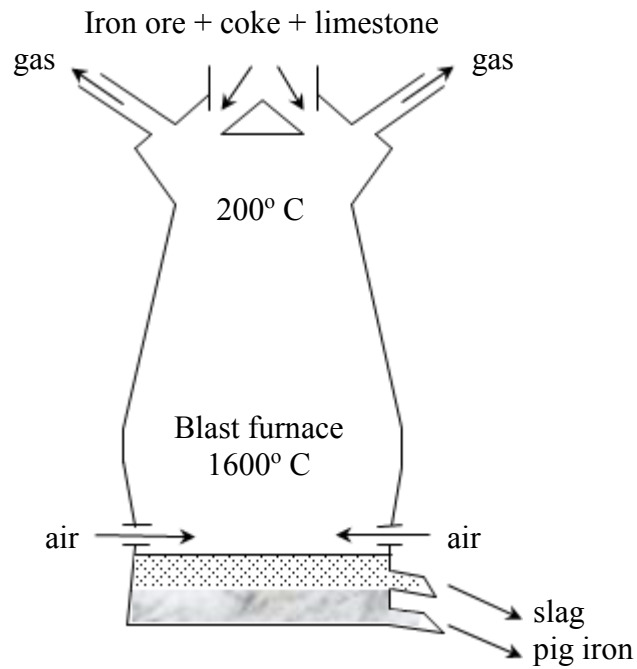


Figure 2.2: The slag floats above the pig iron at the bottom of the blast furnace (Davidovits, 2011)

The blast furnace slag is a molten material that is formed from the manufacturing of the siliceous gangue found in iron ore, the residue of coke combustion, the limestone and other added ingredients. The temperature is in the range between 1400° and 1600° C and is close to that of the molten iron. In the blast furnace, it appears above the pig iron (Figure 2.2) (Davidovits, 2011).

Slag becomes suitable for geopolymeric reaction when quenched from the melt. It is called granulated slag or ground granulated blast furnace slag GGBS. The glassy material is obtained either poured into pits filed with water or by high-pressure water jets at the blast furnace, when it flows out of the spout.

Guidance on its use in concretes, either as a component of composite cements such as Portland blastfurnace cements conforming to BS 146 and BS 42461) or as a direct addition to the concrete mix, can be found in BS 5328, BS 6543 and BS 8110-1. Guidance on its use in mortar as a component of composite cements, such as those conforming to BS 146 and BS 42461) or as a direct addition to the mortar mix, can be found in BS 5262 and BS 5628.

Fly ash (FA), one of the source materials for geopolymer binders, is available abundantly worldwide, and yet its use to date is limited. From the 1998 estimation, the global coal ash production was more than 390 million tonnes annually, but its use was less than 15% (Malhotra, 1999). In the future, fly ash production will increase, especially in countries such as China and India. From these two countries alone, it is estimated that by the year 2010, the amount of the fly ash produced will be 780 million tonnes annually (Malhotra, 2002; Hardjito et al., 2004). Accordingly, efforts to use this by-product material in concrete manufacture are important to make concrete more environmentally friendly. Fly ash is normally grey in colour and can be light dark or even beige depending on the type of coal and the efficiency of combustion. Fly ash is divided into two distinct categories – Class F (low calcium $\text{CaO} < 10\%$) and Class C (high calcium $\text{CaO} > 10\%$) ASTM:C618-12a.

2. For conventional concrete, water used for hydration of cement. But in the case of geopolymer, the source materials would not react with the presence of water. Alkaline activator are used as a substitute of water during the mixing of the raw materials of geopolymer concrete. The hydroxyl ions (OH^-) from the alkaline activator are known

to increase the hydration rate by enhancing the dissolution of aluminate and silicate in the source materials.

2.5 Mixture proportions of geopolymer concrete

Geopolymer concrete is a new type of concrete, and there is no standard mix design or well-known method available (Hardjito & Rangan, 2005). The principal difference between the OPC concrete and the geopolymer concrete is the cement or binder. To produce geopolymer concrete, the source material reacts with alkaline activator to form geopolymer paste that binds the fine, coarse and other un-reacted materials. The volume of coarse and fine aggregates represents about 75 to 80 per cent of the overall volume to be geopolymer concrete (Hardjito & Rangan, 2005), similar to the conventional OPC concrete. The mechanism of OPC concrete, its hydration process and reactions are well established due to vast number of researches performed during the last century. On the contrary, the mechanism of geopolymer concrete are still not recognized. Therefore, the mix proportion of this novel concrete needs more attention due to its constituent materials.

Hardjito & Rangan (Hardjito & Rangan, 2005) conducted a study on the low-calcium fly ash-based geopolymer concrete and open a new milestone in the field of geopolymer concrete. They reported:

- Higher concentration of NaOH solution produce higher compressive strength of geopolymer concrete.
- Higher the ratio of Na_2SiO_3 solution-to-NaOH solution by mass, produce higher compressive strength of geopolymer concrete.
- The addition of naphthalene sulphonate-based super plasticizer, up to approximately 4% of fly ash by mass, improves the workability of the fresh

geopolymer concrete; however, there is a slight degradation in the compressive strength of hardened concrete when the super plasticizer dosage is greater than 2%.

- The slump value of the fresh geopolymer concrete increases when the water content of the mixture increases.
- As the H₂O-to-Na₂O molar ratio increases, the compressive strength of geopolymer concrete decreases.

Kupaei et al. (2013) developed fly ash (FA) based OPS geopolymer concrete. They reported:

- The conventional mixture methods are not suitable for OPSGC.
- Loss of water during heat curing would result in strength reduction in OPSGC
- The strength of OPSGC are significantly decreases as the increase in water, OPS and fine aggregate contents increases.
- The strength of OPSGC beyond 14 M of activator solution does not increase significantly.

Table 2.1 shows the summary of mix proportion of geopolymer concrete carried out by previous researchers. It is revealed that molarity of NaOH and oven curing temperature used in their mixes were 10 – 15 M and 60 – 65 °C, respectively. The quantity of water used is very low.

Table 2.1: Summary of mix proportion (by weight) of geopolymer concrete

References	Constituents	Mix proportion	NaOH solution	Activator / binder ratio	Water / binder ratio	SP / binder ratio	Curing	Compressive strength at 28-day (MPa)
Kupaei et al. (2013)	FA/NS/OPS ^a	1/0.74/0.66	14 M	0.35	0.17	0.013	65 °C OD (48 h)	28
Wallah and Rangan (2006)	FA/NS/CG ^a	1/1.36/3.17	14 M	0.35	0.06	0.015	60 °C OD (24 h)	45
Tho-in et al. (2012)	FA/CG ^a	1/8	15 M	0.45	0	0	60 °C OD (48 h)	11
Yusuf et al. (2014a)	(POFA+GGBS) /NS/CG ^a	(0.8+0.2)/1.8/3.3	10 M	0.50	0	0	60 °C OD (24 h)	71

^a FA-fly ash, NS- conventional mining sand, OPS-oil palm shell, CG-crushed granite, GGBS-ground granulated blastfurnace slag

2.6 Mortar for geopolymer

The manufacturing of geopolymer concrete is similar to that of the conventional concrete. For the preparation of mortar, binding raw materials and fine aggregates were first dry-mixed together in a pan mixer for about three minutes. The alkaline liquid was then mixed with the super plasticiser and the extra water, if any. The liquid component of the mixture was then added to the dry materials and the mixing continued usually for another four minutes (Hardjito & Rangan, 2005; Wallah & Rangan, 2006). Subsequently, immediately after mixing, the geopolymer mortar was cast into 50 x 50 x 50 mm cube moulds, in two layers. The specimens were started moulding within a total elapsed time of not more than 2 min and 30 s after completion of the original mixing of the mortar batch. A layer of geopolymer mortar was placed approximately one half of the depth of the mould in all of the cube compartments. The mortar in each cube compartment was tamped 32 times in about 10 s in 4 rounds as illustrated in Figure 2.3. When the tamping of the first layer in

the entire cube compartment was completed, the compartments with the remaining mortar was then filled and tamped as specified for the first layer [ASTM:C109/C109M-12].

1	2	3	4
8	7	6	5

Figure 2.3: Order of tamping in moulding of test specimens [ASTM:C109/C109M-12]

The compressive strength of geopolymer concrete is influenced by the wet-mixing time. Test results show that the compressive strength increased as the wet-mixing time increased (Hardjito & Rangan, 2005).

2.7 Effect of water-to-geopolymer solids ratio

Hardjito and Rangan (2005) conducted a study on the effect of water-to-geopolymer solids ratio by mass on the compressive strength and the workability of geopolymer concrete. Figure 2.4 shows that the compressive strength decreases as the water-to-geopolymer solids ratio by mass increases.

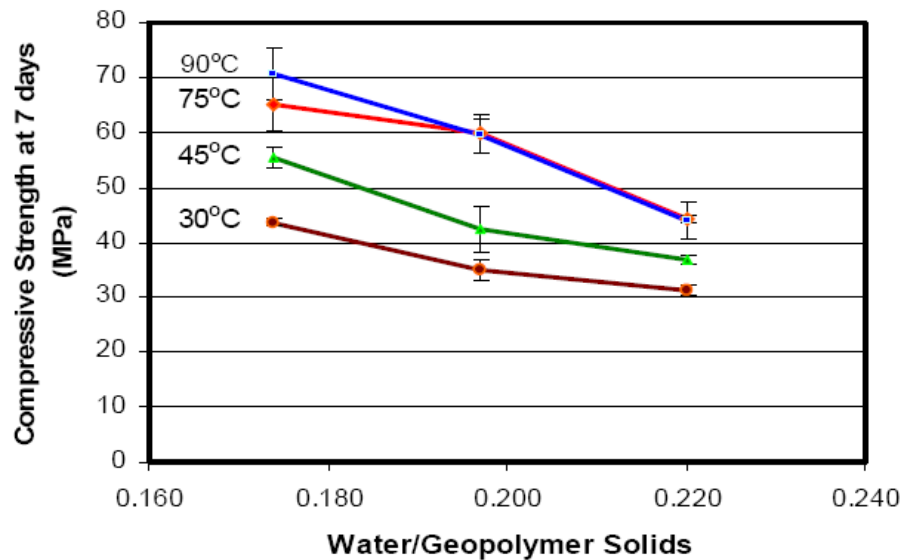


Figure 2.4: Effect of water-to-geopolymer solids ratio by mass on compressive strength of geopolymer concrete (Hardjito & Rangan, 2005)

2.8 Curing of geopolymer concrete

Heat accelerates the chemical reaction during the heat-curing in the geopolymer paste. Both curing time and curing temperature affect the compressive strength of geopolymer concrete. During the first 24 hours of curing, the rate of increase in strength is rapid and beyond this time, the gain in strength is not substantial. Therefore, in practical heat-curing time need not be more than 24 h (Hardjito & Rangan, 2005).

Davidovits (2011) opined that the slag based geopolymer mortar cured under heat and non-heat conditions achieves similar strength at later age of 28-day compared to early ages of 3-, and 7-day strength. Geopolymerization starts with the depolymerisation (break down, cleavage of Si-O-Si-O- and others in the aluminosilicate structures of the raw materials: slag (mellilite) or metakaolin). This step requires energy (heat) or time (at room temperature). However, at the end, the chemical mechanism remains the same.

2.9 Lightweight concrete

Lightweight concrete (LWC) is a concrete which has been made lighter than conventional concrete. LWC has been in use in construction industry for many years in Europe and America but did not find enough attention due to lack of understanding about the production techniques and structural performance of lightweight aggregates (LWA) (Chandra & Berntsson, 2002). Structural lightweight concrete have been in use in both reinforced and pre-stressed concrete for many years. The use of LWC permits greater design flexibility, reduced dead load, improved cyclic loading for structural response, longer spans, better fire rating, thinner sections, smaller structural sections, less reinforcing steel, 10-20% cost saving and lower foundation cost.

For structural concrete, the pragmatic requirements are generally that any lightweight aggregate is suitable that has a crushing strength sufficient to have reasonable resistance to fragmentation while enabling concrete strength in excess of 20 N/mm^2 (Newman & Choo, 2003; Clarke, 2005). The density of structural lightweight aggregate concretes can range from approximately $1200 - 2000 \text{ kg/m}^3$ compared with 2300 to 2500 kg/m^3 for normal weight concrete (NWC) (Clarke, 2005). The oven-dry density range as specified in EN 206-1 (2000) for lightweight concrete and NWC are $800 - 2000 \text{ kg/m}^3$ and $2000 - 2600 \text{ kg/m}^3$, respectively. The density of concrete that exceeds 2600 kg/m^3 is known as heavyweight concrete. The minimum strength for structural lightweight concrete, as identified by several codes are shown in Table 2.2 (Clarke, 2005).

Table 2.2: Minimum strength for structural lightweight concrete (Clarke, 2005)

Code	Reinforced	Pre-stressed
BS 8110	20	30 ^a and 40 ^b
BS 5400	25	Not permitted
ACI 318	30	30
ENV 1992-1-4	12	25 ^a and 30 ^b
AS 3600	25	25
NS 3473	25	35
JASS 5	25	25

^a post-tensioned

^b pre-tensioned

2.10 Development of new LWC and OPS used as a coarse aggregate

Malaysia is the second largest palm oil producing country in the world (Pakiam, 2013), and producing a large quantity of palm oil wastes. But there is not many reports on use of OPS as coarse aggregate. To sustain the environment few researchers have taken initiative of the utilization of OPS as a LWA (Mannan & Ganapathy, 2002; Teo et al., 2006; Alengaram et al., 2013). Proposals were made to substitute OPS as road based materials instead of asphalt on various occasion (Okafor, 1988; Basri et al., 1999). Teo et al. (2006) use OPS to build one story building and foot bridge which are being monitored for their structural behaviour.

2.11 Fibre reinforced geopolymer concrete

Fibre-reinforced concrete is concrete containing fibrous material which increases its structural integrity. Bernal et al. (2010) carried out a study on the effect of steel fibre on the mechanical properties of slag-based geopolymer concrete and reported that utilization of steel fibre reduces the compressive strength but largely improve splitting tensile and flexural strength. They reported that alkali-activated fibre reinforced slag concrete shows a mechanical performance better than the corresponding mixes of ordinary Portland

cement concrete. A reduction of compressive strength of about 23% at 28-day was observed for the slag based fibre reinforced geopolymer concrete (FRGC) containing 40kg/m^3 steel fibres compared to plane control geopolymer concrete and increase in steel fibre content from 40kg/m^3 to 120kg/m^3 , there was a greater reduction in compressive strength.

Puertas et al. (2003) conducted a study on the on polypropylene (PP) fibre reinforced FRGC, no such reduction in compressive strength was observed as reported (Bernal et al., 2010). In their study, three different types of source materials such as slag, fly ash and slag/fly ash combination were used. The polypropylene (PP) fibres of 0.5% and 1% by volume of mortar were used. The addition of 0.5% and 1% PP fibre did not affect the compressive strength of slag based FRGC at 2- and 28-day. Though, in fly ash based FRGC the 2-day compressive strength was increased due to increase of PP fibre contents but a slight reduction was observed at 28 days in the same composite. In the case of combined slag/fly ash based FRGC, slight increase in compressive strength was noticed by increasing the PP fibres from 0.5% to 1.0% at both ages.

In another study reported the early improvement of PP FRGC compressive strength compared to the plane concrete (Zhang et al., 2009). The source material used in that study was fly ash and calcined kaolin. The compressive strength of FRGC containing 0.5% PP fibre (by wt.) reached about 52 MPa at 3-day; though beyond this fibre content reduced compressive strength.

2.12 Impact Test

Impact test is a method of determining behaviour of material subjected to impact loading in bending. Usually, the energy absorbed in breaking the specimen is measured. Drop hammer impact test is performed by subjecting the specimen failure to multiple blows.

Rao et al. (2011) conducted impact test under drop weight impact load on concrete specimens that contained using recycle aggregate of 15 years old demolished reinforced concrete culvert. Results showed that beyond 25% replacement of recycle aggregate, impact resistance reduced significantly.

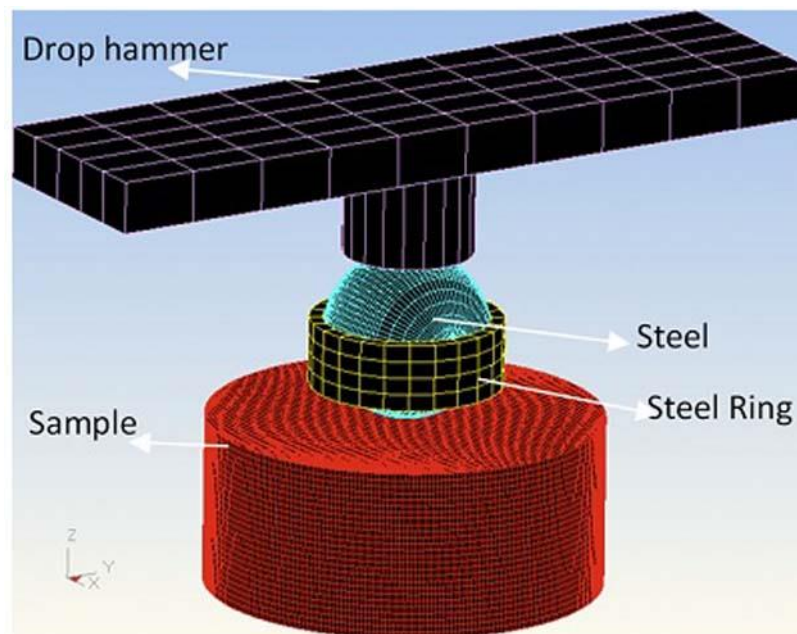


Figure 2.5: Finite element model of impact test (Nia et al., 2012)

Another study (Nia et al., 2012) of impact test was performed using the method of drop weight impact load in accordance with the ACI committee 544. They used two different types of fibres namely steel and polypropylene fibres and reported that steel fibres

significantly increased impact resistance compared to polypropylene fibres. This could be attributed to larger length of hooked-ends steel fibres, high tensile strength and better cohesion due to their hooked-ends. They compared numerical and experimental data (Figure 2.5) and found that the impact resistance development for normal strength concrete is higher than high-strength concrete.

There is no study has been done on impact test on geopolymer concrete and OPS in geopolymer concrete. The drop weight impact test for OPS conventional concrete with conventional mining sand and OPC was performed by Mo et al. (2014b). They produced OPS concrete using two different sizes of OPS coarse aggregates called uncrushed and crushed OPS of maximum sizes 14 mm and 9 mm, respectively. They reported that the impact energy of the concrete produced by uncrushed OPS is higher compared to crushed OPS because of its energy absorption capability compared to the corresponding crushed OPS.

2.13 Application of geopolymer concrete

Geopolymer concrete is well-suited to manufacture precast concrete products that can be used in infrastructure developments (Lloyd & Rangan, 2010) and main building structure (Aldred & Day, 2012) as well. The University of Queensland's Global Change Institute (GCI), Australia is the world's first building to successfully use slag/fly ash-based geopolymer concrete for structural purpose (Figure 2.6). This precast geopolymer concrete is useful for faster construction process, better quality maintain due to factory production, reuse of formwork as well as saving of formwork cost.



(a)



(b)

Figure 2.6: (a) Queensland's University GCI building with 3 suspended floors made from structural geopolymer concrete, (b) precast slag/fly ash - based geopolymer concrete floor parts, Australia (Aldred & Day, 2012)



Figure 2.7: Composite pultruded girder and Grade 40 geopolymer deck bridge in Brisbane (Aldred & Day, 2012)

Another application of geopolymer concrete is the precast deck bridge (Aldred & Day, 2012). Figure 2.7 shows a composite pultruded girder and Grade 40 geopolymer deck bridge structure constructed in West Moggill, Brisbane, Australia.

2.14 Research gap addressed in this research

Author	Past research works	Significance of current research	
Bagheri and Nazari (2014)	Performed compressive strength test using class C fly ash and GGBS based geopolymer concrete using NWA. Two types of curing namely oven-dry and water were carried out and found that oven-oven dry cure samples are more effective.	<p>It was observed from literature review that there is no research carried out on the sustainable sand to replace conventional sand; one of the means to attain sustainability is to reduce conventional sand (NS); in Malaysia the availability of two different fine aggregates – manufactured sand (MS) and quarry dust (QD) paves way to use alternative materials for sand. Thus, this work focusses on using MS and QD as replacement material for conventional sand in the development of geopolymer concrete.</p> <p>The use of local waste materials – fly ash (FA), palm oil fuel ash (POFA) and ground granulated Blastfurnace slag – as binder, in the development of geopolymer mortar and concrete is another significance of this research work.</p> <p>Another salient feature of this research work is the use of another local waste material – oil palm shell (OPS) to replace conventional crushed granite aggregate; its ability to resist high impact resistance is being explored by means of mechanical and impact tests.</p>	
Yusuf et al. (2014a)	POFA-GGBS based geopolymer concrete using conventional aggregate. Different curing temperature and varying alkaline activators to binder ratio were observed. Results show that the alkaline activators to binder ratio between 0.50 to 0.55 is suitable for moderate workability and good structural strength.		
Yusuf et al. (2014b)	Test conducted on POFA-GGBS based geopolymer paste and found that the optimum ratio is 80/20.		

Author	Past research works	Significance of current research
Altwair et al. (2012)	High volume of POFA used by cement replacement for conventional concrete to investigate the flexural performance and reported that higher content of POFA tends to reduce the crack width.	<p>The mechanical properties – compressive strength, splitting tensile strength, flexural strength, Young’s modulus and Poisson’s ratio have been investigated and reported.</p> <p>The ability of steel fibres to enhance the ductility of the OPSGC is another significant contribution and the fibre reinforced OPSGC was investigated for impact characteristic.</p> <p>The comparison of OPSGC with geopolymer concrete prepared from normal weight aggregate is also an important part of the present work.</p>
Kupaei et al. (2013)	Development of fly ash based OPS geopolymer concrete using conventional mining sand (NS) and 48 hours oven curing. They found the optimum mix ratio of FA/NS/OPS is 1/0.74/0.66.	

CHAPTER 3 : MATERIALS AND METHODS

3.1 Introduction

This chapter explains the materials and methods used to carry out various types of tests as shown in Table 3.1. Materials used include ground granulated blastfurnace slag (GGBS), palm oil fuel ash (POFA), fly ash (FA), mining sand (NS), manufactured sand (MS), quarry dust (QD), oil palm shell (OPS), crushed granite and steel fibre. Materials tests include water absorption, specific gravity, bulk density, particle size distribution, aggregate impact value (AIV) etc. Further, the X-ray fluorescence (XRF) test was conducted to determine the chemical composition of source materials. Specimens were prepared using OPS of target compressive strength of 30 MPa. A brief flowchart is presented in Appendix D.

Table 3.1: Specimen details and test conducted with code of practice

Test		Specimen	Specimen dimensions (mm)	Test age (day)	Code of practice
Physical properties of materials	Specific gravity & water absorption	N/A	N/A	N/A	BS EN 1097-6:2013
	Bulk density	N/A	N/A		BS 3N: 1097-3:1998
	Sieve analysis	N/A	N/A		BS EN 933-1:2012
	Moisture content	N/A	N/A		BS EN 1097-5:2008
	Workability	N/A	N/A		BS EN 12350-2:2009
	Oven-dry density	N/A	N/A	28	BS EN 12390-7:2009
Compressive strength		Cube	100×100×100	3, 7, 28, 56, 90	BS EN 12390-3:2009
Splitting tensile strength		Cylinder	100Ø×200	28	BS EN 12390-6:2009
Flexural strength		Prism	100×100×500	28	BS EN 12390-5:2009
Young's modulus & Poisson's ratio		Cylinder	150Ø×300	28	ASTM: C469/C469M-10
Impact test		Panel	600×600×50	28	ACI 544.1R-96
Ultrasonic pulse velocity (UPV)		Cube	100×100×100	28	BS EN 12504-4, 2004

3.2 Materials used to develop geopolymer mortar and concrete

3.2.1 Characterisation of materials

The materials used for this study are ground granulated blastfurnace slag (GGBS), palm oil fuel ash (POFA), fly ash (FA), mining sand (NS), manufactured sand (MS), quarry dust (QD), oil palm shell (OPS), crushed granite and steel fibre. The followings explain each material used and its characteristics. A brief introductory is shown in Appendix E.

3.2.2 Ground granulated blastfurnace slag

Ground granulated blast furnace slag (GGBS) (Figure 3.1a) was obtained from YTL Cement Marketing Sdn Bhd, Malaysia. The slag activity index of GGBS was 62% and 108% for 7 and 28 days respectively. The specific gravity was 2.89 g/cm³, specific surface area was 405 m²/kg and the soundness was 1 mm. The particle size distribution of GGBS is shown in Figure 3.2. It is off-white in colour and substantially lighter than Portland cement. The chemical composition of GGBS is shown in Table 3.2; while its physical properties are given in Table 3.3. GGBS shall contain at least two-thirds by mass of glassy slag. The slag shall consist of at least two-thirds by mass of the sum of CaO, MgO and SiO₂. The remainder contains Al₂O₃ together with small amounts of other oxides. The ratio by mass (CaO + MgO)/(SiO₂) shall exceed 1.0 (BS 146, 1996). This GGBS fulfil these requirements.

Table 3.2: Chemical compositions of source materials as determined by X-ray fluorescence (XRF) analysis (wt. %)

Chemical compounds	CaO	SiO ₂	Al ₂ O ₃	MgO	Na ₂ O	SO ₃	P ₂ O ₅	K ₂ O	TiO ₂	MnO	Fe ₂ O ₃	SrO	Cl	CuO	LOI
GGBS	45.83	32.52	13.71	3.27	0.25	1.80	0.04	0.48	0.73	0.35	0.76	0.08	0.02	-	0.60
Fly-ash	5.31	54.72	27.28	1.10	0.43	1.01	1.12	1.00	1.82	0.10	5.15	0.36	0.01	0.01	6.80
POFA	4.34	63.41	5.55	3.74	0.16	0.91	3.78	6.33	0.33	0.17	4.19	0.02	0.45	6.54	6.20

3.2.3 Palm oil fuel ash

Palm oil fuel ash (POFA) was obtained from Jugra Palm Oil Mill Sdn Bhd, Malaysia. It was then dried in an oven for at least 24 h at 100⁰ C to remove the moisture and then it was sieved through 300 µm sieve. Forty mild steel rods of 10 mm diameter and 400 mm length were placed in the rotating drum to grind approximately 10 kg of POFA that was sieved through 300 µm. The grinding of POFA was carried out for 30,000 cycle in 16 h to obtain the desired level of fineness (>66%). ASTM:C618-12a (2008) stipulates that the mass of fly ash and natural pozzolan passing through 45-µm by wet sieving shall be at least 66% and POFA exceeded this target as 88% passed through the sieve. Its particle size distribution is shown in Figure 3.2. Table 3.2 and Table 3.4 show the chemical composition and physical properties of POFA, respectively. The fineness of POFA was checked at every 4 h of grinding interval using a 45-µm sieve according to ASTM:C 430 (2009). The sieve fineness of POFA for different grinding period is shown in Figure 3.3. It was darker in colour. It was found that after processing of raw POFA, the processed POFA obtained was about 57%.



(a) GGBS



(b) POFA



(c) Fly ash

Figure 3.1: Source materials used in the present study

Table 3.3: Physical properties of source materials

Label	Specific gravity	Specific surface area, (m ² /kg)	Soundness, (mm)	Colour
GGBS	2.89	405 (min 275 m ² /kg, BS6699:1992)	1	off-white
POFA	2.14	172	-	Dark
FA	2.40	341	-	Grey

Legend: (P) - Passing, (R) – Retained

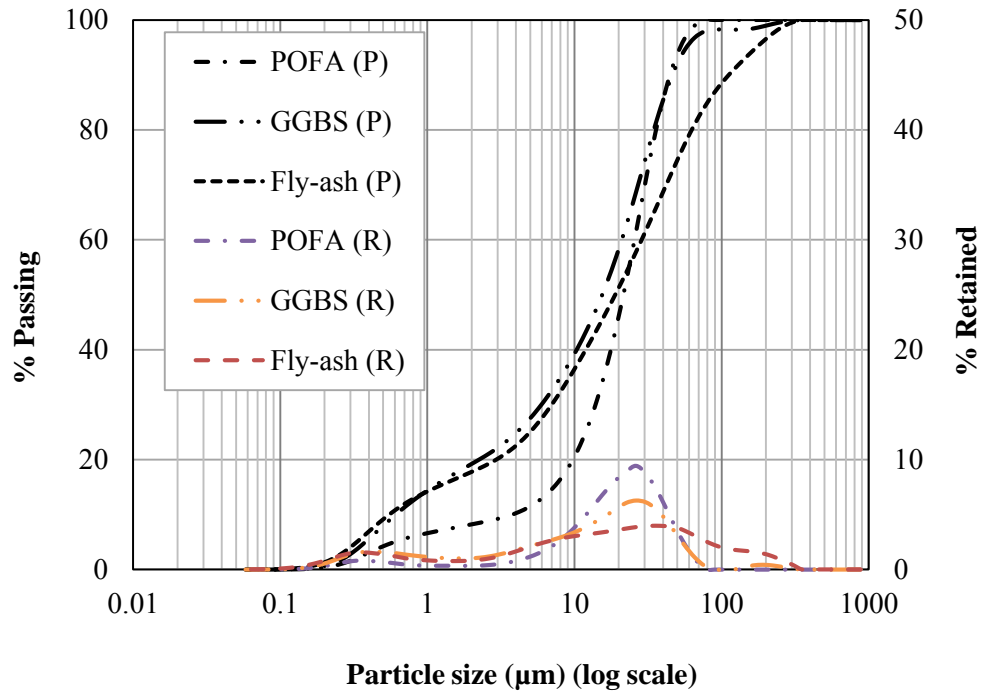


Figure 3.2: Particle size distribution of GGBS, POFA and FA

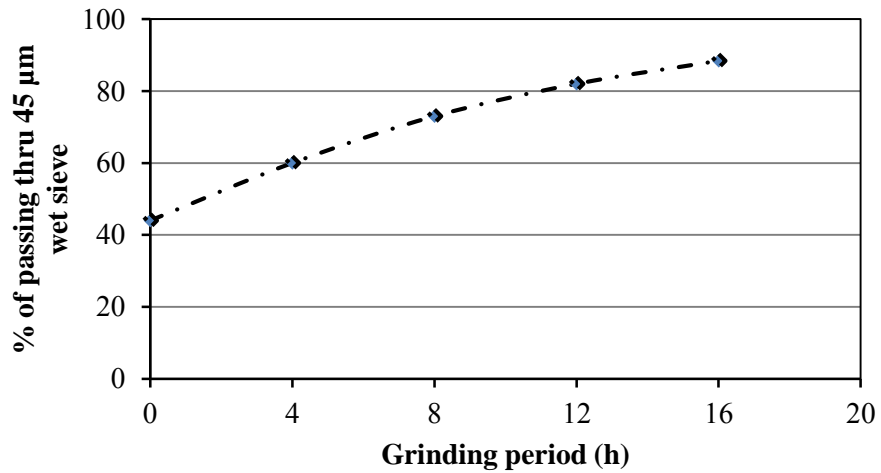


Figure 3.3: Fineness of POFA with different grinding periods

3.2.4 Fly ash

Fly ash (FA) was obtained from Lafarge Malayan Cement Bhd, Malaysia. According to ASTM:C618-12a (2008), FA is divided into two distinct categories i.e., low-calcium fly ash (Class F, CaO<10%) and high-calcium fly ash (Class C, CaO>10%) (ASTM:C618-

12a, 2008). In this study low-calcium fly ash was used. The chemical composition and physical properties of FA are shown in Table 3.2 and Table 3.3, respectively.

3.2.5 Fine aggregates

Three different fine aggregates (Figure 3.5) were used to produce concrete mixes. Local mining sand (NS) with a specific gravity, fineness modulus and maximum nominal size of 2.63, 2.69 and 4.75 mm, respectively was used.

Two other local waste materials, namely, manufactured sand (MS) and quarry dust (QD) were also used to study the feasibility of these materials in the development of sustainable lightweight geopolymer concrete; their physical and mechanical properties were investigated and compared with the conventional mixes using mining sand. The maximum nominal size of 4.75 mm was kept constant for all fine aggregates. The specific gravity and fineness modulus of MS were found as 2.60 and 3.19, respectively; however, QD with irregular and flaky particles had higher specific gravity and fineness modulus of 2.64 and 3.84, respectively. The physical properties and particle size distribution of all three fine aggregates are shown in Table 3.4 and Figure 3.4.

Table 3.4: Physical properties of mining sand, manufactured sand and quarry dust

Physical property	Mining sand (NS)	Manufactured sand (MS)	Quarry dust (QD)
Maximum size (mm)	4.75	4.75	4.75
Specific gravity (SSD)	2.63	2.6	2.65
24 h water absorption (%)	1.1	1.8	1.87
Fineness modulus	2.69	3.19	3.84
Grading zone (BS882:1992)	F	M	C

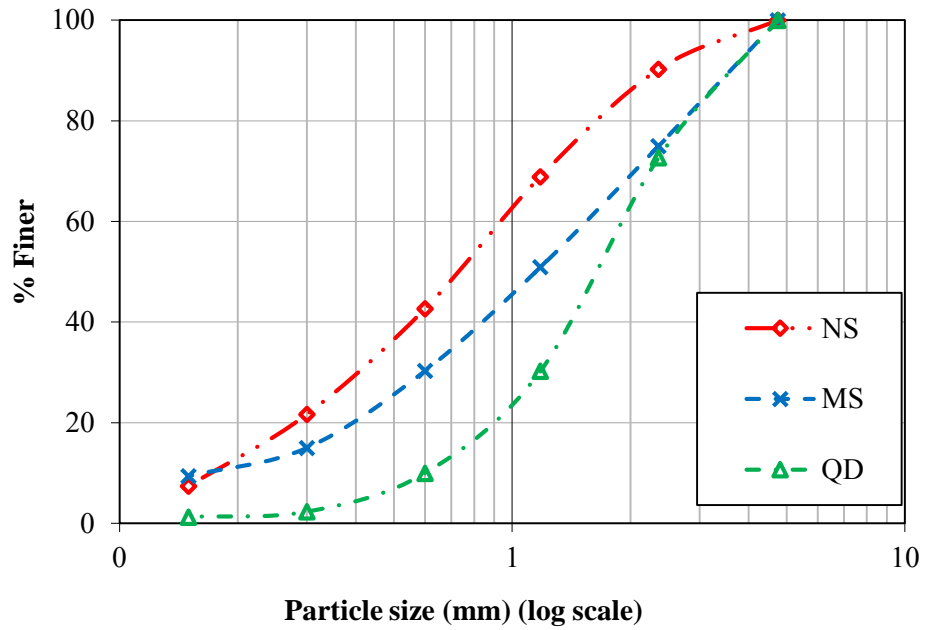


Figure 3.4: Particle size distribution of NS, MS and QD

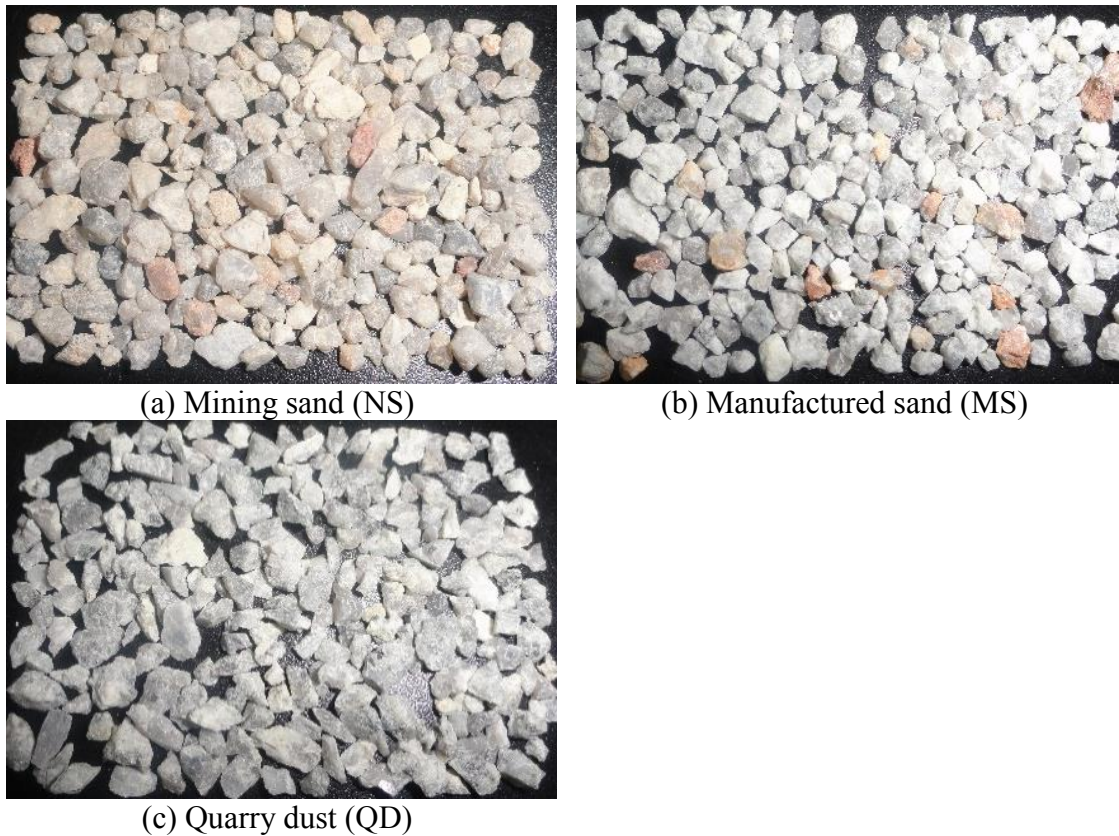


Figure 3.5: Coarse fraction of fine aggregate (a) Mining sand (NS); (b) Manufactured sand (MS) and (c) Quarry dust (QD)

3.2.6 Coarse aggregates

The coarse aggregate used in this study were oil palm shell (OPS) collected from local palm oil factory, in both uncrushed and crushed conditions (Figure 3.6), with maximum

sizes of 14 mm and 9 mm, respectively (Table 3.5). Generally, the raw OPS collected from factory have oily surface that could affect the bond and hence these were washed and then air dried in the laboratory to saturated surface dry (SSD) condition; for the crushed OPS, the cleaned ones were crushed to the required size.

Table 3.5: Physical properties of OPS and crushed granite

Physical property	Uncrushed OPS	Crushed OPS	Crushed granite
Maximum size (mm)	14	9	20
Compacted bulk density (kg/m ³)	633	655	1468
Specific gravity	1.34	1.33	2.62
24 h water absorption (%)	25.7	24.7	0.95
Aggregate impact value (AIV) (%)	2.63	3.13	11.9



(a)



(b)



(c)

Figure 3.6: Coarse aggregate (a) uncrushed OPS; (b) crushed OPS; and (c) crushed granite

The uncrushed OPS have concave and convex surfaces and the outer convex surface has smoother surface compared to concave surface. The crushed OPS have more spiky edges than the uncrushed OPS (Figure 3.6) (Mo et al., 2014b). The physical properties of the uncrushed and crushed OPS along with conventional crushed granite aggregate are given in Table 3.5. Both the crushed and the uncrushed OPS have lower aggregate impact value (AIV) and bulk density than the crushed granite aggregate. As seen from Table 3.5, the 24 h water absorption of OPS is very high (about 25%) compared to NWA (0.95%). Higher water absorption characteristics of OPS shows that pre-soaking is necessary or higher water content must be used to compensate for loss of water due to absorption (Alengaram et al., 2010a).

3.3 Activator solution

A combination of sodium silicate ($\text{Na}_2\text{O}= 12\%$, $\text{SiO}_2=30\%$, and water = 57% by mass) and sodium hydroxide solution (NaOH) was used as alkaline activator. The solution of 12 molarity (M) NaOH prepared with 99% purity such that 361 g of pellets was dissolved in 1 kg of solution (Wallah & Rangan, 2006). The ratio of $\text{Na}_2\text{SiO}_3/\text{NaOH}$ was kept constant at 2.5 for all the mixes and the mixture contained additional water.

The specific gravity of the combined alkaline activators was found about 1.57; while the specific gravities of Na_2SiO_3 and NaOH were 1.65 and 1.38, respectively. The specific gravity of NaOH solution varied depends on the molarity of the solution. The increase in concentration, increase in specific gravity and vice-versa. The formula for the combined specific gravity is as follows:

$$\frac{G_{NaOH} \times 1}{1 + 2.5} + \frac{G_{Na_2SiO_3} \times 2.5}{1 + 2.5} \quad (2)$$

$$= 1.57$$

Where, G_{NaOH} and $G_{Na_2SiO_3}$ are the specific gravities of NaOH and Na_2SiO_3 respectively.

3.4 Water

Tap water was used in the mixing of concrete.

3.5 Fibres

The fibres in this study include hooked-end steel fibre (aspect ratio = 65 and length = 35 mm) Figure 3.7. The specific gravity of steel fibre is 7.9.

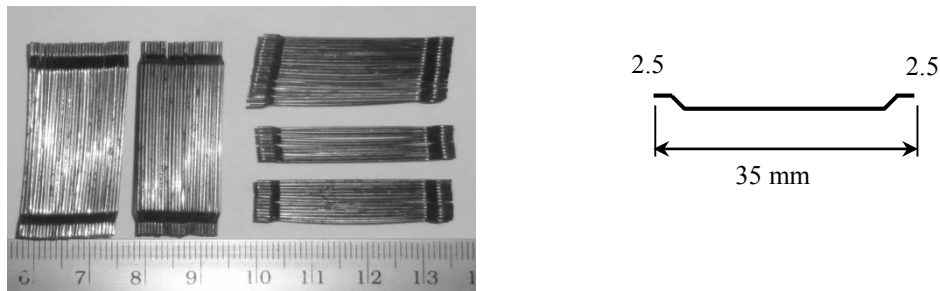


Figure 3.7: Steel fibres used to reinforced geopolymer concrete

3.6 Mix proportion and casting of specimens

Three steps of casting were performed to prepare the geopolymer specimens.

Step 1: At the beginning of the research, mortar casting was carried out to develop appropriate mix design of geopolymer mortar. At this step, the binder effect in mortar based on their chemical properties and compressive strength was investigated and reported.

Step 2: After obtaining the optimum mix proportion of mortar, trial casting of geopolymer concrete was conducted to develop structural grade of concrete and nine (9) mix design were performed with three different fine and coarse aggregates. From this step, the MS was kept constant as the fully replacement of conventional mining sand. The mix ratio for structural concrete grade was obtained as well. The mechanical properties of these geopolymer concrete also investigated.

Step 3: Finally, impact behaviour and mechanical properties of geopolymer concrete were carried out incorporating steel fibre and varying OPS contents as coarse aggregate to investigate the effect of fibre and OPS. The mixture proportions of three steps of casting are discussed in the following sections.

3.6.1 Preparation of fresh geopolymer mortar and casting

A total of 11 mixes were prepared by varying the POFA, FA and GGBS contents. The sand and activators contents were kept constant to investigate the effect of the binders. The proportion of binder to fine aggregate ratio was 1:4. The mixture proportions for mortar are given in Table 3.6. The binder content, solution to binder ratio, molarity of sodium hydroxide solution and curing temperature are given in Table 3.7.

The binder and the MS were first mixed together in a rotary mixer for about 3 minutes (min). The alkaline liquid was then added to the dry materials followed by water and the mixing was continued for further 4 min to produce the fresh geopolymer mortar as shown in Figure 3.8. The fresh mortar was compacted and the excess mortar removed. The

moulds were covered by plastic film to avoid evaporation of water. For each mortar mixture, twelve (12) 50 mm cube specimens were cast to determine the compressive strength.



Figure 3.8: Preparation of geopolymer mortar

Table 3.6: Mixture proportion of geopolymer mortar (kg/m³)

Mix No.	Binding raw materials					
	GGBS ^a		POFA ^b		FA ^c	
	(%)	Weight (kg/m ³)	(%)	Weight (kg/m ³)	(%)	Weight (kg/m ³)
M1	100	460	0	0	0	0
M2	0	0	100	460	0	0
M3	0	0	0	0	100	460
M4	50	230	50	230	0	0
M5	0	0	50	230	50	230
M6	50	230	0	0	50	230
M7	50	230	25	115	25	115
M8	40	184	60	276	0	0
M9	40	184	30	138	30	138
M10	60	276	40	184	0	0
M11	70	322	30	138	0	0

^a Ground granulated blastfurnace slag

^b Palm oil fuel ash

^c Class F fly ash

Table 3.7: Experimental parameters for geopolymer mortar

Binder : MS	Binder	MS	Activator (1:2.5)		Added water	s/b	w/b	Curing temp. (°C)
			NaOH solution (12 M)	Na ₂ SiO ₃				
	(kg/m ³)					(wt/wt)		
1:4	460	1840	53	131	184	0.4	0.4	65

s/b: Activator solution to binder weight ratio, w/b: water to binder weight ratio

3.6.2 Mix proportions of geopolymer concrete

A total of nine (9) mixes were prepared using variables of three different coarse aggregates (crushed granite, uncrushed and crushed OPS) and fine aggregates (NS, MS and QD) and two different curing conditions – oven and ambient curing. The effect of fine aggregates on the fresh and hardened concrete properties; the comparison between the mechanical properties from the experimental results and code of practice and published results was also performed. A normal weight geopolymer concrete (NWGC) using crushed granite aggregate was prepared as a control mix to compare the mechanical properties of the OPSGC.

The mix proportions and experimental parameters of all the concrete mixes are shown in Table 3.8 and Table 3.9, respectively, while the graphical representation of mix proportions and the casting specimens are presented at Figure 3.9 and Figure 3.10. Initially the coarse and fine aggregates were mixed in the rotary mixer followed by GGBS and POFA for about 5 min. This was followed by the addition of water and alkaline activator and the mixing continued for another 4 min. As the polycarboxylic-based superplasticizer reduces the fluidity of the mixture in geopolymer concrete, free water was added to enhance the workability. The alkaline solution/binder ratio (s/b) of 0.40 was kept constant for all the mixes. The water/binder ratio (w/b) of 0.64 and 0.30 was used

for NWGC and OPSGC, respectively. The material estimation of the mixes are presented in Appendix A.

Table 3.8: Mixture proportion of geopolymer concrete (kg/m³)

Mix	Binder				Fine Aggregate						Coarse Aggregate					
	GGBS		POFA		NS		MS		QD		Granite		OPS (C)		OPS (UC)	
	(%)	Wt.	(%)	Wt.	(%)	Wt.	(%)	Wt.	(%)	Wt.	(%)	Wt.	(%)	Wt.	(%)	Wt.
NWGC with crushed granite																
NWGC-NS	60	132	40	88	100	884	-	-	-	-	100	994	-	-	-	-
NWGC-MS	60	132	40	88	-	-	100	884	-	-	100	994	-	-	-	-
NWGC-QD	60	132	40	88	-	-	-	-	100	884	100	994	-	-	-	-
OPSGC with crushed OPS																
OPSGC-NS-C	60	255	40	170	100	1064	-	-	-	-	-	-	100	255	-	-
OPSGC-MS-C	60	255	40	170	-	-	100	1064	-	-	-	-	100	255	-	-
OPSGC-QD-C	60	255	40	170	-	-	-	-	100	1064	-	-	100	255	-	-
OPSGC with uncrushed OPS																
OPSGC-NS-UC	60	255	40	170	100	1064	-	-	-	-	-	-	-	-	100	255
OPSGC-MS-UC	60	255	40	170	-	-	100	1064	-	-	-	-	-	-	100	255
OPSGC-QD-UC	60	255	40	170	-	-	-	-	100	1064	-	-	-	-	100	255

Table 3.9: Experimental parameters of geopolymer concrete

Label	Binder : Fine aggregate : Coarse aggregate (wt. ratio)	Binder (kg/m ³)	s/b (wt/wt)	Activators (kg/m ³)		w/b (wt/wt)	Added water (kg/m ³)	Curing Temp. (°C)
				NaOH solution (12 M)	Na ₂ SiO ₃ solution			
				(1 : 2.5)				
NWGC	1 : 4 : 4.5	220	0.4	25	63	0.64	141	65
OPSGC	1 : 2.5 : 0.6	425	0.4	49	122	0.30	128	65

NWGC: normal weight geopolymer concrete, OPSGC: oil palm shell geopolymer concrete, s/b: solution to binder weight ratio, w/b: water to binder weight ratio

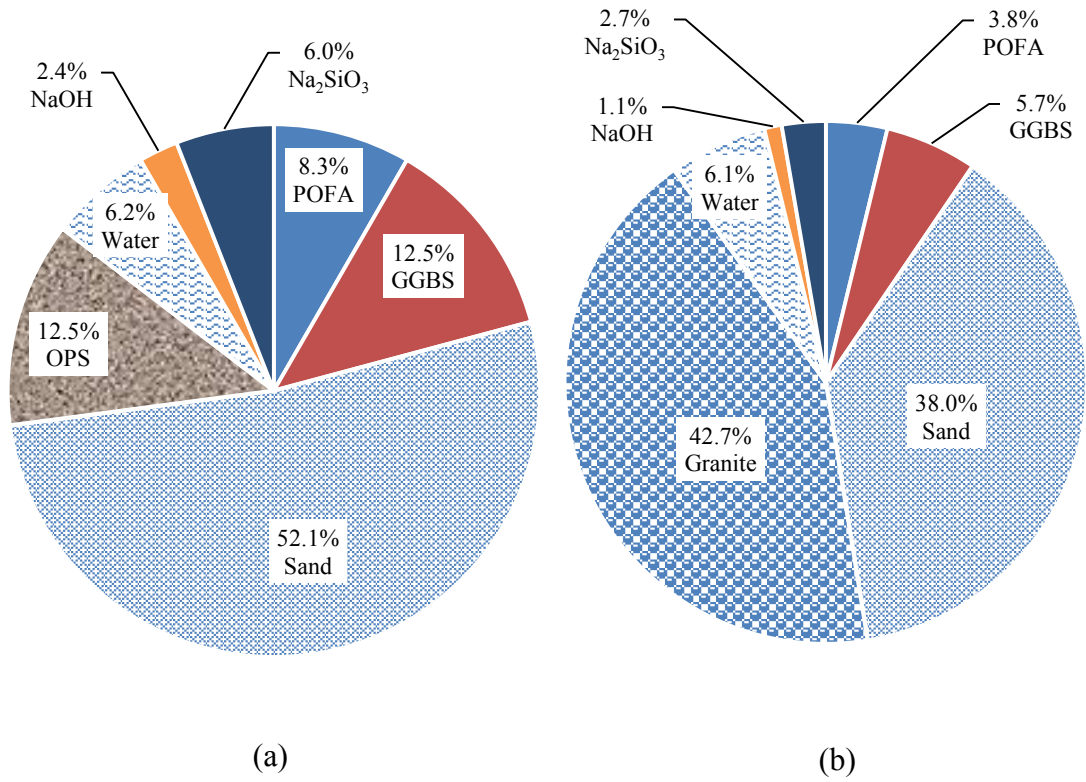


Figure 3.9: Graphical representation of fresh concrete mix ratio by volume (a) OPSGC; (b) NWGC



Figure 3.10: Casting specimens for compressive strength, splitting tensile strength, flexural strength and Young's modulus test

3.6.3 Mix proportions of geopolymer concrete with and without fibre

Another fourteen mixes were prepared using variables of three different OPS as coarse aggregates of which the OPS to binder weight ratio 0.4, 0.6, 0.8 (for OPS both in crushed (C) and uncrushed (UC) condition). In addition, 0.5% of steel fibre added and the effect of varying OPS contents on the fresh and hardened concrete properties; the comparison between the mechanical properties and impact behaviour with and without fibre was also performed. A normal weight geopolymer concrete (NWGC) using crushed granite aggregate was prepared as a control mix to compare the mechanical properties and impact behaviour of the OPSGC.

Table 3.10: Mixture proportion of geopolymer concrete with and without fibre (kg/m³)

No.	Mix	Binder		Fine Aggregate	Coarse Aggregate			Activator	Added water	Steel fibre (%) volume
		GGBS	POFA	MS	OPS (UC)	OPS (C)	Granite			
OPSGC with Uncrushed OPS (UC)										
1	OPSGC4-NF-UC	227	227	1134	181	-	-	204	114	-
2	OPSGC4-F-UC	227	227	1134	181	-	-	204	114	0.5
3	OPSGC6-NF-UC	212	212	1061	255	-	-	191	106	-
4	OPSGC6-F-UC	212	212	1061	255	-	-	191	106	0.5
5	OPSGC8-NF-UC	200	200	998	319	-	-	180	100	-
6	OPSGC8-F-UC	200	200	998	319	-	-	180	100	0.5
OPSGC with crushed OPS (C)										
7	OPSGC4-NF-C	227	227	1134	-	181	-	204	114	-
8	OPSGC4-F-C	227	227	1134	-	181	-	204	114	0.5
9	OPSGC6-NF-C	212	212	1061	-	255	-	191	106	-
10	OPSGC6-F-C	212	212	1061	-	255	-	191	106	0.5
11	OPSGC8-NF-C	200	200	998	-	319	-	180	100	-
12	OPSGC8-F-C	200	200	998	-	319	-	180	100	0.5
NWGC with crushed granite										
13	NWGC-NF	154	154	618	-	-	1235	139	77	-
14	NWGC-F	154	154	618	-	-	1235	139	77	0.5

The mix proportions and experimental parameters are shown in Table 3.10 and Table 3.11, respectively, while the casting specimens and the graphical representation of mix proportions are presented at Figure 3.11 and Figure 3.12, respectively. Initially, the coarse and fine aggregates were mixed in the rotary mixer followed by GGBS and POFA for about 5 min. Those mixes contained fibre, it was added during the mixture of coarse and fine aggregates. This was followed by the alkaline activators and addition of water and the mixing continued for another 4 min. Free water was added to enhance the workability. The alkaline solution to binder ratio (s/b) of 0.45 and water to binder ratio (w/b) of 0.25 was kept constant for all the mixes. The mix designs are presented in Appendix B.

Table 3.11: Experimental parameters of geopolymer concrete with and without fibre

Label	Binder : Fine aggregate : Coarse aggregate (wt. ratio)	Binder (kg/m ³)	s/b (wt/wt)	Activators (kg/m ³)		w/b (wt/wt)	Added water (kg/m ³)
				NaOH solution (12 M)	Na ₂ SiO ₃ solution		
				(1 : 2.5)			
OPSGC	1:2.5:0.4	454	0.45	58	145	0.25	114
	1:2.5:0.6	424		55	137		106
	1:2.5:0.8	400		51	128		100
NWGC	1 : 2 : 4	308		40	100		77



Figure 3.11: Casting specimens for impact test, compressive strength, splitting tensile strength, flexural strength and Young's modulus test

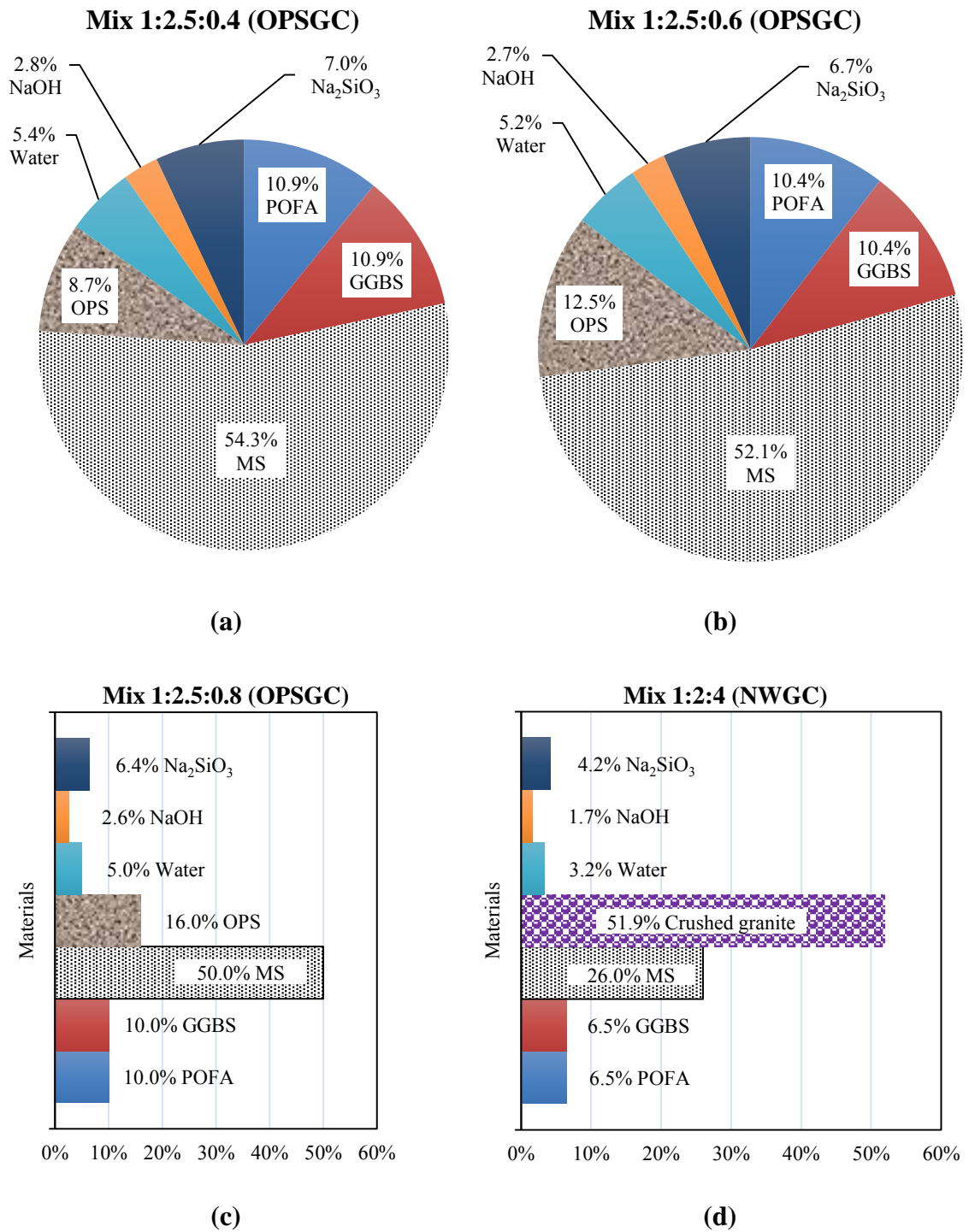


Figure 3.12: Graphical representation of fresh concrete mix ratio by volume (a) 1:2.5:0.4 (OPSGC); (b) 1:2.5:0.6 (OPSGC); (c) 1:2.5:0.8 (OPSGC); and (d) NWGC

3.7 Workability and oven-dry density tests

The workability of fresh concrete was then measured using slump test in accordance with BS EN 12350-2 (2009). The density of concrete was measured based on BS EN 12390-7 (2009).



Figure 3.13: Slump test

3.8 Curing regime

3.8.1 Curing of 50-mm cube specimens for geopolymer mortar

Immediately after casting, the test specimens were covered with plastic film to minimise the water evaporation during curing at an elevated temperature as shown in Figure 3.14. The test specimens were cured in an oven at 65° C for 24 hours. After the curing period, the test specimens were left in the moulds for at least six hours and demoulded. After demoulding, the specimens were left to air-dry condition in the laboratory with the temperature and humidity of 27° C and 70%, respectively until the day of test (Hardjito & Rangan, 2005; Wallah & Rangan, 2006).



Figure 3.14: Test specimens covered with plastic film and specimens in air drying condition

3.8.2 Curing of geopolymer concrete specimens

After casting, the test specimens were covered with plastic sheeting to minimise the evaporation of water. Two types of curing were used in this study, i.e., oven-dry curing and ambient curing. For oven-dry curing, the specimens were first kept in laboratory for about 1 hour and then cured in an oven for 24 h at 65 °C. The specimens were then demoulded and kept in ambient condition till the age of testing. The ambient cured specimens were kept in laboratory at temperature and humidity of 26-29° C and 75-80%, respectively till the age of testing.

3.8.3 Curing of geopolymer concrete with and without fibre

Only ambient curing was adopted. After casting, all the test specimens were kept in laboratory at temperature and humidity of 26–29° C and 75–80%, respectively till the age of testing.

3.9 Specimen moulding and testing

3.9.1 Compressive strength test of mortar

The cubes were tested in compression in accordance with the test procedures given in ASTM:C109/C109M-13 (2013). The compressive strength value was determined as the average of three specimens. The testing machine and the failure mode of the specimens are shown in Figure 3.15.

Compressive strength, $f_c = \text{Failure load } (P) / \text{Loaded area } (A)$



Figure 3.15: Compression testing machine and failure mode of cubes

3.9.2 Mechanical properties tests of geopolymer concrete

The concrete was cast in 100 mm cubes, Ø150 × 300 mm cylinders, Ø100 × 200 mm cylinders and 100 × 100 × 500 mm prisms for testing the compressive strength, modulus of elasticity, splitting tensile strength and flexural strength test, respectively. The compressive strength, modulus of elasticity, splitting tensile strength and flexural strength tests were done in accordance to BS 1881: Part 118, ASTM: C469/C469M, BS EN 12390-6:2009 and BS EN 12390-5:2009, respectively. The cube compressive test was carried

out at 3-, 7- and 28-days, while the modulus of elasticity, splitting tensile strength and flexural strength were tested at the age of 28-day.

3.9.3 Mechanical properties tests of geopolymer concrete with and without fibre

This section is similar to that of the Sec 3.9.2 . The difference is only the incorporation of steel fibre, variation of OPS content to investigate their effectiveness and subsequently material mixing proportion during casting that already described in Section 3.6.3

3.9.4 Ultrasonic pulse velocity (UPV)

Ultrasonic pulse velocity (UPV) test is a non-destructive test of concrete. UPV test is based on the pulse velocity method to provide information on the uniformity of concrete, cavities, cracks and defects. The pulse velocity in a material depends on its density and its elastic properties which in turn are related to the quality and the compressive strength of the concrete. It is easy to use and the results can be quickly obtained on site. The UPV of a homogeneous solid can be easily related to its physical and mechanical properties.



Figure 3.16: Measurement of UPV

3.9.5 Poisson's ratio

The ratio of the lateral strain to the longitudinal strain is called Poisson's ratio. If the lateral and longitudinal strain is Δx and Δy , respectively (Figure 3.17), the Poisson's ratio can be expressed as:

$$\mu = \frac{\Delta x}{\Delta y} \quad (3)$$

where, μ is the Poisson's ratio.

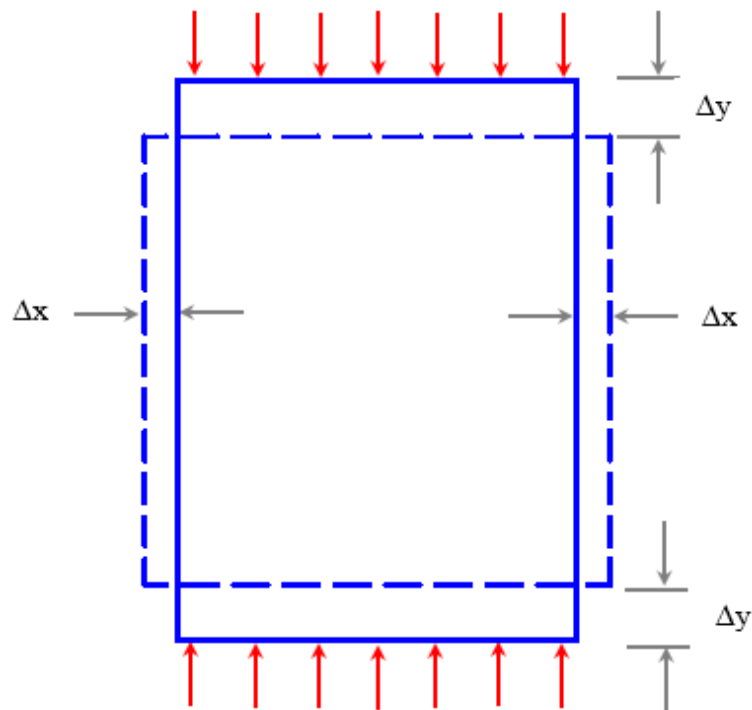


Figure 3.17: Poisson's ratio

3.9.6 Drop hammer impact test of fibre reinforced oil palm shell geopolymer concrete (FROPSGC)

The concrete was cast in $600 \times 600 \times 50$ mm panel for testing the impact resistance with and without fibre. The panels were demoulded after 24 h of casting and left in the

laboratory at temperature and humidity of 26–29 °C and 75–80%, respectively, till the age of testing. The impact capacity of panels were tested at 28-day.



Figure 3.18: Impact test arrangement

The drop hammer impact test was done based on modification of the recommendations by ACI Committee 544 in which an impact specimen is subjected to repeated blows on the same spot. In this modified impact test, a 10 kg drop hammer was released from a height of 300 mm on the panel specimen (Figure 3.18). The number of blows to cause the first visible crack and failure was observed and used to calculate the first crack and failure impact energy of the concrete, respectively. The impact energy is given in the following equation:

$$E_{\text{impact}} = mgh \times N \quad (4)$$

where, E_{impact} = impact energy in Joule (J); m = mass of drop hammer = 10 kg; g = 9.81 m/s²; h = releasing height of drop hammer = 300 mm; N = number of blows.

The ratio of the number of blows to cause failure, N_f to the number of blows to cause the first crack, N_c is defined as impact ductile index, $\mu_i = N_f / N_c$ (Mo et al., 2014b). Crack widths of all the geopolymer panel were measured using a high magnification crack microscope, immediately after the first crack development and during the propagation of cracks to the panel. Figure 3.19 shows the crack width measurement system using magnification microscope.

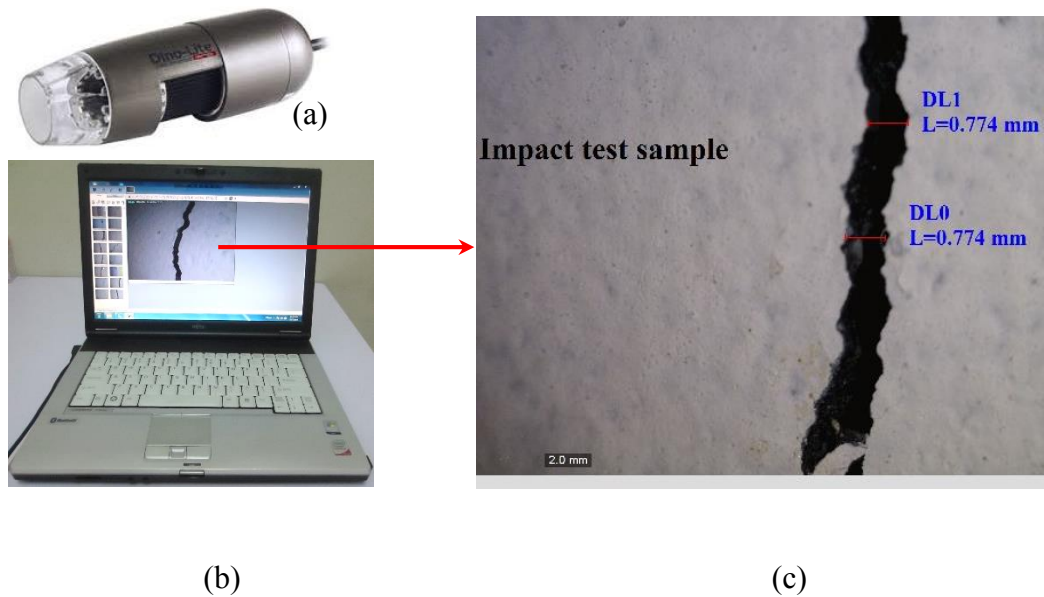


Figure 3.19: Crack width measurement (a) microscope, (b) laptop, and (c) impact test specimen

3.10 Data collection and analysis

From the impact test, a number of data have been collected and analysed for the suitability of new developed concrete on the impact resistance, such as first crack impact energy, ultimate (final) impact energy, failure mode of geopolymer concrete specimens, crack development resistance. Impact resistance of concrete specimens using crushed and uncrushed OPS and the effects of the variation of OPS contents with and without steel fibre have been compared and reported in Section 4.10 .

3.11 Carbon footprint

A carbon footprint is historically defined as “the total sets of greenhouse gas emissions caused by an organization, event, product or person”. A details calculation of carbon footprint is presented in Appendix C.

CHAPTER 4 : RESULTS AND DISCUSSION

4.1 Introduction

The results obtained for all the five objectives are listed and discussed in this chapter; the results include the material characteristics, compressive strength of mortar, mechanical properties of geopolymer concrete, the effect of fibre etc. The effects of materials properties in the development of concrete strength are discussed. The impact behaviour of lightweight concrete incorporating steel fibre and three different proportions of OPS aggregates are also discussed and compared with control mix. In addition, the effect of crushed and uncrushed OPS on the mechanical properties and impact behaviour are discussed and reported.

4.2 Density of the source materials of geopolymer mortar mix

4.2.1 Effect of specific gravity and fineness on the density

Table 4.1 shows the 3-day oven-dry density (ODD) of the specimens. The ODD depends on the specific gravity and fineness of the materials. The mix with 100% GGBS that has higher specific gravity and fineness produced the highest density of 2163 kg/m³ (mix M1). On the contrary, the mix M2 with 100% POFA produced the lowest density of 2014 kg/m³. Another factor that influences the density is the ability of finer particle to fill the voids within the mortar. Figure 3.2 (Chapter 3) shows that POFA has relatively coarser particles within a narrow range compared to that of GGBS and FA. Thus, GGBS with finer particles enhanced its density of about 7.5% compared to mortar with POFA. It was observed that the density of mortar varies between 2014 kg/m³ and 2163 kg/m³. As indicated earlier, in the previous works (Sata et al., 2004; Tangchirapat et al., 2009; Tangchirapat et al., 2012) investigations on the effects of ash particle size on properties

of geopolymer showed that the finer the particle size, the better the properties in terms of strength.

Table 4.1: Average oven-dry density (ODD) (kg/m^3) of geopolymer mortar at 3-day

Mix No.	M1	M2	M3	M4	M5	M6	M7	M8	M9	M10	M11
(kg/m^3)	2163	2014	2020	2116	2021	2135	2121	2107	2112	2157	2159

4.2.2 Density reduction

Figure 4.1 shows the change in density of mortar specimens left in the laboratory at temperature of 26 – 29° C and relative humidity of 75 – 80%. The ODD of the mortar decreased slightly in the order of about 2 percent in the first few weeks but remained almost constant thereafter. Similar finding was reported by Wallah and Rangan (2006).

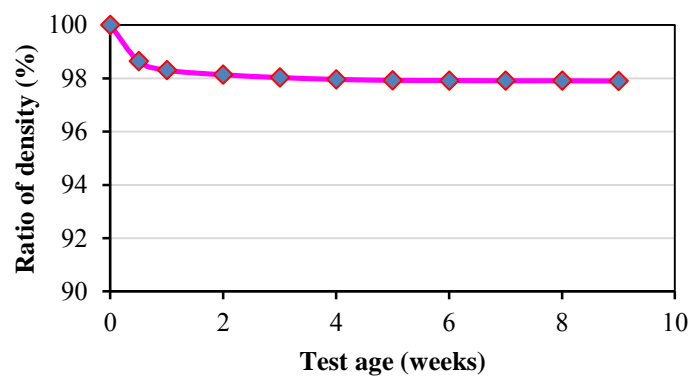


Figure 4.1: Reduction in density of mortar specimen

4.3 Development of compressive strength in geopolymer mortar

The development of compressive strength at 3-, 7-, 14- and 28-days are shown in Figure 4.2. It can be observed from Figure 4.2 that the mixture M3 that contains 100% FA and cured at 65 °C for 24 h produced the lowest compressive strength. Bakharev (2006)

reported that alkali activated cementitious pastes prepared using Class F fly ash (FA) produced higher initial compressive strength for specimens cured at 100 °C compared to specimens cured at 80 °C. The mixes in this investigation were cured at 65 °C that contained Class F FA, GGBS and POFA. Hence, the reduction in the curing temperature allowed the mixes with high Ca content able to achieve the desired strength. It is also reported that long pre-curing at room temperature is beneficial for strength development of geopolymeric materials utilising FA; while curing at elevated temperature allows shortening the time of heat treatment to achieve high strength (Bakharev, 2005b). For materials utilising FA activated by sodium silicate, 6 h heat curing is more beneficial for the strength development than 24 h heat treatment (Bakharev, 2005b). The curing at 65 °C for 24 h was chosen in this investigation for practical reasons even though the effect of short curing period is beneficial for FA based geopolymer mortars. The mixture M2 contained 100% POFA and when it was mixed with GGBS, the strength was increased significantly. This might be attributed to the packing ability of finer particles. On the contrary, the mixture M1 and M11 produced higher compressive strength which contained higher Ca and Al₂O₃. POFA contained very less Al₂O₃ and Ca but when it was mixed with GGBS, the compressive strength increased. So it is observed that Ca and Al₂O₃ influenced the compressive strength of the mortar (Khale & Chaudhary, 2007; Li et al., 2010). The average compressive strength and standard deviation are given in Table 4.2. Wongpa et al. (2010) reported that higher solution to binder ratios (s/b) and higher paste to aggregate (P/Agg) ratios result in lower compressive strength and higher water permeability.

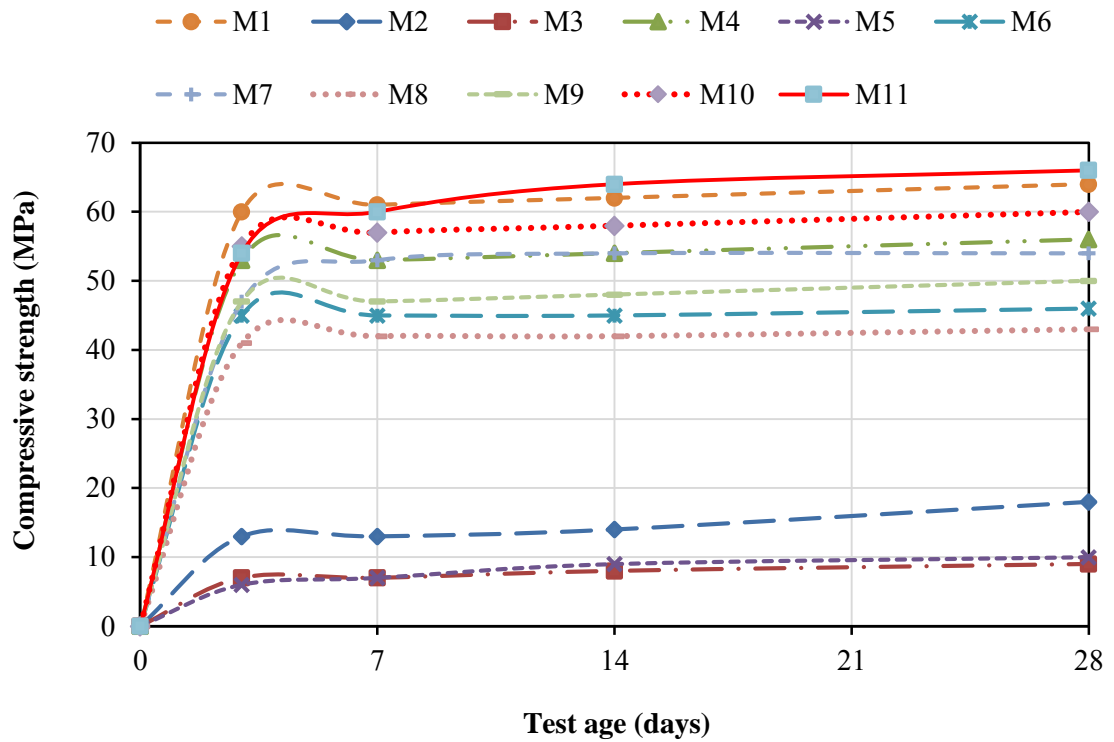


Figure 4.2: Development of compressive strength of mortar with varying binder content ratio

Table 4.2: Development of the compressive strength (MPa) and standard deviation of 3 mortar cubes at different ages

Label	M1	M2	M3	M4	M5	M6	M7	M8	M9	M10	M11
3-day	60 (1.45)	13 (0.125)	7 (1.03)	53 (2.4)	6 (0.38)	45 (1.18)	47 (0.05)	41 (1.76)	47 (4.03)	55 (8.7)	54 (1.62)
7-day	61 (1.3)	13 (2.05)	7 (0.95)	53 (0.56)	7 (0.43)	45 (1.3)	53 (1.76)	42 (1.3)	47 (0.73)	57 (1.26)	60 (0.39)
14-day	62 (1.26)	14 (0.73)	8 (0.26)	54 (0.5)	9 (0.29)	45 (1.26)	54 (1.46)	42 (1.83)	48 (2.19)	58 (2.19)	64 (0.12)
28-day	64 (0.39)	18 (0.05)	9 (0.54)	56 (1.3)	10 (0.48)	46 (0.4)	54 (0.4)	43 (0.73)	50 (0.58)	60 (1.45)	66 (0.5)

Note: () The data in parentheses are the standard deviation of the corresponding compressive strength

Table 4.3 shows the increase in the compressive strength between 3 and 28 days expressed as a percentage. The 28-day compressive strength was taken as the reference and the 3-, 7-, and 14-days and the ratio of increase in the strength was calculated. Most of the

specimen achieved 86% of the 28-day strength at 3-day. Similarly the 7-day and 14-day strength were 90% and 94%, respectively of the 28-day strength.

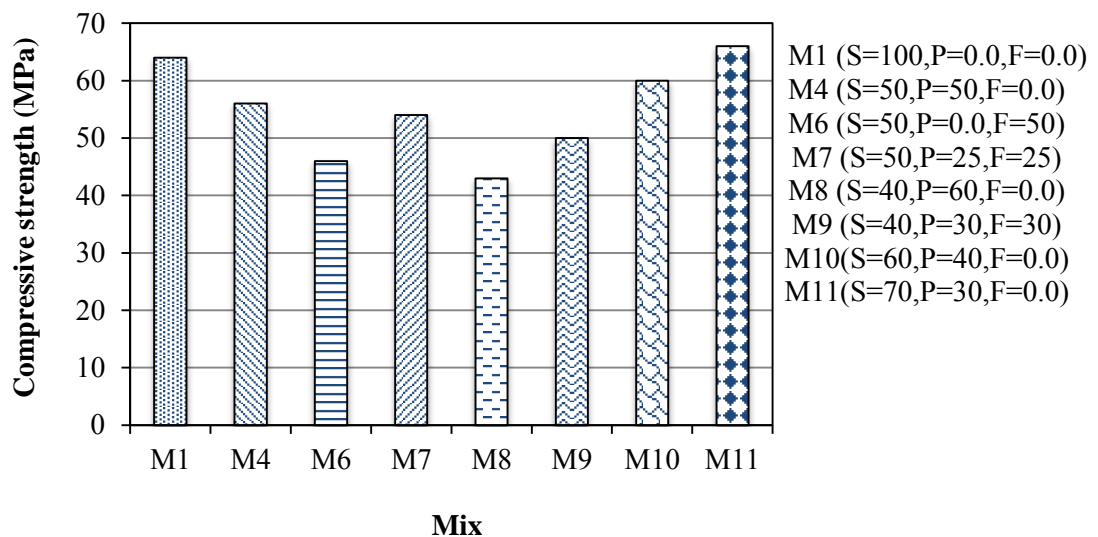
Table 4.3: The comparison of increase in the compressive strength (%) with respect to that of 28 days

Test age (day)	M1	M2	M3	M4	M5	M6	M7	M8	M9	M10	M11
3	94	72	78	95	60	98	87	95	94	92	82
7	95	72	78	95	70	98	98	98	94	95	91
14	97	78	89	96	90	98	100	98	96	97	97

4.4 Effect of GGBS on the compressive strength of the mortar

The ground blast furnace slag employed is a latent hydraulic product, which can be activated by suitable activators. Without an activation, the development of the strength of the GGBS is extremely slow and the development of the slag necessitates a $\text{pH} \geq 12$ (Davidovits, 2011). GGBS plays an important role in the development of the compressive strength. Higher concentrations of GGBS (slag) result in higher compressive strength of geopolymer concrete (Naidu et al., 2012). Figure 4.3 shows that the compressive strength of mortar with 70% of GGBS (mix no. M11) produced the highest strength while further increase in the GGBS content (mix no. M1) reduces the compressive strength. The mixture M1 contains 100% GGBS while the mix M11 contains 70% GGBS and 30% POFA. A comparison between the mixes M1 and M11 shows that the former with 100% GGBS produces 3% lower compressive strength compared to the mix with 70% GGBS and 30% POFA. The mixes M10, M4 and M8 show that the reduction of GGBS contents of 10%, 20% and 30%, respectively and the remainder is replaced by POFA. Thus, the effect of GGBS replacement with POFA shows that the mixes M10, M4 and M8 with

high content of POFA produced lower strength of about 9%, 15%, 35%, respectively compared to the mix M11 (with 70% GGBS and 30% POFA). The effect of POFA in enhancing the compressive strength can be seen from Figure 4.3 as the mix M4 (50% GGBS and 50% POFA) produced 22% higher strength than the mix M6 (50% GGBS and 50% FA). Further comparison between the mixes M6 and M7 (50% GGBS, 25% POFA and 25% FA) shows an increase of about 17% for the latter. As explained earlier that GGBS has finer particles compared to POFA and its contribution in the strength development cannot be ignored. However, further tests are required to validate the compactness of the structure within the mortar.



Legend: S – Slag (GGBS), P – POFA, F – Fly ash and mix compositions are shown in bracket in percentage (%)

Figure 4.3: The effect of GGBS on the compressive strength of mortar mixed with POFA and FA at 28-day

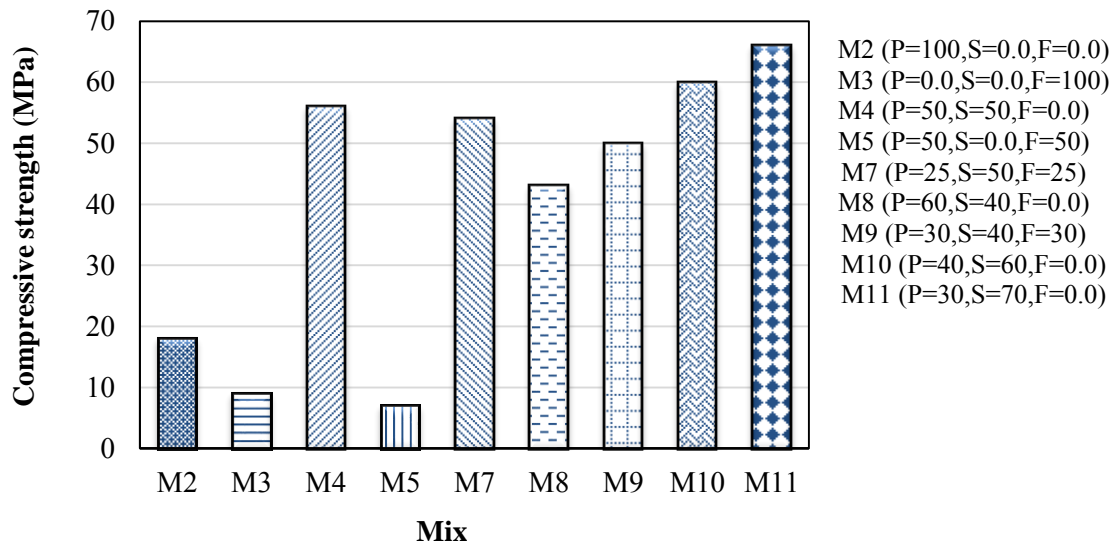
Naidu et al. (2012) reported that the compressive strength of geopolymer concrete increases with increase in percentage of replacement of fly-ash with GGBS and 90% of

the compressive strength was achieved in 14 days and from this investigation most of the mortar specimens achieved it in 7 days.

Shafiqh et al. (2013b) used lightweight concrete with high volume of GGBS and reported that 30% of cement replacement by GGBS increased the workability of OPS concrete. However, they reported further increase in GGBS content decreased the workability. They also reported that by introducing initial heating at 60 °C for 20 h after demoulding, it is possible to improve the compressive strength of GGBS OPS concrete at early ages.

4.5 Effect of POFA on the compressive strength of the mortar

Figure 4.4 shows the effect of POFA content on the compressive strength at 28-day. The compressive strength of the mixes M2 and M3 that contain 100% POFA and 100% FA, respectively shows that the latter produced about 50% lower compressive strength than the mix M2. As seen from the Figure 4.4, increase beyond 30% in POFA content decreases the strength. Safiuddin et al. (2011) reported that a POFA content higher than 40% may adversely affect the properties and durability of concrete which was reflected in the geopolymer mortar as well. The mix M11 with 30% of POFA and 70% of GGBS produced the highest strength of 66 MPa. The coarser particles of the POFA with cohesive characteristic could not be mixed properly and hence the strength development was poor. The ground POFA with high fineness ($d_{50} = 10.1 \mu\text{m}$) is a reactive pozzolanic material and can be used to produce high-strength concrete. The suggested level of POFA content as cement replacement in normal concrete was 20% to produce high-strength concrete (Sata et al., 2004; Kroehong et al., 2011).



Legend: S – Slag (GGBS), P – POFA, F – Fly ash and mix compositions are shown in bracket in percentage (%)

Figure 4.4: The effect of POFA on the compressive strength of mortar mixed with GGBS and FA at 28-day

4.6 Analysis of chemical composition

The rate of polymerization is influenced by parameters such as curing temperature, water content, alkali concentration, initial solids content, silicate and aluminate ratio, pH and the type of activators used. Khale and Chaudhary (2007) reported in their review that certain synthesis limits existed in the formation of strong geopolymer products (Table 4.4) but the ratio changes while working with the waste.

Table 4.4: Oxide-mole ratios of the reactant mixture (Khale & Chaudhary, 2007; Davidovits, 2011)

Composition	M_2O/SiO_2	SiO_2/Al_2O_3	H_2O/M_2O	M_2O/Al_2O_3
Range	0.2 to 0.48	3.3 to 4.5	10 to 25	0.8 to 1.6

where, M_2O represents either Na_2O , or K_2O , or the mixture (Na_2O, K_2O).

Table 4.5 and Figure 4.5 represent the major oxide composition of the three materials i.e., GGBS, POFA and FA. The mixes M1 and M11 achieved higher strength and the mix M3 achieved the lowest strength compared to other mixes. However, the mix M11 produced slightly higher strength than the mix M1. It can be seen in Table 4.5 and Figure 4.5, the mix M1 contains more lime (CaO) than the mix M11. Nevertheless, the SiO₂ content in the mix M11 is slightly higher than the M1 and the ratio of SiO₂/Al₂O₃ of M11 is 3.7 (Table 4.6) which compiled those tabulated in Table 4.4. On the contrary, this ratio (SiO₂/Al₂O₃) for M1 is 2.37 and for M3 is 2.01. The lowest compressive strength of mix M3 that contains 100% FA might be attributed to the lowest SiO₂/Al₂O₃ ratio of 2.01 as seen from Table 4.6. Lime (CaO) plays a very important role. It controls strength and soundness but any excess in the lime content makes the material unsound and causes expansion and disintegration. Excessive quantity of lime (CaO) is the essence of the hardening mechanism of mortar (Davidovits, 2011). It has been reported that the formation of Ca compounds in geopolymers is greatly dependent on the pH and Si/Al ratio (Yip et al., 2005). The SiO₂ content provides greater strength but at the same time it prolongs its setting time though mix M2 contains the maximum percentages (%) of SiO₂ among all the mixes but the silicate and aluminate ratio is very high (11.4). Also M2 contains higher percentages of K₂O and MgO which are harmful ingredients in cement. If the amount of Na₂O and K₂O exceeds 1%, it leads to the failure of concrete and if the content of MgO exceeds 5%, it causes cracks in the hardened concrete.

Table 4.5: Major chemical composition of mortar and 28-day compressive strength

Mix No.	CaO	SiO ₂	Al ₂ O ₃	MgO	Fe ₂ O ₃	Na ₂ O	K ₂ O	28-d Comp. Strength (MPa)
M1	45.83	32.52	13.71	3.27	0.76	0.25	0.48	64
M2	4.34	63.41	5.55	3.74	4.19	0.16	6.33	18
M3	5.31	54.72	27.28	1.10	5.15	0.43	1.00	9
M4	25.09	47.97	9.63	3.51	2.48	0.21	3.41	56
M5	4.83	59.07	16.42	2.42	4.67	0.30	3.67	10
M6	25.57	43.62	20.50	2.19	2.96	0.34	0.74	46
M7	25.33	45.79	15.06	2.85	2.72	0.27	2.07	54
M8	20.94	51.05	8.81	3.55	2.82	0.20	3.99	43
M9	21.23	48.447	15.333	2.76	3.11	0.28	2.39	50
M10	29.23	44.88	10.45	3.46	2.13	0.21	2.82	60
M11	33.38	41.79	11.26	3.41	1.79	0.22	2.24	66

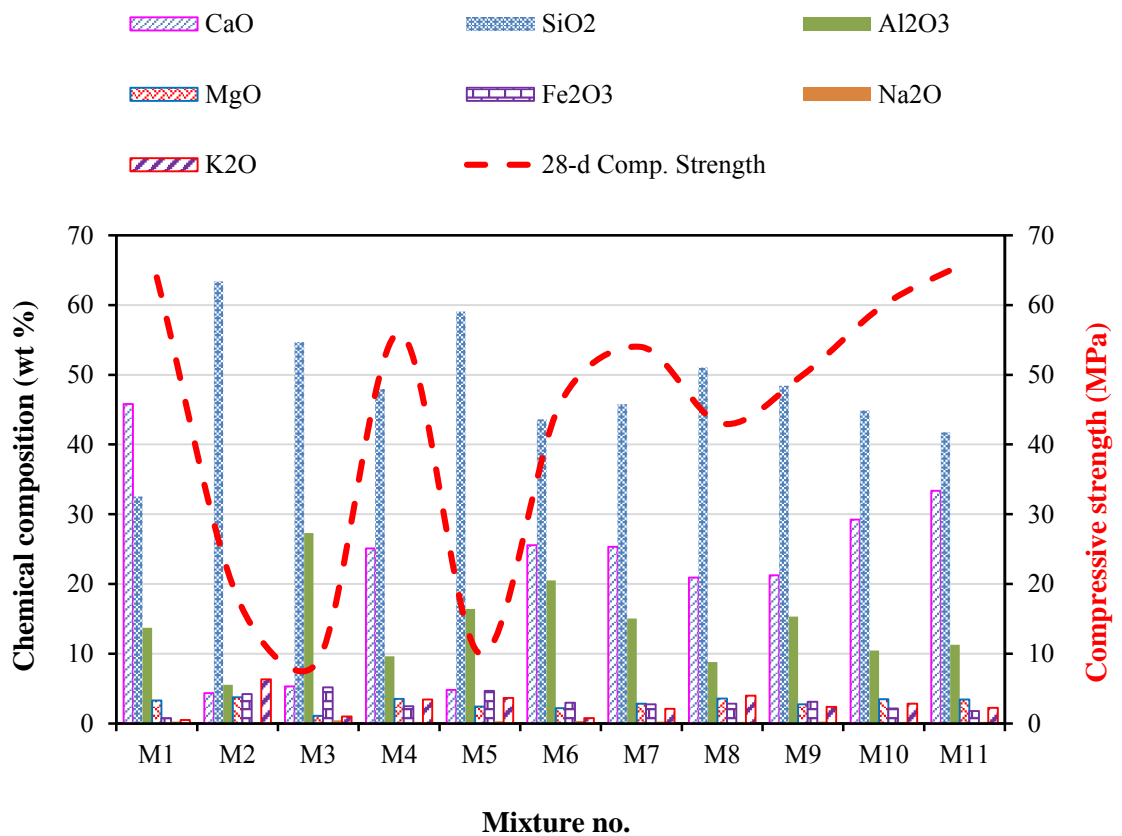


Figure 4.5: The comparison between major chemical composition and compressive strength of mortar

Table 4.6: SiO₂/Al₂O₃ and CaO/Al₂O₃ ratios of mortar mixes

Mix No.	M1	M2	M3	M4	M5	M6	M7	M8	M9	M10	M11
SiO ₂ /Al ₂ O ₃	2.37	11.43	2.01	4.98	3.60	2.13	3.04	5.79	3.16	4.29	3.71
CaO/ Al ₂ O ₃	3.34	0.78	0.19	2.60	0.29	1.25	1.68	2.38	1.38	2.80	2.96

4.7 Properties of geopolymer concrete with OPS as coarse aggregate

The following sections describe the fresh and hardened concrete properties of POFA-GGBS based geopolymer concrete developed using OPS as coarse aggregate. The OPS used had two forms, namely crushed and uncrushed; the sizes of crushed and uncrushed OPS varied in the range of 5-10 mm and 5-14 mm, respectively.

4.7.1 Workability

The workability of the concrete measured using the slump test shows the values of 5 to 12 mm and 50 to 63 mm, respectively, for NWGC and OPSGC (Table 4.9). The solution to binder ratio was kept constant at 0.4 for all mixes; the water/binder ratios were 0.64 and 0.30 for NWGC and OPSGC, respectively (Table 3.9). The mixes using fine aggregate as quarry dust (QD) produced slightly lower workability compared to the mixes with conventional mining sand and MS, which might be attributed to the angular edges of the aggregate, coarser particle size, high silt and dust content in the QD (Raman et al., 2011). The setting of NWGC was found to be faster compared to OPSGC, which could be attributed to the dry condition of NWA. It should be noted that the OPS was pre-soaked for about 24 h in water before use and the workability of the OPSGC mixes was found to be medium (Neville, 1995). Although most of the mixes did not produce high workability, the cohesive concrete mixes achieved sufficient compaction upon vibration using vibration table. The smooth surface of the OPS aggregate also enhanced the workability

compared to the conventional coarse aggregate, as reported in previous studies (Basri et al., 1999; Shafiqh et al., 2013b). It is important to note that the workability test using a slump cone for the sticky and cohesive geopolymer concrete might not be an appropriate test. Thus, it can be concluded that the slump values do not reflect the actual workability for the cohesive geopolymer concrete, and that suitable workability tests as designed for self-compacting concrete (SCC) have to be designed and used.

4.7.2 Density

Table 4.9 shows the test results for the 24 h oven dry density (ODD) for all mixes from which it can be seen that the OPSGC produced a density in the range of 1900–1935 kg/m³. EN 206-1 (2000) defines lightweight concrete (LWC) as concrete having an oven-dry density (ODD) of not less than 800 kg/m³ and not more than 2000 kg/m³ that is produced using lightweight aggregate for all or part of the total aggregate. As seen in Table 4.9, all the OPS concrete in this investigation produced ODD of less than 2000 kg/m³ and thus could be categorized as LWC.

4.8 Mechanical properties of geopolymer concrete

4.8.1 Development of compressive strength in geopolymer concrete

4.8.1.1 Development of compressive strength between 3 and 28-day

Table 4.9 shows the compressive strength developed between 3 and 28 days expressed as a percentage. The 28-day compressive strength was taken as the reference and the ratios achieved in the strength for 3 and 7 days were calculated. The 3-day compressive strength of 35, 30 and 28 MPa were obtained for NWGC-NS, OPSGC-NS-C & OPSGC-NS-UC,

respectively, which developed 92, 94 and 93% of the 28-day strength, as shown in Table 4.9. Most of the specimens achieved 90% of the 28-day strength at the age of 3 days for OD curing, while the AD curing specimens achieved 57–82%; however, the final strength of the AD curing specimens were found to be slightly higher than the corresponding OD cured specimens at 28 days. The 7-day compressive strength of geopolymer concrete (GC) reached 92–100% and 81–97% of the 28-day compressive strength, respectively, for OD and AD curing.

Table 4.7: Chemical composition of binder based on 60% of GGBS and 40% of POFA

Label	CaO	SiO ₂	Al ₂ O ₃	MgO	Na ₂ O	SO ₃	P ₂ O ₅	K ₂ O	TiO ₂	MnO	Fe ₂ O ₃	SrO	Cl	CuO	LOI
Binder (GGBS & POFA)	29.23	44.88	10.45	3.46	0.21	1.44	1.54	2.82	0.57	0.28	2.13	0.06	0.19	2.62	2.84

Table 4.7 shows the chemical composition of binder based on 60% of GGBS and 40% of POFA and the additional composition of Na₂O, SiO₂ and H₂O from the activator solution and the additional water are as follows (based on solution to binder mass ratio (s/b) and water to binder mass ratio (w/b) are 0.40 and 0.3, respectively, and NaOH solution of 12M):

Na₂O= 3.43%, SiO₂=8.57%, and H₂O = 53.59% by mass.

For the formation of early high-strength polysialate geopolymers, the oxide-mole ratios proposed by Davidovits (2011) and the experimental mixes (based on the binder, activator solution and added water contents) is shown in Table 4.8.

Table 4.8: Comparison of oxide-mole ratio proposed by Davidovits (2011) and those obtained from experimental

Oxide-mole ratio	Proposed by Davidovits (2011)	Experimental (for OPSGC)
M_2O/SiO_2	0.21 to 0.36	0.12
SiO_2/Al_2O_3	3.00 to 4.12	5.11
H_2O/M_2O	12 to 20	8.3
M_2O/Al_2O_3	0.60 to 1.36	0.62

where, M_2O represents either Na_2O , or K_2O , or the mixture (Na_2O , K_2O).

The molar ratios proposed by Davidovits (2011) are for the formation of high strength concrete while the experimental molar ratios in this research are based on the 30 grade concrete, and, hence, the ratios of H_2O/M_2O M_2O/SiO_2 fall short of the proposed values by Davidovits (2011) (Table 4.8). Hardjito and Rangan (2005) reported that, as the H_2O/Na_2O molar ratio increases, the compressive strength of geopolymer concrete decreases. The high early strength might be attributed to the addition of GGBS in the presence of alkalis as it could generate more heat due to the calcium and alumina contents, as was reported in earlier studies (Bakharev et al., 1999). During mixing, the Ca^{++} reacts with OH^- in the alkaline aqueous system to form $Ca(OH)_2$, which then reacts with CO_2 in the atmosphere, forming calcite, $CaCO_3$. At the same time, the dissolution of alumina-silica precursor continues to take place. In essence, these reactions produce the high early strength as reported in earlier studies (Davidovits, 2011). Based on the scanning electron microscopy image (SEM) analysis, it is reported that a high volume of GGBS (50% replacement by cement) produces more ettringite ($CaO.Al_2O_3.3SO_3.32H_2O$) at an early age, which results in the higher early strength (Razak & Sajedi, 2011).

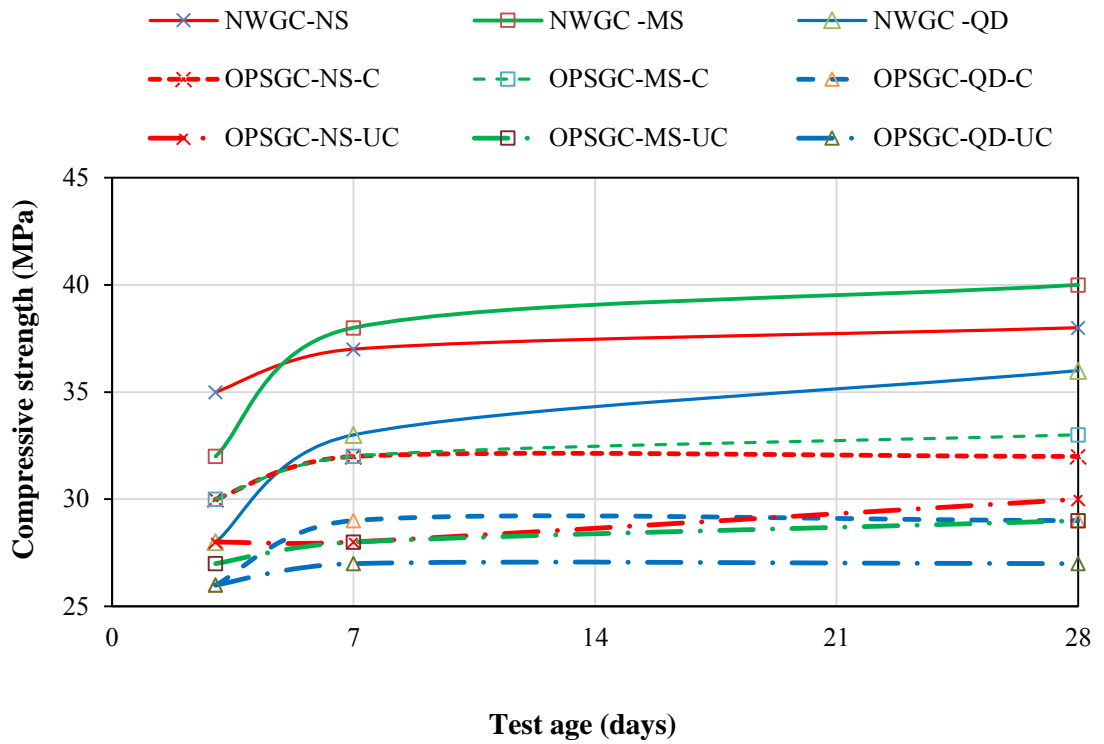


Figure 4.6: Development of compressive strength at initial 24 h oven-dry curing

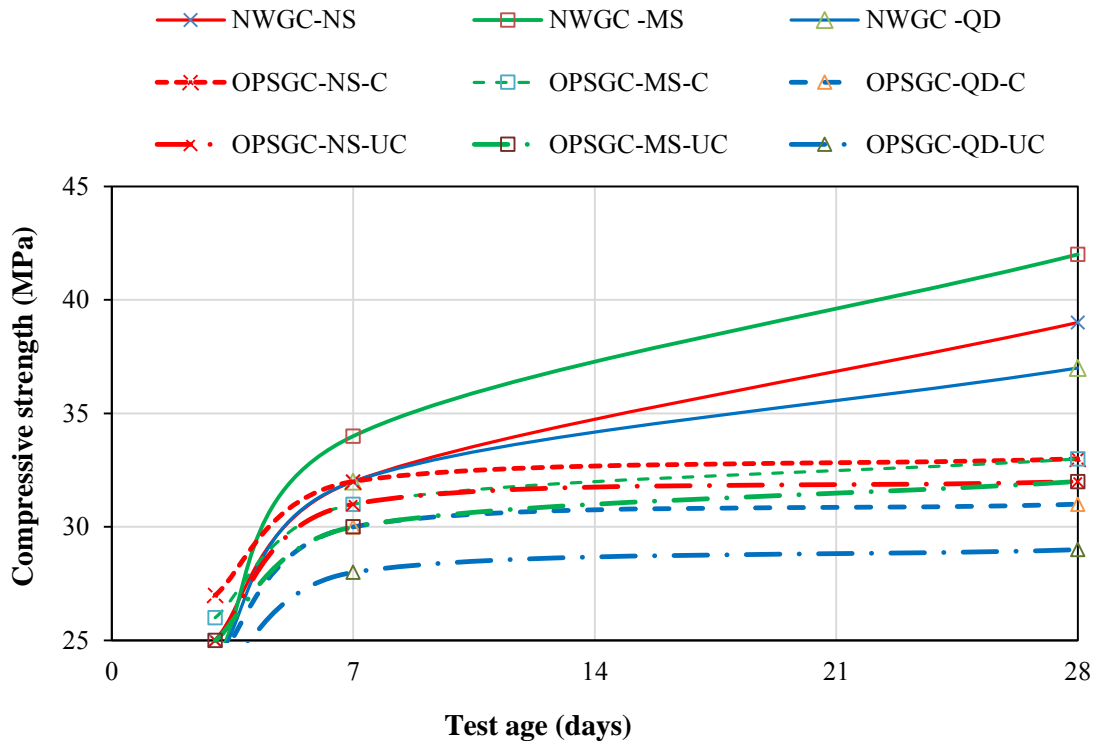


Figure 4.7: Development of compressive strength at ambient curing

The development of the compressive strength between 7 and 28 days seems to be lower compared to that between 3 and 7 days, as shown in Figure 4.6 and Figure 4.7. This could be attributed to the geopolymerisation that happens at the early age (Puligilla & Mondal, 2013; Yusuf et al., 2014a). The rate of development of strength between 7 and 28 days for NWGC was found to be higher compared to that of OPSGC (NWGC: 2 to 9% for OD curing and 15 to 21% for AD curing; OPSGC: 0 to 7% for OD curing and 3 to 7% for AD curing). This could be due to the stronger bond between the NWA and the matrix. In contrast, the convex surface of the OPS leads to a poor bond that reduces the compressive strength (Alengaram et al., 2011).

4.8.1.2 Failure modes of cube

This sub-section explain the failure mode of concrete cubes as specified in standard code (BS EN 12390-3, 2009) and the experimental specimens.

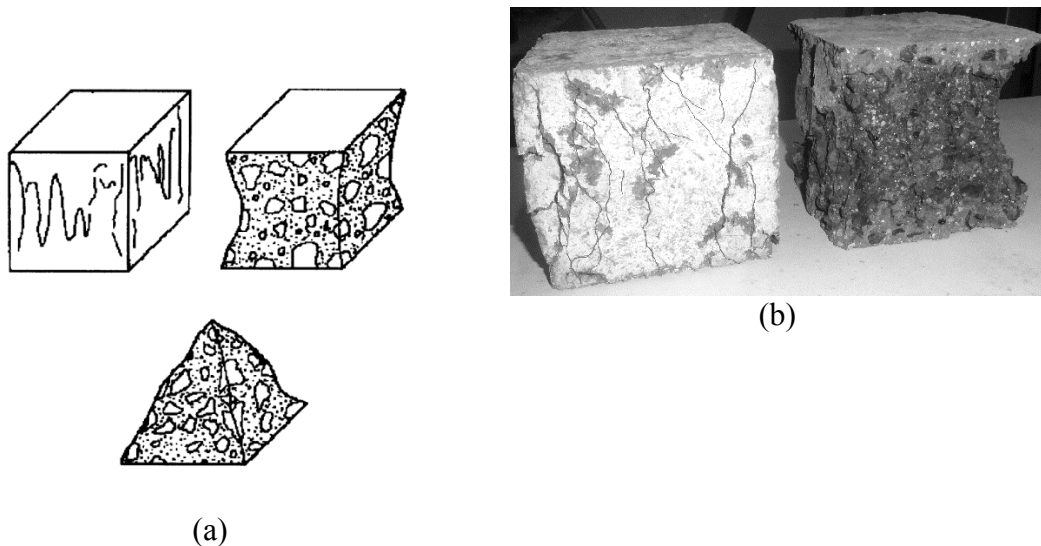


Figure 4.8: Failure mode of 100-mm cube (a) satisfactory failure (BS EN 12390-3, 2009); and (b) experimental specimen failure

The satisfactory failure mode(s) of 100-mm cube as specified in (BS EN 12390-3, 2009) and the experimental 100-mm cube specimens are shown in Figure 4.8a and 4.6b, respectively. As can be seen in Figure 4.8b, all four exposed faces failed similar to that of shown in the BS EN 12390-3.

4.8.1.3 Effect of curing conditions on the compressive strength

The 3-, 7-, and 28-day compressive strength of the ambient and oven-cured concrete specimen mixes are shown in Table 4.9. As can be seen in Table 4.9, the compressive strength of the oven-cured mixes at early ages of 3 and 7 days were found to be higher than the corresponding specimens cured in ambient conditions. However, the 28-day strength of the ambient cured specimens was found to be slightly higher than that of the oven-cured specimens (Table 4.9 & Figure 4.9). The increase of the ambient cured specimens was found to be between 3 and 10%. Davidovits (2011) opined that the slag based geopolymer mortar cured under heat and non-heat conditions achieves similar strength at a later age of 28 days compared to the early 3- and 7-day strength. Geopolymerisation starts with the depolymerisation (break down, cleavage of Si-O-Si-O- and others in the aluminosilicate structures of the raw materials: slag (mellilite) or metakaolin). This step requires energy (heat) or time (at room temperature). However, ultimately, the chemical mechanism remains the same.

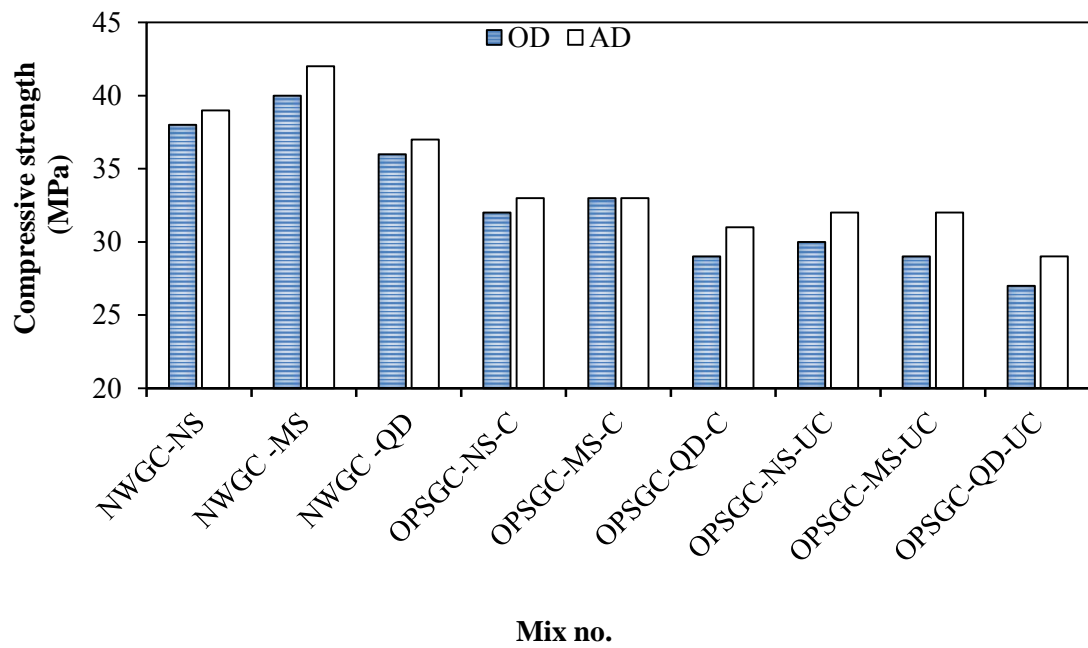


Figure 4.9: Compressive strength at 28 days of age of geopolymer concrete subjected to initial 24 h OD in relative to those of AD curing

The difference in the increase of the compressive strength of the specimens cured in OD and AD conditions shows 2.63–5.0% for NWGC. However, for OPSGC with crushed and uncrushed OPS it was found to be in the range of 0–6.90% and 6.70–10%, respectively (Table 4.9).

Table 4.9: Workability, oven-dry density (ODD) and compressive strength of NWGC and OPSGC

Mix no.	Slump (mm)	24 h ODD (kg/m ³)	Mean compressive strength (MPa) ^a						% higher ^b at 28-day
			Initial 24 h oven-dry curing (OD)			Ambient-curing (AD)			
			3-d	7-d	28-d	3-d	7-d	28-d	
NWGC									
NWGC-NS	10	2366	35 (92)	37 (97)	38	25 (64)	32 (82)	39	2.63
NWGC -MS	12	2323	32 (80)	38 (95)	40	24 (57)	34 (81)	42	5.00
NWGC -QD	5	2358	28 (78)	33 (92)	36	24 (65)	32 (86)	37	2.78
OPSGC with crushed OPS									
OPSGC-NS-C	58	1935	30 (94)	32 (100)	32	27 (82)	32 (97)	33	3.13
OPSGC-MS-C	60	1918	30 (91)	32 (97)	33	26 (79)	31 (94)	33	0.00
OPSGC-QD-C	50	1928	26 (90)	29 (100)	29	24 (77)	30 (97)	31	6.90
OPSGC with uncrushed OPS									
OPSGC-NS-UC	60	1915	28 (93)	28 (93)	30	25 (78)	31 (97)	32	6.67
OPSGC-MS-UC	63	1900	27 (93)	28 (97)	29	25 (78)	30 (94)	32	10.34
OPSGC-QD-UC	55	1909	26 (96)	27 (100)	27	23 (79)	28 (97)	29	7.41

^a () The data in parentheses are percentages of 28-day compressive strength.

^b % of compressive strength higher at 28-day cured in AD compared to OD condition.

Based on the compressive strength development of both the OD and AD of the OPSGC, it can be concluded that the AD cured specimens produce nearly 95% of the 28-day strength in 7 days and is preferred over the OD specimens. This also reduces the energy required for the elevated temperature in oven curing and thus reduces the cost.

4.8.1.4 Effect of three types of fine aggregates on the compressive strength

Table 4.9 shows the compressive strength development for the mixes with three different types of fine aggregate, namely, conventional mining sand (NS) as control, MS and QD. The 28-day compressive strength of the control mixes NWGC-NS, OPSGC-NS-C and

OPSGC-NS-UC, which were prepared using conventional mining sand and initially 24 h cured in the oven were 38, 32, 30 MPa, respectively. In contrast, the compressive strength of the mixes NWGC-MS, OPSGC-MS-C and OPSGC-MS-UC prepared using MS were 40, 33 and 29 MPa, respectively, which were comparable to the control mixes. Similar findings are shown in the case of AD curing (Table 4.9). All the mixes (NWGC-QD, OPSGC-QD-C and OPSGC-QD-UC) with QD produced a slightly lower strength compared to the other mixes with mining sand. Reddy (2012) investigated both in mortar and concrete specimens using NS and MS, and found that the specimens prepared using MS had higher strength. The slight difference among the mixes with three different fine aggregate shows that MS could be considered to be an ideal replacement for the conventional sand. However, QD with angular and flaky particles, could lead to a reduction in compressive strength and workability (Lohani et al., 2012).

Raman et al. (2011) reported that the compressive strength of self-compacting concrete (SCC) slightly decreased after 20% replacement of QD due to the non-uniform grading of QD and also due to the large amount of fine particles smaller than 150 μ m and 300 μ m sieve sizes in QD. Thus, the use of MS could be more appropriate as a replacement material for conventional mining sand.

4.8.1.5 Relationship between 28-day compressive strength of NWGC and OPSGC under AD and OD curing conditions

Figure 4.10 shows a linear relationship between the compressive strength of the specimens cured under oven and ambient curing; the trend line shows a strong correlation between those two curing regimes.

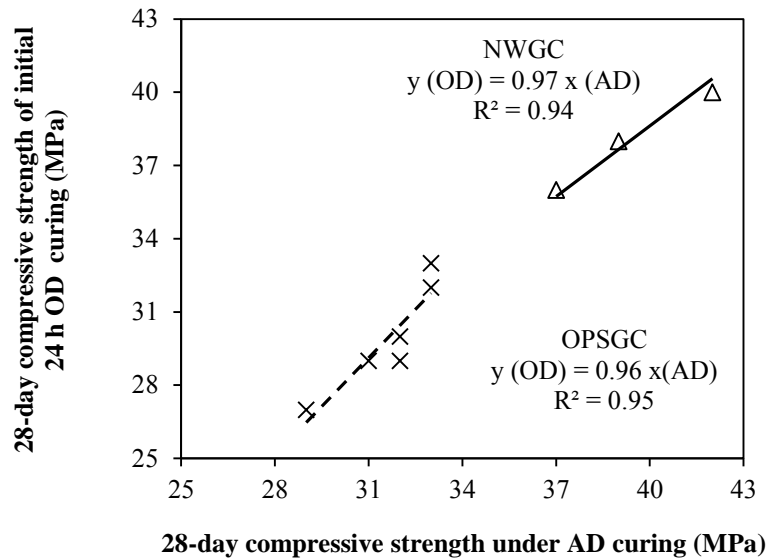


Figure 4.10: Relationship between 28-day compressive strength of NWGC and OPSGC under AD and OD curing conditions

Based on the experimental results the following equations could be obtained to relate the compressive strength of the specimens cured under two different regimes:

NWGC,

$$y_{(OD)} = 0.9656 x_{(AD)} \quad R^2 = 0.94 \quad (5)$$

OPSGC,

$$y_{(OD)} = 0.9557 x_{(AD)} \quad R^2 = 0.95 \quad (6)$$

Atiş and Bilim (2007) proposed the following equations for normal Portland cement (NPC) concrete and GGBS concrete.

NPC concrete:

$$y_{(dry)} = 0.94 x_{(wet)} \quad R^2 = 0.87 \quad (7)$$

GGBS concrete (up to 80% replacement of cement):

$$y_{(dry)} = 0.85 x_{(wet)} \quad R^2 = 0.89 \quad (8)$$

Shafigh et al. (2013a) reported the following relationship between OPS concrete containing GGBS up to 50% replacement of cement under two different curing conditions (air-dry and wet curing):

$$y_{(dry)} = 0.80 x_{(wet)} \quad R^2 = 0.94 \quad (9)$$

A similar type of equation proposed by Shafigh et al. (2013a) shows a good correlation could be established between the compressive strength of specimens cured under two different environments. The following equation proposed to predict the compressive strength for OPS concrete containing fly ash up to 50% replacement of cement:

$$f'c_{(dry)} = 0.81 f'c_{(wet)} \quad R^2 = 0.93 \quad (10)$$

Based on the above equations for two different lightweight concretes of OPSGC and OPSC, the relationship between the oven and air cured specimens of OPSGC shows a stronger relationship compared to the air and wet curing. This could be attributed to the geopolymerization of the specimens cured in oven and ambient conditions. For OPSC, the compressive strength depends on the hydration of cement and subsequent formation of C-S-H gel, while for the OPSGC, the strength development is dependent on the formation of calcium-silicate-hydrate (C-S-H) and aluminosilicate-hydrate (A-S-H) that enhanced the compressive-strength (Pangdaeng et al., 2014; Yusuf et al., 2014a). In the presence of alkaline activator and calcium from GGBS, the additional SiO₂ and Al₂O₃ could react and form C-S-H or C-A-S-H and N-A-S-H gels and led to a higher strength geopolymer (Phoo-ngernkham et al., 2014).

4.8.1.6 Effect of uncrushed and crushed OPS on compressive strength

Figure 4.11 and Figure 4.12 show the 28-day compressive strength of OPSGC prepared using crushed and uncrushed OPS and cured under OD and AD conditions. The results show that OPSGC with crushed OPS achieved a slightly higher compressive strength compared to the corresponding mixes prepared using uncrushed OPS cured in OD and AD conditions, and in the ranges of about 7–14% and 3–7%, respectively.

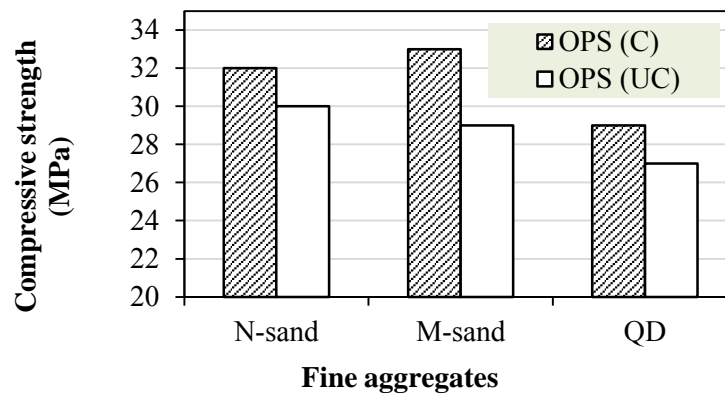


Figure 4.11. 28-day compressive strength of OPSGC (initial 24 h OD curing)

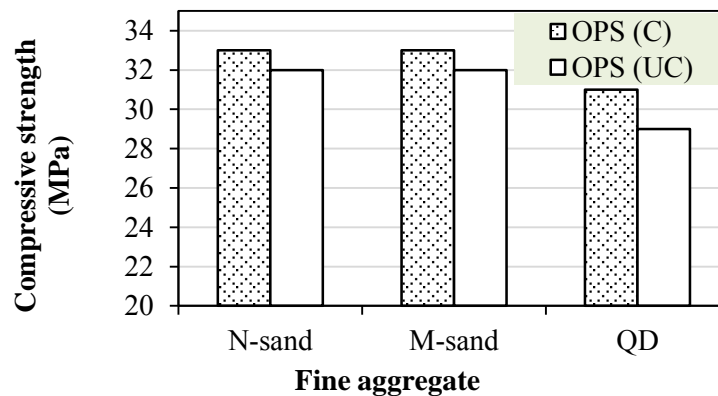


Figure 4.12. 28-day compressive strength of OPSGC (ambient curing)

Previous studies (Alengaram et al., 2010b; Shafigh et al., 2011b; Mo et al., 2014b) reported that OPSC with crushed aggregate produced a higher compressive strength compared to OPSC with uncrushed aggregate. Crushed OPS is hard and has a strong physical bond with the hydrated cement paste. The crushing of OPS reduces the smooth

concave and convex surfaces and increases the rough and spiky broken edges of OPS. This enhances the bond between the OPS and the cement paste (Shafigh et al., 2011b). Alengaram et al. (2010b) reported that the convex smooth surfaces of larger OPS particles produce a weaker interfacial bond strength. (Mannan et al., 2006) reported that the failure of concrete specimens in compression is initially due to the failure of the adhesion between the OPS and the cement paste.

4.8.2 Ultrasonic pulse velocity (UPV)

Ultrasonic pulse velocity (UPV) is an indicator of compressive strength of concrete and quality of aggregates used (Solís-Carcaño & Moreno, 2008). Low UPV value indicates the presence of the internal voids or porous aggregates in the concrete. Table 4.10 shows the UPV values of NWGC and OPSGC.

Table 4.10: Development of ultrasonic pulse velocity (UPV) of NWGC and OPSGC at 28-day

Mix	UPV (km/s)
NWGC-NS	3.76
NWGC-MS	3.64
NWGC-QD	3.51
OPSGC-NS-C	3.48
OPSGC-MS-C	3.23
OPSGC-QD-C	3.21
OPSGC-NS-UC	3.44
OPSGC-MS-UC	3.24
OPSGC-QD-UC	3.19

The UPV values for all the mixes were found to be within the range of 3.19–3.76 km/s, as shown in Ultrasonic pulse velocity (UPV) is an indicator of compressive strength of concrete and quality of aggregates used (Solís-Carcaño & Moreno, 2008). Low UPV

value indicates the presence of the internal voids or porous aggregates in the concrete.

Table 4.10 shows the UPV values of NWGC and OPSGC.

Table 4.10. Geopolymer concrete is very cohesive, which makes the compaction of concrete more difficult compared to that of normal concrete; thus, inappropriate compaction is likely to cause voids within the concrete leading to reduced UPV values.

The mixes with normal weight aggregate (NWA) produced 28-day UPV values between 3.51 and 3.76 showing that the quality of the concrete is “good” (BS EN 12504-4, 2004). Bogas et al. (2013) reported that in LWC with more porous aggregate and rich mortar there is a greater relative variation for UPV than for the compressive strength. In this investigation, all the mixes with OPS produced UPV values of 3.19 and 3.48 for 100-mm concrete cubes at 28 days, which is lower than for NWGC and proves that OPSGC contains more porous aggregate compared to NWGC; thus, showing that the quality of the concrete is “medium” (BS EN 12504-4, 2004).

4.8.3 Splitting Tensile Strength (STS)

The splitting tensile strength of NWGC and OPSGC are shown in Table 4.11 and Table 4.12 and the relationship between splitting tensile and compressive strength are shown in Figure 4.13 and Figure 4.15, respectively. It can be observed that the splitting tensile strength increases with the increasing compressive strength. The experimental 28-day splitting tensile strength was found in the range of 2.61–2.94 MPa for NWGC, 1.88–2.44 MPa for OPSGC with crushed OPS and 1.92–2.94 MPa for OPSGC with uncrushed OPS. It is found from the experimental results that irrespective of the OPS coarse aggregates

(crushed or uncrushed), the mixes containing conventional mining sand (NS) produced higher tensile strength compared to the splitting tensile strength of the mixes prepared with MS and QD.

The mixes NWGC-QD, OPSGC-QD-C and OPSGC-QD-UC produced lower tensile strength of about 11%, 23% and 30 % compared to NWGC-NS, OPSGC-NS-C and OPSGC-NS-UC, respectively. This might be due to the angular and flaky particles of QD that could influence the bond between the aggregate and matrix in the interfacial transition zone (ITZ), which has a significant role in the tensile strength of concrete.

The empirical formulae proposed in Eq. (11) shows the relationship between the compressive strength (f'_c) and splitting tensile strength (f_i) (Zain et al., 2002).

$$f_i = k (f'_c)^n \quad (11)$$

where, f_i is the splitting tensile strength (MPa); f'_c is the compressive strength (MPa); k , n : constants. The constants k and n are obtained through a regression analysis of the experimental data. In general, the value of n ranges between 0.5 and 0.75.

4.8.3.1 Splitting tensile strength for NWGC

Based on the basic equation, ACI 363R-92 (1992) and CEB-FIP (1993), the models as expressed in Eqs. (12) and (13) to predict the cylinder splitting tensile strength (f_i) from

the compressive strength of cylinder for normal weight concrete. Ryu et al. (2013) suggested a formula to predict cylinder splitting tensile strength from the cylinder compressive strength for fly ash-based geopolymer concrete as shown in Eq. (14).

$$\text{ACI 363R-92: } f_t = 0.590 \sqrt{f'_c} \quad (\text{for } 21 \text{ MPa} < f'_c < 83 \text{ MPa}) \quad (12)$$

$$\text{CEB-FIP (1993): } f_t = 0.301 (f'_c)^{\frac{2}{3}} \quad (13)$$

$$\text{Ryu et al. (2013): } f_t = 0.170 (f'_c)^{\frac{3}{4}} \quad (14)$$

Table 4.11: Splitting tensile strength of NWGC

Mix no.	Compressive strength, f'_c (MPa)	Splitting tensile strength, f_t (MPa)				$(\frac{f_t}{f'_c} \times 100)\%$
		Experimental	Predicted by Eq. (12) $f_t = 0.59 \sqrt{f'_c}$	Predicted by Eq. (13) $f_t = 0.301 (f'_c)^{\frac{2}{3}}$	Predicted by Eq. (14) $f_t = 0.17 (f'_c)^{\frac{3}{4}}$	
			Using conversion factor 0.77*			
NWGC-NS	38	2.94	3.19	2.89	2.14	7.74
NWGC-MS	40	2.87	3.27	2.99	2.22	7.18
NWGC-QD	36	2.61	3.11	2.79	2.05	7.25

*Conversion factor is to convert cube compressive strength to cylinder compressive strength. Lower value of conversion for 100 mm cube compressive strength to 150 mm diameter cylinder was taken based on previous data from published researchers (Wong, 2013).

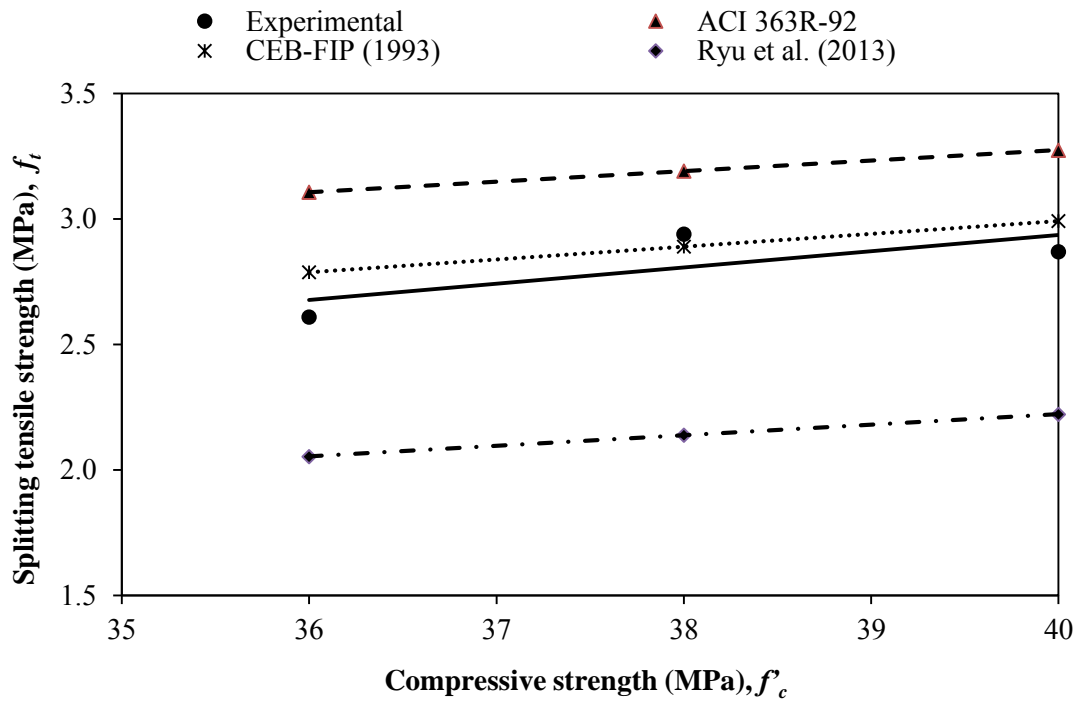


Figure 4.13. Relationship between splitting tensile and compressive strength of NWGC at 28-day

The comparison of the experimental results and the formulae proposed by ACI 363R-92 (ACI 363R-92, 1992), CEB-FIP (CEB-FIP, 1993) and the other researchers (Ryu et al., 2013) is shown in Table 4.11 and Figure 4.13. It is found that the splitting tensile strength obtained from the experimental results for POFA-GGBS-based geopolymer concrete is lower than that the values calculated using the proposed formula by ACI 363R-92. However, it was found closer values obtained from the equations proposed by CEB-FIP. Ryu et al. (2013) proposed an equation to predict the splitting tensile strength for fly ash based geopolymer normal weight aggregate concrete. The experimental results of GGBS-POFA based geopolymer concrete produced higher splitting tensile strength than that of the equation proposed by Ryu et al. (2013). The difference between the splitting tensile strength of specimens prepared using MS and NS is negligible compared to the specimen with QD. As mentioned earlier in Section 4.8.1.4, the QD particles have angular and flaky

particles that could result in more air voids entrapped surrounding QD and hence the interfacial zone is weaker compared to specimens with MS and NS.

4.8.3.2 Splitting tensile strength of lightweight OPSGC

The ratio of 28-day splitting tensile strength to compressive strength expressed as percentage of the crushed OPSGC was found in the range of 6–8%; while the uncrushed OPSGC produced slightly higher values of 7–9%. The lower range in crushed OPSGC might be due to the large quantity of OPS used in these mixes. The smaller size of crushed OPS, which leads to larger number of crushed OPS particles compared to that of uncrushed OPS for a given weight of OPS. Generally, the splitting tensile strength of normal weight concrete (NWC) is 8–14% of the compressive strength (Kosmatka et al., 2002). In comparison to NWC, the tensile/compressive strength ratio is lower for LWAC of equivalent grade (Haque et al., 2004). It could be due to the weaker bond between the OPS and the matrix than that of NWGC. Figure 4.14 shows the experiment of splitting tensile strength and the failure of the specimen after the test. It can be seen that the generally the bond failure between the OPS and the matrix occurred along with failure of the OPS itself. However, the tensile/compressive strength ratio of OPSGC obtained in this study is comparable with that of the OPS concrete (not geopolymer, but lightweight OPS concrete prepared from OPC) containing fly ash of an equivalent grade, as reported by Shafigh et al. (2013a).

The following equation was suggested to predict the splitting tensile strength from the compressive strength of OPS normal concretes made from OPC (Shafigh et al., 2012).

$$f_t = 0.49 \sqrt{f'_c} \quad (15)$$

where f_t is the splitting tensile strength obtained from 100×200-mm cylinders and f_c' is the 100-mm cube compressive strength at 28-day.

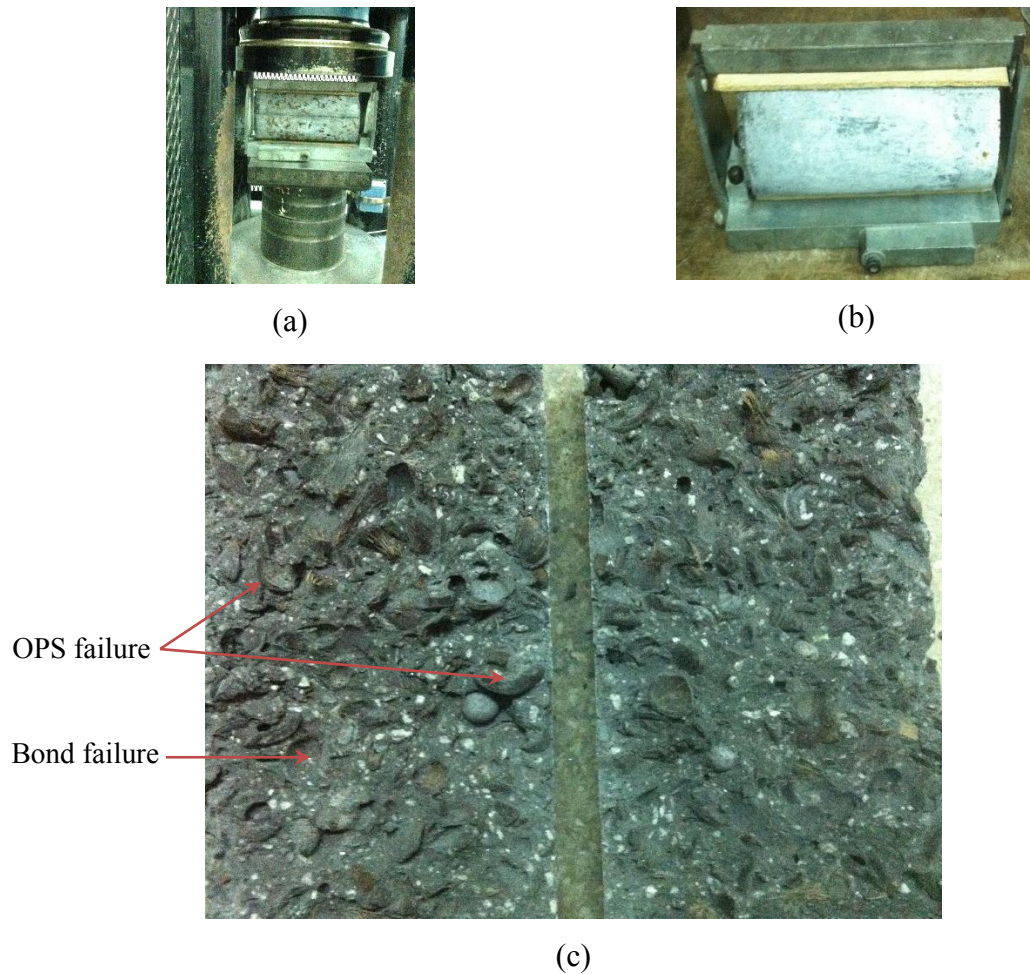


Figure 4.14: (a) Splitting tensile testing; (b) placement of cylinder specimen; (c) specimen after testing

For OPS normal concrete containing fly ash, the following equation is proposed to predict the splitting tensile strength based on the compressive strength (Shafiqh et al., 2013a).

$$f_t = 0.23 f_c'^{0.64} \quad R^2 = 0.91 \quad (16)$$

Gesoğlu et al. (2004) suggested the following equation for structural lightweight aggregate normal concrete made of an artificial lightweight aggregate, namely, cold-bonded fly ash, to predict the splitting tensile strength from the compressive strength (compressive strength in the range of 21–47 MPa):

$$f_t = 0.27 f_c^{0.67} \quad (17)$$

Table 4.12: Splitting tensile strength of OPSGC

Mix	Compressive strength, f_c (MPa)	Splitting tensile strength, f_t (MPa)				Experimental: $\left(\frac{f_t}{f_c} \times 100\right)\%$
		Experimental	Predicted by Eq. (15) $f_t = 0.49 \sqrt{f_c}$	Predicted by Eq. (16) $f_t = 0.23 f_c^{0.64}$	Predicted by Eq. (17) $f_t = 0.27 f_c^{0.67}$	
OPSGC-NS-C	32	2.44	2.77	2.11	2.75	7.63
OPSGC-MS-C	33	2.09	2.81	2.16	2.81	6.33
OPSGC-QD-C	29	1.88	2.64	1.98	2.58	6.48
OPSGC-NS-UC	30	2.74	2.68	2.03	2.64	9.13
OPSGC-MS-UC	29	2.37	2.64	1.98	2.58	8.17
OPSGC-QD-UC	27	1.92	2.55	1.90	2.46	7.11

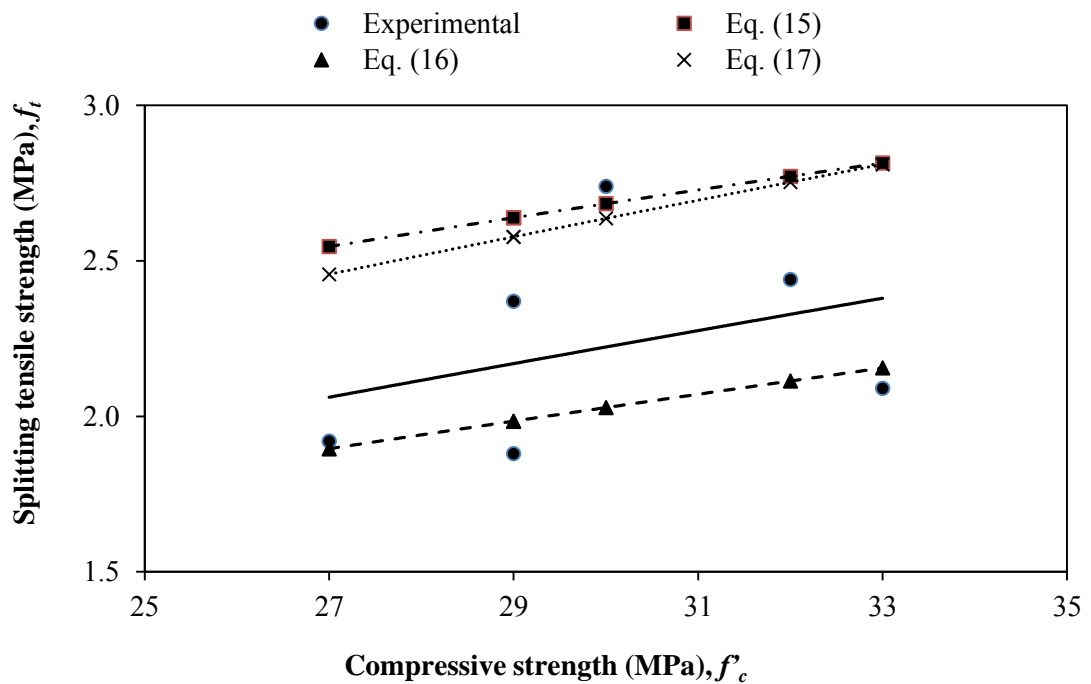


Figure 4.15. Relationship between splitting tensile and compressive strength of OPSGC at 28-day

Table 4.12 and Figure 4.15 show the comparison among the experimental results with the formulae proposed by other researchers (Eq. (15), (16) and (17)) and results show that the

splitting tensile strength produced by the POFA-GGBS-based OPSGC based on the compressive strength is lower than that provided by the formulae Eq. (15) and (17) and comparable with the formulae Eq. (16). It should be noted that the specimens prepared in this investigation has two variables namely, the crushed and uncrushed OPS and three different types of sand (NS, MS and QD). The equations proposed by researchers are for the lightweight concrete prepared with OPC, conventional sand, OPS and cold bonded lightweight fly ash aggregate.

It is worth noting that according to ASTM:C330 , a minimum splitting tensile strength of 2.0 MPa is a requirement for structural grade lightweight aggregate concrete. It can be seen that according to this criteria, all mixes except OPSGC-QD-C and OPSGC-QD-UC fulfilled the criterion for minimum splitting tensile strength.

4.8.4 Flexural Strength

The flexural strength of NWGC and OPSGC and its comparison with compressive strength is shown in Table 4.13. Generally for conventional concrete having a compressive strength of more than 25 MPa, the ratio of flexural strength to compressive strength expressed as percentage is in the range of 8–11% (Shetty, 2005). As can be seen in Table 4.13, this ratio was found within this range for all the mixes.

Table 4.13: Comparison of compressive strength, splitting tensile strength, flexural strength and elastic modulus

Mix no.	Compressive strength, f'_c (MPa)	Splitting tensile strength, f_t (MPa)	Flexural strength, f_r (MPa)	Elastic modulus, E (GPa)	$\left(\frac{f_t}{f'_c}\right) \times 100$ %	$\left(\frac{f_r}{f'_c}\right) \times 100$ %	$\left(\frac{f_r}{f_t}\right)$
NWGC-NS	38	2.94	3.62	16.86	7.74	9.53	1.231
NWGC-MS	40	2.87	3.83	14.80	7.18	9.58	1.334
NWGC-QD	36	2.61	3.20	13.74	7.25	8.89	1.226
OPSGC-NS-C	32	2.44	3.00	11.12	7.63	9.38	1.229
OPSGC-MS-C	33	2.09	3.03	8.93	6.33	9.18	1.450
OPSGC-QD-C	29	1.88	2.79	8.51	6.48	9.62	1.485
OPSGC-NS-UC	30	2.74	3.10	10.08	9.13	10.33	1.131
OPSGC-MS-UC	29	2.37	3.19	8.05	8.17	11.00	1.346
OPSGC-QD-UC	27	1.92	2.94	7.36	7.11	10.89	1.532

In this investigation, the flexural/splitting tensile strength ratios for NWGC-NS, NWGC-MS and NWGC-QD mixes were found as 1.23, 1.33 and 1.23, respectively; while for OPSGC-NS-C, OPSGC-MS-C, OPSGC-QD-C, OPSGC-NS-UC, OPSGC-MS-UC and OPSGC-QD-UC mixes the ratios were 1.23, 1.45, 1.48, 1.13, 1.35 and 1.53, respectively.

Alengaram et al. (2008b) reported that the ratio $\left(\frac{f_r}{f_t}\right)$ for OPC based OPS concrete between 1.4 and 1.7. In general, as reported by Zheng et al. (2001), the flexural strength of concrete is 35% higher than the splitting tensile strength.

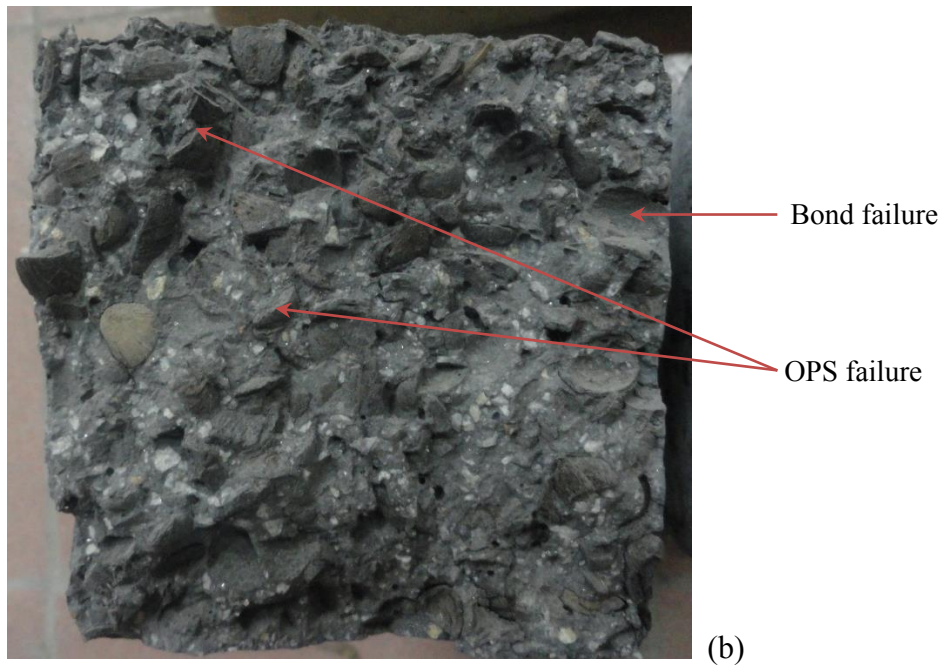


Figure 4.16: (a) Flexural strength testing and (b) specimen after testing

The mixes NWGC-NS, OPSGC-NS-C and OPSGC-NS-UC using conventional mining sand show the flexural strength of 3.62, 3.00 and 3.10 MPa. On the contrary, the flexural strength of the mixes using MS (NWGC-MS, OPSGC-MS-C, OPSGC-MS-UC) and QD (NWGC-QD, OPSGC-QD-C, OPSGC-QD-UC) were 3.83, 3.03, 3.19 and 3.20, 2.79, 2.94, respectively. The result shows that the mixes NWGC-MS, OPSGC-MS-C and OPSGC-MS-UC are 6, 1.0 and 3% higher than the corresponding mixes using conventional mining sand. In contrast, the corresponding mixes using QD show 12, 7 and 5% lower flexural strength compared to the corresponding mixes using conventional

mining sand. Hence, it can be concluded that the use of MS could be considered as an ideal replacement for conventional mining sand.

Figure 4.16 shows that bond failure occurred between the OPS and the mortar and it could be due to the smooth surface of the OPS. And as explained in the Section 4.8.3.2, OPS failure along the failure plane is visible and it is due to the weaker stiffness of OPS. The weaker bond and OPS failure result in lower flexural strength value of OPSGC compared to NWGC.

Previous researchers proposed following relationship to predict the flexural strength from the compressive strength of OPS concrete.

Alengaram et al. (2008b) have reported OPS concrete with compressive strength ranging from 15 to 37 MPa and the relationship with the flexural strength can be expressed as follows:

$$f_r = 0.30 \sqrt[3]{f'_c} \quad (18)$$

Meanwhile, Lo et al. (2004) have reported expanded clay lightweight aggregate concrete with cube compressive strength ranging from 29 to 43 MPa and the relationship with the flexural strength can be expressed as follows:

$$f_r = 0.69 \sqrt{f'_c} \quad (19)$$

Smadi and Migdady (1991) reported high strength lightweight concrete with compressive strength of 60 MPa, which was prepared with Tuff lightweight aggregate and the relationship with the flexural strength can be expressed as follows:

$$f_r = 0.58 \sqrt{f'_c} \quad (20)$$

Shafigh et al. (2013a) investigated OPS concrete with compressive strength ranging from 30 to 44 MPa, with 0 – 50 % fly ash replacement with cement and the above relationship expressed as follows:

$$f_r = 0.09 f'_c \quad (21)$$

Table 4.14: Flexural strength of OPSGC

Mix	Compressive strength, f'_c (MPa)	Flexural strength, f_r (MPa)					Experimental: $(\frac{f_r}{f'_c} \times 100)\%$
		Experimental	Predicted by Eq. (18) $f_r = 0.30 \sqrt[3]{f'^2_c}$	Predicted by Eq. (19) $f_r = 0.69 \sqrt{f'_c}$	Predicted by Eq. (20) $f_r = 0.58 \sqrt{f'_c}$	Predicted by Eq. (21) $f_r = 0.09 f'_c$	
OPSGC-NS-C	32	3.00	3.02	3.90	3.28	2.88	9.38
OPSGC-MS-C	33	3.03	3.08	3.96	3.33	2.97	9.18
OPSGC-QD-C	29	2.79	2.83	3.72	3.12	2.61	9.62
OPSGC-NS-UC	30	3.10	2.89	3.78	3.18	2.7	10.33
OPSGC-MS-UC	29	3.19	2.83	3.72	3.12	2.61	11.00
OPSGC-QD-UC	27	2.94	2.70	3.59	3.01	2.43	10.89

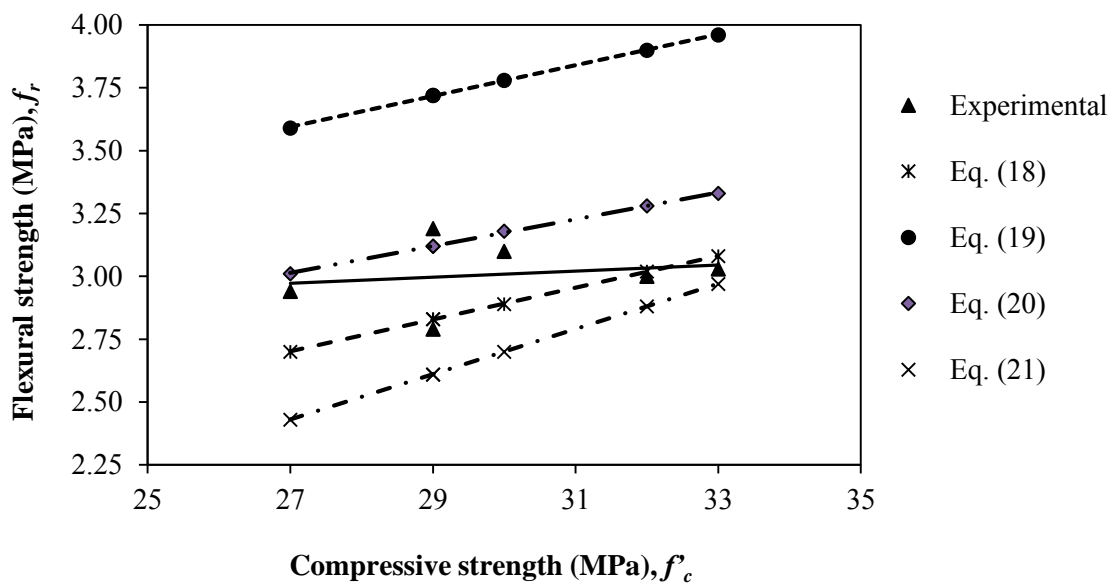


Figure 4.17: Relationship between flexural strength and compressive strength of OPSGC

Table 4.14 and Figure 4.17 show the comparison among the experimental results with the formulae proposed by other researchers (Smadi & Migdady, 1991; Lo et al., 2004; Alengaram et al., 2008b; Shafigh et al., 2013a) and the results show that the flexural strength produced by the POFA-GGBS-based OPSGC based on the compressive strength is lower than that provided by the formulae Eq. (19) (Lo et al., 2004) and comparable with the formulae Eq. (18), (20) and slightly higher than the Eq. (21). The higher difference between the formulae Eq. (19) and the experimental results could be attributed to the formula proposed for high strength concrete Eq. (19) (cube compressive strength ranging from 29 to 43 MPa) and the aggregates used in this study were crushed and uncrushed OPS and three different types of sand (NS, MS and QD) discussed earlier in Section 4.8.3.2, while the equations proposed by researchers (Lo et al., 2004) are for the lightweight concrete prepared with OPC, conventional sand, expanded clay lightweight aggregate.

4.8.5 Modulus of elasticity (E- value)

The modulus of elasticity (MOE) or E-value of concrete is one of the most important parameters for structural concrete as it is required when assessing deflections and cracking of a structure. Table 4.15 shows the experimental and predicted static moduli of elasticity (E) of all mixes.

The moduli of LWA particles are generally lower than NWA and though most LWA concretes contain higher cement contents it follows that the overall moduli of lightweight aggregate concretes will be lower than normal weight concretes

(Clarke, 2005). Generally, for LWAC with natural and artificial LWA, the value of the static MOE ranges between 10 and 24 kN/mm² (FIP Manual, 1983).

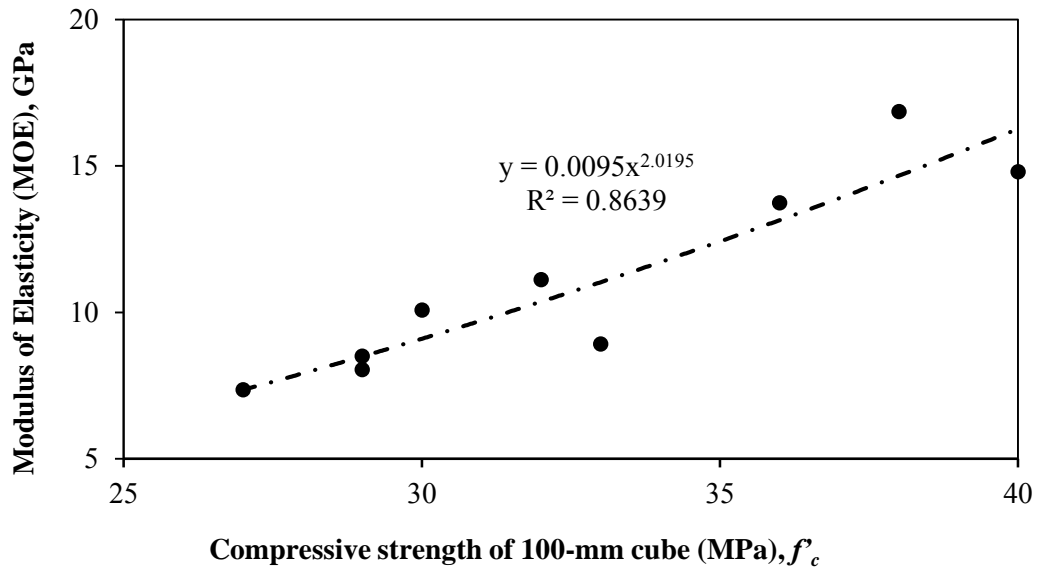


Figure 4.18. The relationship of MOE and compressive strength at 28-day

The experimental E-values for the OPSGC and NWGC vary in the range of 7.4–11.12 GPa and 13.74 –16.86 GPa, respectively (Table 4.15), and the MOE increases as the compressive strength increases (Figure 4.18). The E-values of OPSGC are lower than the values obtained for NWGC; as stated, NWA has higher stiffness and establishes a stronger bond between the aggregate surface and the matrix compared to the OPS. The E-values of OPSGC depend on the stiffness of the aggregate, the hardened cement matrix, the bond between the OPS and the cement matrix and the quantity of OPS. A higher LWA content lowers the modulus value, because the concrete stiffness decreases (Short & Kinniburgh, 1978; FIP Manual, 1983). Alengaram et al. (2011) opined that the use of higher OPS content in mixes reduces the E-values. They reported values ranging between 5.5 and 7.1 kN/mm². The E-values reported in this investigation were higher than the values reported by Alengaram et al. (2011) for OPSC, which could be attributed to reasons such as water to binder (w/b) ratio, sand to binder (s/b) ratio and the quantity of OPS in the OPSGC.

Table 4.15: Elastic moduli and Poisson's ratios of concrete at 28-day

Mix	Compressive strength, f'_c (MPa)	ρ_{28-d} (kg/m ³)	Poisson's ratio	Elastic modulus, E (GPa)	Predicted by Eq. (22) $E_{c,28} = 20 + 0.2 f'_{c,28}$	Predicted by Eq. (23) $E_{c,28} = \rho^2 \sqrt{f'_c} \times 10^{-6}$	Predicted by Eq. (24) $E_c = \left[\frac{\rho}{2400} \right]^2 \times (f'_c)^{1/3} \times 5.0$
NWGC-NS	38	2341	0.19	16.86	27.60	NA	NA
NWGC-MS	40	2285	0.27	14.80	28.00	NA	NA
NWGC-QD	36	2320	0.20	13.74	27.20	NA	NA
OPSGC-NS-C	32	1970	0.15	11.12	NA	21.95	10.70
OPSGC-MS-C	33	1949	0.16	8.93	NA	21.82	10.58
OPSGC-QD-C	29	1957	0.16	8.51	NA	20.62	10.21
OPSGC-NS-UC	30	1948	0.16	10.08	NA	20.78	10.24
OPSGC-MS-UC	29	1934	0.17	8.05	NA	20.14	9.98
OPSGC-QD-UC	27	1940	0.17	7.36	NA	19.56	9.80

Note: NA- not applicable

4.8.5.1 Effect of aggregates on E-value of geopolymer concrete

It can be seen from Table 4.15 that the E-values obtained using conventional mining sand are 16.86, 11.2 and 10.08 GPa for mixes NWGC-NS, OPSGC-NS-C and OPSGC-NS-UC, respectively. In contrast, the E-values obtained using MS to the corresponding mixes are 14.80, 8.93 and 8.05, which are 12, 19 and 20% lower than the values obtained for mixes with NS. One possible explanation for this difference could be due to low stiffness of OPS and the bond between aggregate and the paste, as discussed earlier. All the mixes with QD show lower E-value and it could be attributed to QD as explained in earlier Sections 4.8.1.4.

4.8.5.2 Comparison of E-value with the previous research

In the literature, the following equations were suggested to predict the elastic modulus of concrete from the compressive strength.

For normal-weight concrete,

$$\text{BS8110 : } E_{c,28} = K_0 + 0.2 f'_{c,28} \quad (22)$$

where

$E_{c,28}$ is the static modulus of elasticity at 28 days (in kN/mm²);

$f'_{c,28}$ is the characteristic cube strength at 28 days (in N/mm²);

K_0 is a constant closely related to the modulus of elasticity of the aggregate (taken as 20 kN/mm² for normal-weight concrete and 14 to 26 kN/mm² for unknown aggregates)

For structural lightweight aggregate concrete, it is reported (Clarke, 2005):

$$E_{c,28} = \rho^2 \sqrt[3]{f'_c} \times 10^{-6} \quad (23)$$

where E , ρ and f'_c are modulus of elasticity (GPa), nominal density (kg/m³) and cube strength (MPa), respectively.

Kosmatka et al. (2002) reported for structural lightweight conventional concrete, the MOE varied between 7 and 17 GPa.

Alengaram et al. (2011) established for OPS lightweight normal concrete incorporated cement, fly ash and silica fume, the MOE can be expressed as:

$$E_c = \left[\frac{\rho}{2400} \right]^2 \times (f'_c)^{1/3} \times 5.0 \quad (24)$$

where, f'_c = cube compressive strength (MPa)

Based on the Young's modulus comparisons between experimental and three equations (Eq. (22), (23) and (24)), it could be concluded that the equation proposed by Alengaram et al. (2011) (modified based on FIP manual) predicts the E-values closer to the experimental. The difference between the experimental and predicted values are 0.16–2.44 MPa.

4.8.5.3 Stress-strain relationship

Figure 4.19 shows the stress-strain relationship for all nine mixes including NWGC. The draft European code (ENV 1992–1–1: Part 1, 1991) gives special provisions for lightweight aggregate concrete. It defines an idealised bilinear stress-strain diagram for concrete, with a peak stress of 0.77 times the design strength of the concrete in most situations. For normal weight concrete, the factor is 0.85. The transition from the linearly increasing portion of the curve to the uniform is at a strain of 0.00135 for normal weight concrete, but increases to 0.0022 for lightweight aggregate concrete. The ultimate strain for most structural concretes is approximately 0.0035, irrespective of the strength of the concrete (Mosley & Bungey, 1990).

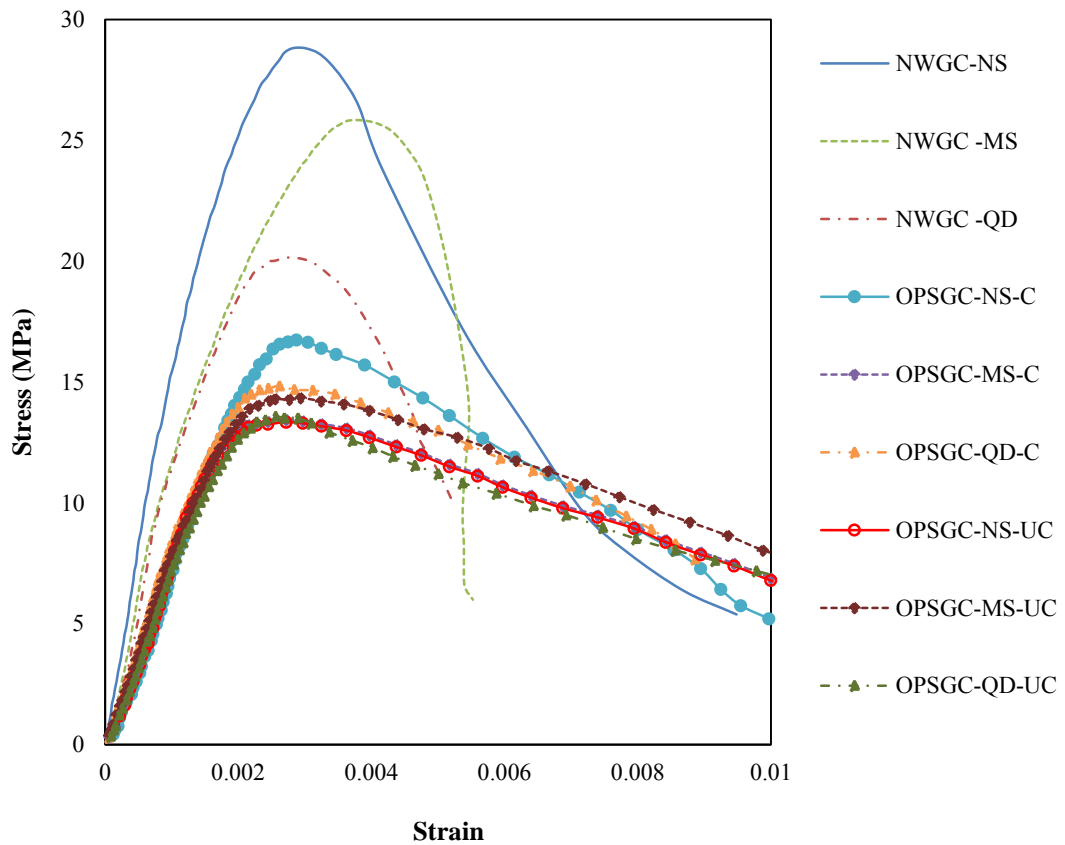


Figure 4.19. Stress-strain curve

It can be seen from Figure 4.19, that, in the beginning, as the load is applied, the stress-strain curve is approximately linear, irrespective of the type of concrete; both NWGC and OPSGC behave almost as an elastic material with virtually a full recovery of displacement if the load is removed. Eventually, the curve is no longer linear and the concrete behaves more and more as a plastic material. The peak stress of the geopolymer concrete (GC) using conventional mining sand is higher compared to the concrete using MS and QD, but MS gives a good result compared to QD. Figure 4.19 shows that the stress-strain relationship of OPSGC is more linear compared to NWGC. It is reported that lightweight aggregate concretes are typically linear to levels approaching 90% of the failure strength, indicating the relative compatibility of the constituents and the reduced occurrence of micro-cracking (Chandra & Berntsson, 2002).

4.8.6 Poisson's ratio

The Poisson's ratio of NWGC and OPSGC are presented in Table 4.15. The values of Poisson's ratio for OPSGC (mixes OPSGC-NS-C, OPSGC-MS-C, OPSGC-QD-C, OPSGC-NS-UC, OPSGC-MS-UC and OPSGC-QD-UC) were found within the range of 0.15–0.17, while in the case of NWGC (mixes NWGC-NS, NWGC –MS and NWGC - QD), the ratios' shows slightly higher values of 0.19-0.27 as shown in Table 4.15. The mixes with uncrushed OPS coarse aggregate shows a slight increment in Poisson's ratio (5.9 - 6.3 %) compared to the mixes using crushed OPS (0.15 – 0.16) and this could be attributed to higher strains in uncrushed OPS. The OPSGC with conventional mining sand show the Poisson's ratio values 0.15 and 0.16 in the mixes OPSGC-NS-C and OPSGC-NS-UC, respectively; while the corresponding mixes using MS and QD show 0.16–0.17, in both cases.

There is no published literature available on the Poisson's ratio of OPS based geopolymer concrete. Depending on the properties of aggregate used, Poisson's ratio of concrete lies generally in the range of 0.15-0.22 (Neville, 1995). Neville (1995) reported for lightweight aggregate conventional concrete the Poisson's ratio could be of lower value compared to NWA concrete.

Poisson's ratio effect has a considerable influenced in construction. Due to Poisson's effect, the concrete may laterally expand and shorten its length. If a single slab concrete highway is cast without any expansion joint, it may show crack within a short time due the effect of Poisson's ratio. Impact strength in compression is improved by the use of aggregate with a low Poisson's ratio (Neville, 1995). Higher Poisson's ratio could lead to splitting. In each material, the vertical compression results in a lateral expansion due to the Poisson's ratio effect.

4.9 Mechanical properties of OPSGC with and without fibre

In the previous Section (4.8), the effect of three types of fine aggregates along with crushed and uncrushed OPS on the mechanical properties of OPSGC and NWGC was investigated and reported. The specimens with MS produced comparable results to that of NS and hence its use as sustainable material was further investigated using fibres. The variables investigated in this section are OPS to binder contents with crushed and uncrushed OPS; the fibre content was kept constant at 0.5% on volume of concrete. MS was used as fine aggregate and comparison of mechanical properties of NWGC with and without fibre was also done. Based on the findings from the previous Section (4.8), only one curing condition, namely ambient curing was employed.

4.9.1 Density

The 28-day density of oil palm shell geopolymer concrete (OPSGC) and normal-weight geopolymer concrete (NWGC) with and without fibre are shown in Table 4.16. The density of OPSGC and fibre reinforced oil palm shell geopolymer concrete (FROPSGC) ranges 1820–1940 and 1873–1994 kg/m³, respectively, and thus, it could be categorised as LWC (EN 206-1, 2000). Figure 4.20 shows the relationship between density and the compressive strength. As seen from Figure 4.20, the compressive strength increases proportionally with the density.

Table 4.16: Density and compressive strength of OPSGC and NWGC with 0% and 0.5% steel fibre

Mix	28-d density (kg/m ³)	Mean compressive strength (MPa) ^a				
		3-day		7-day		28-day
OPSGC4-NF-UC	1940	23.09	(83.40)	26.78	(97.73)	27.69
OPSGC4-F- UC	1994	19.87	(70.64)	24.12	(85.73)	28.14
OPSGC6-NF- UC	1925	19.56	(80.85)	23.47	(96.98)	24.20
OPSGC6-F- UC	1965	20.94	(83.79)	24.77	(99.13)	24.99
OPSGC8-NF- UC	1843	15.92	(78.79)	17.44	(86.32)	20.21
OPSGC8-F- UC	1885	15.54	(75.27)	18.91	(91.62)	20.64
OPSGC4-NF-C	1929	17.42	(62.54)	25.06	(89.99)	27.85
OPSGC4-F-C	1978	18.44	(64.39)	26.97	(94.17)	28.64
OPSGC6-NF-C	1910	21.33	(75.28)	25.59	(90.32)	28.33
OPSGC6-F-C	1950	21.37	(76.32)	24.28	(86.74)	28.00
OPSGC8-NF-C	1820	16.17	(71.88)	19.77	(87.88)	22.50
OPSGC8-F-C	1873	18.05	(86.08)	19.67	(93.79)	20.97
NWGC-NF	2296	28.42	(69.95)	35.16	(86.54)	40.63
NWGC-F	2330	27.66	(69.97)	32.32	(81.77)	39.53

^a () The data in parentheses are percentages of 28-day compressive strength

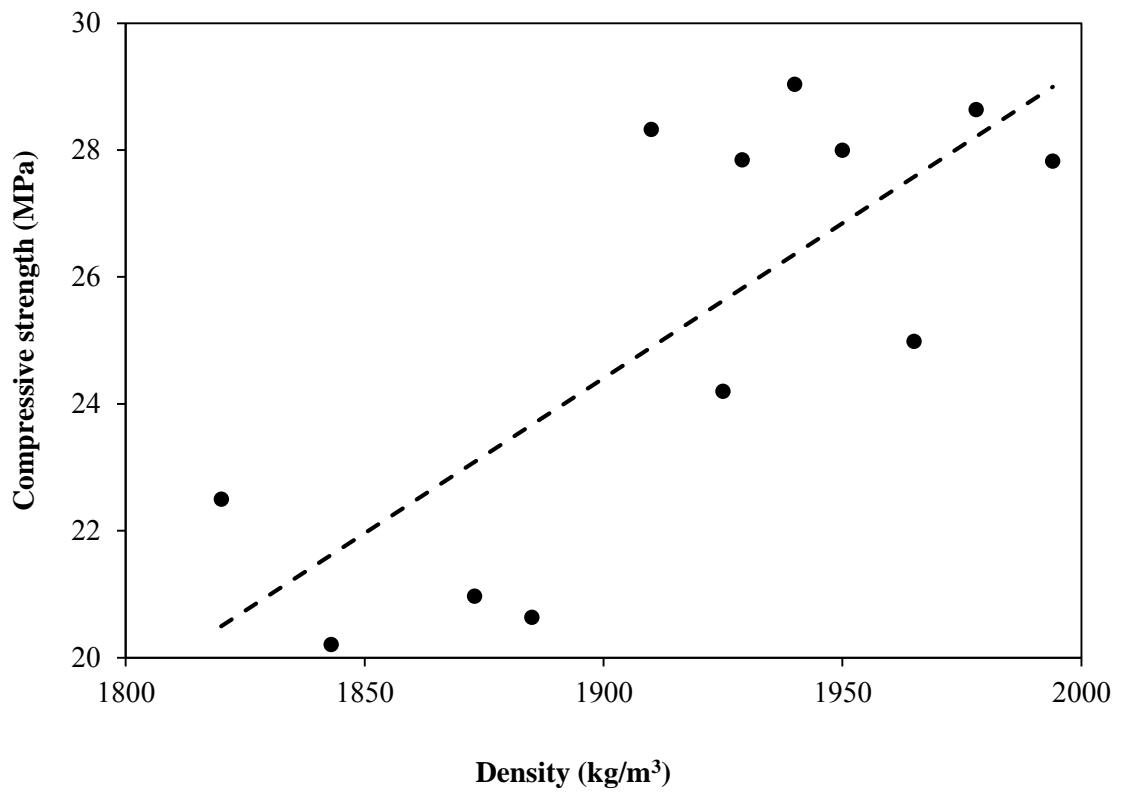


Figure 4.20: Relationship of density and compressive strength of steel fibre reinforced OPSGC

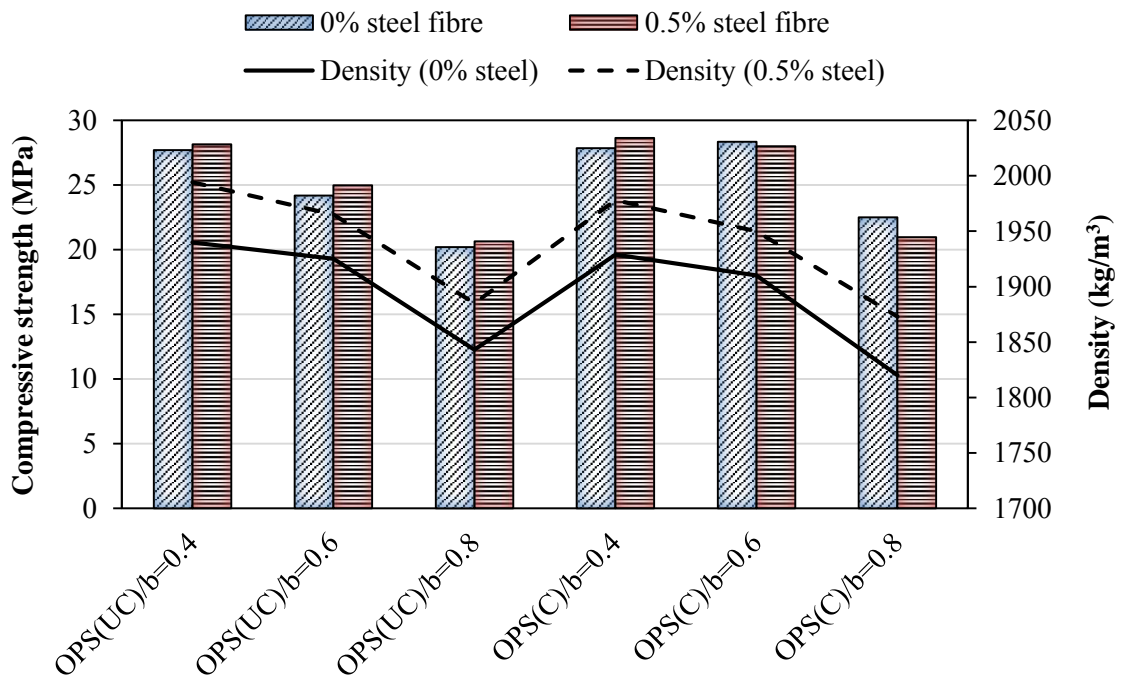


Figure 4.21: Compressive strength with respect to density and OPS contents

The comparison between the compressive strength with and without fibre and the density are shown in Figure 4.21. The mixes OPSGC6-NF-C and OPSGC6-F-C show the higher value of compressive strength with low density compared to the corresponding mixes. The density of OPSGC decreases as the OPS content increases. The density of the mix OPSGC4-NF-UC that contained 181 kg/m³ of OPS (OPS to binder weight ratio of 0.4) was found as 1940 kg/m³. The effect of increase in the OPS content was evident as the mix OPSGC8-NF-UC produced lower density of 1843 kg/m³ compared to OPSGC6-NF-UC of 1925 kg/m³ (for an increase in the OPS content of 74 kg/m³). The addition of 0.5% of steel fibre on volume of concrete, the density of OPSGC increases about 2–3%. The rate of reduction in the density for OPSGC mixes with crushed OPS is similar to that of mixes with uncrushed OPS.

4.9.2 Development of compressive strength in steel fibre reinforced OPSGC

The development of compressive strength of uncrushed and crushed OPSGC with varying OPS contents and NWGC with and without fibres are shown in Table 4.16.

4.9.2.1 Effect of uncrushed and crushed OPS on compressive strength of steel fibre reinforced OPSGC

The 28-day compressive strength of the mixes OPSGC4-NF-C, OPSGC6-NF-C and OPSGC8-NF-C were 27.85, 28.33 and 22.50 MPa, respectively (Table 4.16). These values were 0.6%, 17.1% and 11.3% higher compared to the corresponding mixes using uncrushed OPS. The little difference of compressive strength between the mixes OPSGC4-NF-C and OPSGC4-NF-UC is due to less quantity of OPS and the effect of OPS is less on the development of compressive strength. The non-fibrous OPSGC with crushed OPS aggregate produced higher compressive strength compared to the

corresponding mixes using uncrushed OPS aggregate as discussed earlier in Section 4.8.1.6. However, when fibres were added, the OPSGC with crushed OPS produced the compressive strength close to that of uncrushed OPS. Bernal et al. (2010) reported that utilization of steel fibre reduces the compressive strength of slag-based geopolymer concrete. In general, the addition of fibres slightly improves the compressive strength of normal concrete (Chen & Liu, 2005; Shafiq et al., 2011c).

4.9.2.2 Effect of OPS content on compressive strength steel fibre reinforced OPSGC

The relationship of compressive strength and OPS contents is shown in Figure 4.22. OPS had a significant effect on the compressive strength, both in uncrushed and crushed conditions. The compressive strength decreases linearly as the quantity of OPS increases. As seen from Table 4.16 and Figure 4.22, the increase of OPS content from 181 kg/m³ to 319 kg/m³ (an increase of about 138 kg/m³), the compressive strength decreases by about 27% for uncrushed OPS. In contrast, the reduction in compressive strength for OPSGC prepared using crushed OPS aggregate was about 19% for a similar increase in the OPS content.

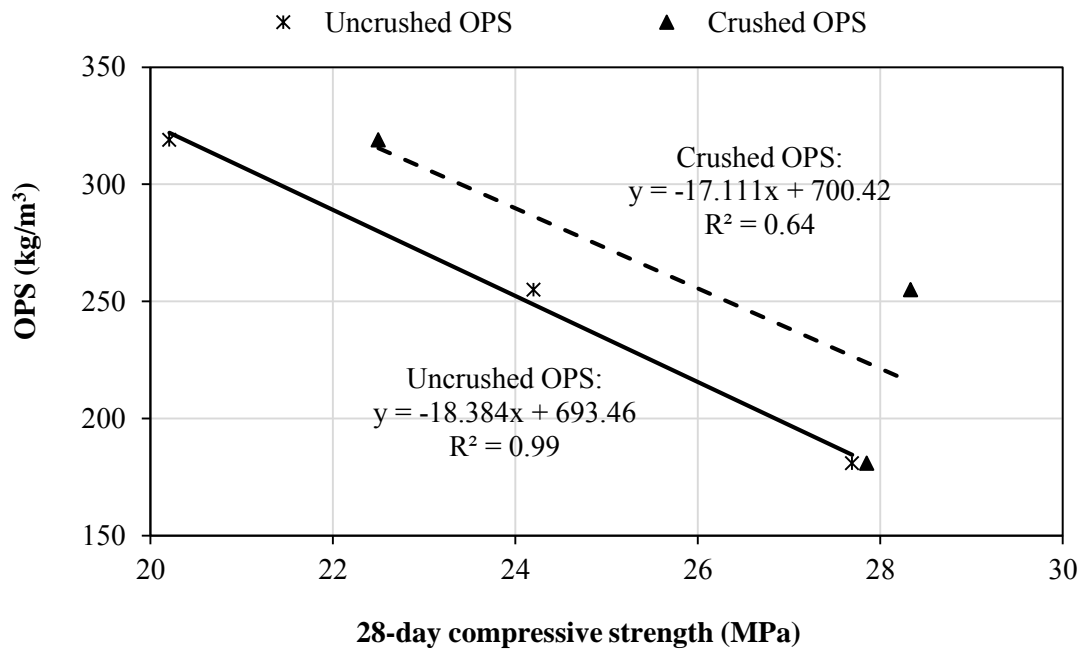


Figure 4.22: Relationship of compressive strength and OPS contents of non and steel fibre reinforced OPSGC

4.9.2.3 Development of compressive strength between 3 and 28-day

The development of compressive strength between 3 and 28 day expressed as a percentage is shown in Table 4.16. The 28-day compressive strength was taken as the reference and the strength achievement in 3- and 7-day was calculated. The development of compressive strength for OPSGC and fibre reinforced OPSGC (FROPSGC) produced using uncruised and crushed OPS along with NWGC are shown in Figure 4.23 and Figure 4.24, respectively. The 3-day compressive strength of non-fibrous OPSGC4-NF-UC, OPSGC6-NF-UC and OPSGC8-NF-UC mixes with uncruised OPS aggregate produced 23, 20 and 16 MPa, respectively. These compressive strength are 83, 81 and 79% of the 28-day strength as shown in Table 4.16. Similarly, the mixes OPSGC4-NF-C, OPSGC6-NF-C and OPSGC8-NF-C prepared using crushed OPS aggregate produced 17, 21 and 16 MPa, respectively, and these developed by 62, 75 and 72% of the 28-day strength as shown in Table 4.16. All the non-fibrous OPSGC achieved 62–83% of the 28-day compressive strength at 3-day. As discussed earlier in Section 4.8.1.1, the 3-day

compressive strength of OPSGC can be achieved 57–82% of the 28-day strength cured in AD condition. The 7-day compressive strength of OPGC reached about 88–97% of 28-day compressive strength. The 3- and 7-day compressive strength of NWGC (mix NWGC-NF) reached 70% and 86% of the 28-day strength.

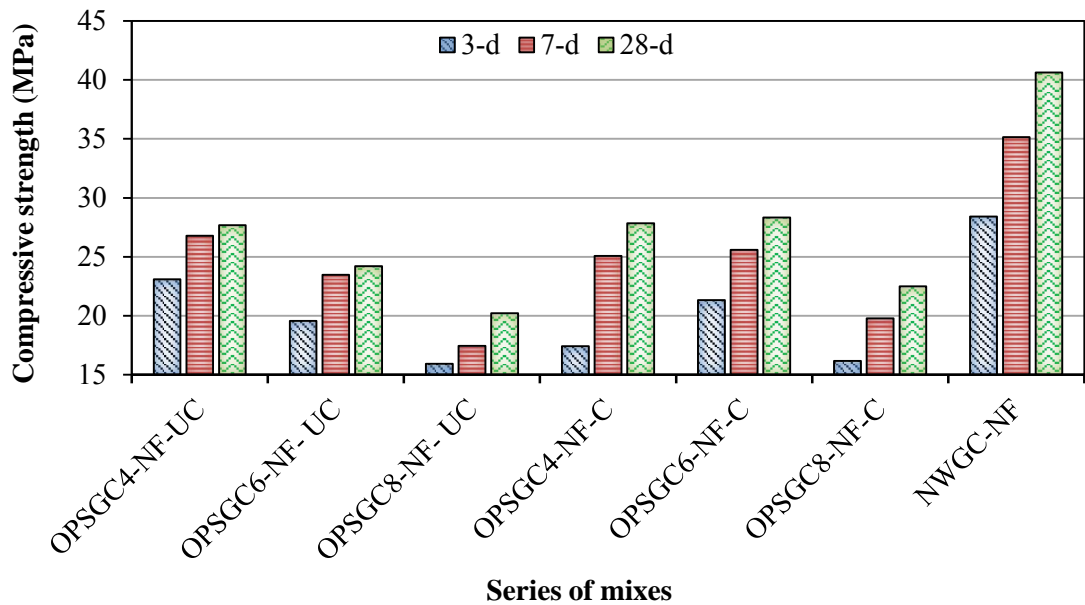


Figure 4.23: Development of compressive strength of OPSGC with 0.0% steel fibre

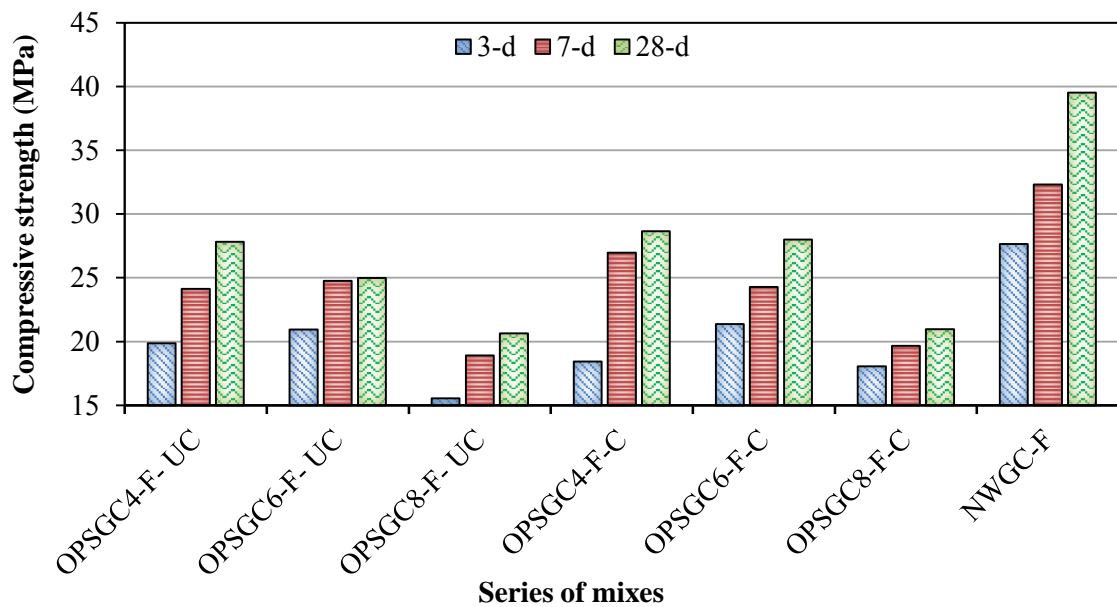


Figure 4.24: Development of compressive strength of OPSGC with 0.5% steel fibre

Figure 4.24 shows the development of compressive strength of FROPSGC with 0.5% fibres by volume of concrete. As seen in Figure 4.23 and Figure 4.24, the rate of development of compressive strength of FROPSGC is close to that of OPSGC of the corresponding mixes. This could be attributed to the less volume of fibres added to the concrete and the effect of fibres is not significant on the development of compressive strength. Previous studies (Chen & Liu, 2005; Shafigh et al., 2011c) show the addition of fibres slightly improves the compressive strength of concrete. Shafigh et al. (2011c) reported that the addition of steel fibres up to 0.5% does not have any effect on the compressive strength. It can be seen in Figure 4.23 and Figure 4.24, the rate of early strength (3- and 7-day) of OPSGC is higher compared to NWGC, both in fibrous and non-fibrous specimens.

4.9.3 Splitting tensile strength

The splitting tensile strength of fibrous and non-fibrous OPSGC and NWGC are shown in Table 4.17. The relationship between splitting tensile and compressive strength of fibrous and non-fibrous OPSGC are shown in Figure 4.25. It can be observed that the splitting tensile strength increases with the increases of compressive strength. The experimental 28-day splitting tensile strength of the mixes OPSGC4-NF-UC, OPSGC6-NF-UC and OPSGC8-NF-UC were found 2.28, 2.07 and 1.64 MPa, respectively. It is evident that the OPS reduces the tensile strength; higher the OPS contents lower the tensile strength. It could be attributed to the bond failure between the OPS and the matrix occurred along with failure of the OPS itself as discussed earlier in Section 4.8.3.2 and Figure 4.14. From this study, it was found that the OPSGC prepared using uncrushed OPS aggregate produced about 11%, 12% and 6% higher compared to the corresponding mixes prepared using crushed OPS aggregate at 28-day.

Table 4.17: Comparison of compressive strength, splitting tensile strength, flexural strength and elastic modulus at 28-day for OPSGC with and without steel fibres

Mix	Compressive strength, f'_c	Splitting tensile strength, f_t	Flexural strength, f_r	Elastic modulus, E	$\left(\frac{f_t}{f'_c} \times 100\right)\%$	$\left(\frac{f_r}{f'_c} \times 100\right)\%$	$\left(\frac{f_r}{f_t}\right)$
	(MPa)	(MPa)	(MPa)	(GPa)			
OPSGC4-NF-UC	27.69	2.28	2.95	3.54	8.25	10.67	1.29
OPSGC4-F- UC	28.14	2.72	4.11	5.74	9.65	14.61	1.51
OPSGC6-NF- UC	24.20	2.07	3.11	3.45	8.55	12.85	1.50
OPSGC6-F- UC	24.99	2.64	3.60	4.68	10.57	14.41	1.36
OPSGC8-NF- UC	20.21	1.64	1.89	2.94	8.12	9.35	1.15
OPSGC8-F- UC	20.64	2.18	2.51	3.15	10.56	12.16	1.15
OPSGC4-NF-C	27.85	2.05	2.77	5.85	7.36	9.96	1.35
OPSGC4-F-C	28.64	2.62	4.01	6.37	9.15	14.00	1.53
OPSGC6-NF-C	28.33	1.84	3.04	5.82	6.49	10.75	1.65
OPSGC6-F-C	28.00	2.54	3.45	5.78	9.07	12.32	1.36
OPSGC8-NF-C	22.50	1.55	1.80	3.87	6.89	8.00	1.16
OPSGC8-F-C	20.97	2.12	2.25	3.53	10.08	10.71	1.06
NWGC-NF	40.63	2.24	3.68	11.39	5.50	9.05	1.64
NWGC-F	39.53	3.01	4.20	10.15	7.60	10.63	1.40

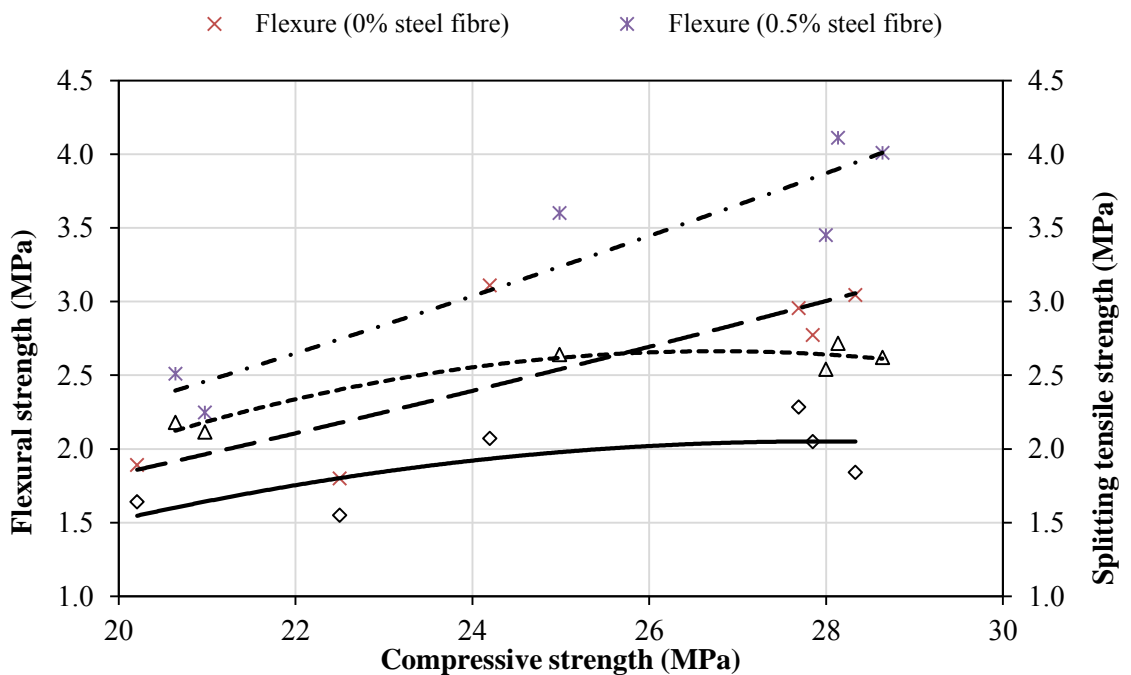


Figure 4.25: Relationship between splitting tensile, flexural and compressive strength of OPSGC with and without fibres at 28-day

Fibres enhance the splitting tensile strength significantly (Shafiqh et al., 2011c). The addition of 0.5% steel fibres, improved the splitting tensile strength of POFA-GGBS based OPSGC of about 19-38% (Figure 4.25) compared to the non-fibrous OPSGC. In this study, the splitting tensile strength for OPSGC and FROPSGC was about 6.5–8.6% and 9–12.3% of the compressive strength, respectively. Previous studies (Shafiqh et al., 2011c) found in the range of about 7.2% and 9.6–12.3% of the compressive strength for non-fibres and fibres oil palm shell concrete, respectively, using Portland cement and conventional mining sand (NS).

4.9.4 Flexural strength

The flexural strength of fibrous and non-fibrous OPSGC and NWGC are shown in Table 4.17. The relationship between the flexural, splitting tensile and compressive strength of fibrous and non-fibrous OPSGC and NWGC are shown in Figure 4.26. As seen in Figure 4.25, the flexural strength increases with the increase of compressive strength. The experimental 28-day flexural strength of the mixes OPSGC4-NF-UC, OPSGC6-NF-UC and OPSGC8-NF-UC were found 2.95, 3.11 and 1.89 MPa, respectively, and these strength are about 6.6%, 2.2% and 5% higher compared to the corresponding mixes prepared using crushed OPS aggregate. As discussed in Section 4.8.3.2., the lower size of crushed OPS particles in OPSGC attributed to the large quantity of OPS used in these mixes. For a given weight of crushed OPS content in a mix, due to the smaller size of crushed OPS a larger number of crushed OPS particles are present compared to that of uncrushed OPS (Mo et al., 2014b). It was found from mixes OPSGC4-NF-UC and OPSGC6-NF-UC that there was a slight improvement of flexural strength by increasing the OPS contents as OPS to binder weight ratio from 0.4 to 0.6 and further increase in OPS reduced the strength. Similar pattern investigated for the specimens prepared using

crushed OPS aggregate for the corresponding mixes. It could be due to the very less quantity of OPS presented to the former that did not affect much on the flexural strength. But excess OPS could cause bond failure between the OPS and the matrix occurred along with failure of the OPS itself as discussed earlier in Section 4.8.3.2 and Figure 4.16.

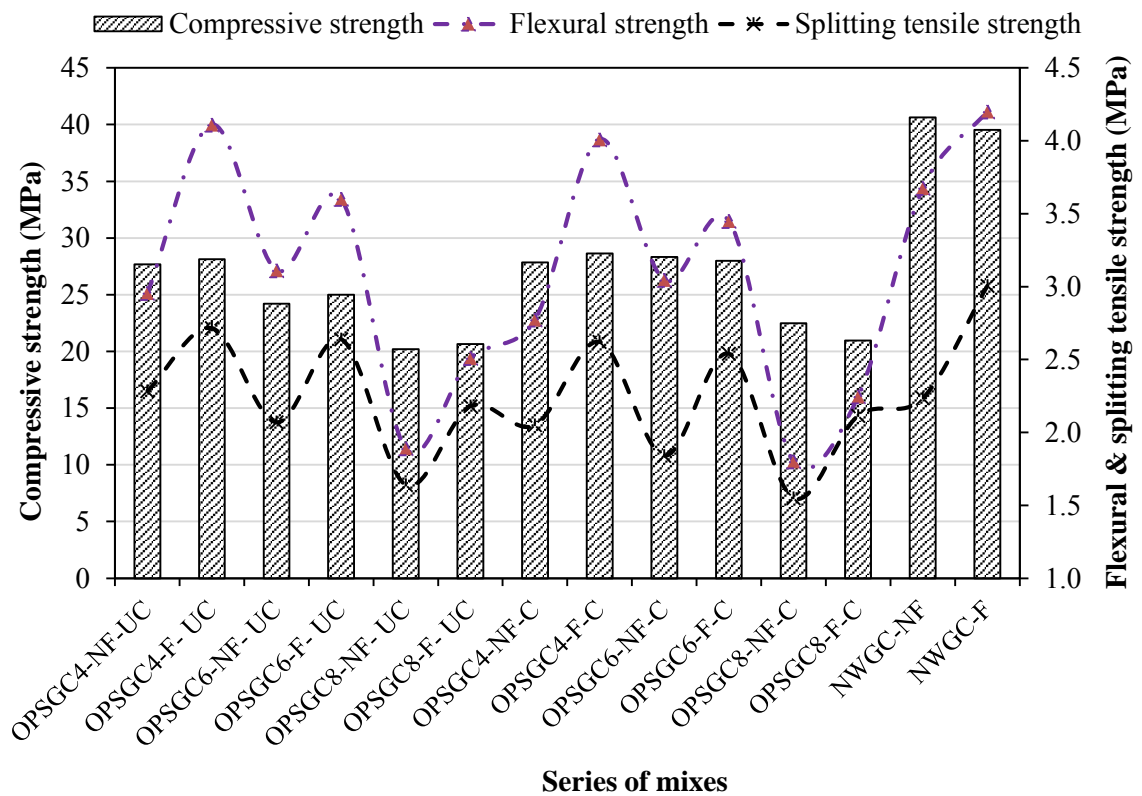


Figure 4.26: Flexural and splitting tensile strength with respect to compressive strength and OPS contents

The addition of steel fibres increases both the splitting tensile and flexural strength. The addition of 0.5% steel fibres, enhanced the flexural strength of POFA-GGBS based OPSGC of about 13-44% (Figure 4.25 and Figure 4.26) compared to the non-fibrous OPSGC. This could be attributed to the strong bond and the matrix between the aggregates and the steel fibres. In this study, the flexural strength for OPSGC and FROPSGC was about 8–13% and 11–15% of the compressive strength, respectively and in average, the flexural strength of lightweight OPSGC and FROPSGC was found

approximately 34% higher than the splitting tensile strength; generally it is 35% as reported earlier investigations (Zheng et al., 2001).

4.9.5 Modulus of elasticity (E- value) for OPSGC with and without steel fibres

The values of static modulus of elasticity (E) of all the mixes with and without fibre are shown in Table 4.17. As seen in Table 4.17 and Figure 4.27, the addition of steel fibres in OPSGC does not have a significant effect on the (E) value. It is reported (Mehta & Monteiro, 2006) that the inclusion of steel fibres in concrete has little effect on the (E) value. It was found from this study that the E-values of NWGC are higher than the values obtained for OPSGC. Generally, the (E) value of OPS concrete is lower than the other types of lightweight aggregate concrete (LWAC) (Shafiq et al., 2010). The reasons already discussed earlier in Section 4.8.5

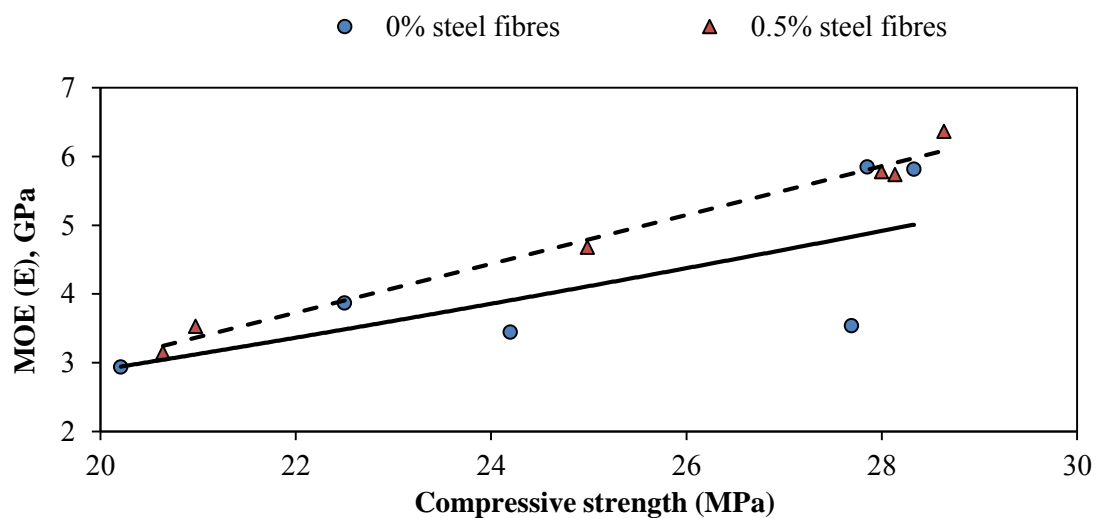


Figure 4.27. The relationship between MOE and compressive strength (at 28-day) of OPSGC with and without steel fibres

4.10 Impact energy

The aggregate impact value (AIV) of OPS is much lower than the crushed granite aggregate and this shows the OPS have high impact energy absorption capacity. Thus,

the impact energy of the OPSGC was investigated using standard panels of 600 mm × 600 mm × 50 mm. To the authors' best knowledge, this is the first time impact test was carried out on geopolymer concrete. Since there is no published literature for the impact capacity of POFA-GGBS based OPSGC, it plays an important role to study the effect of the OPS aggregate in geopolymer concrete both with fibrous and non-fibrous OPSGC.

4.10.1 First crack impact energy

The impact energy and the number of blows to cause first crack are shown in

Table 4.18 and Figure 4.28, respectively. The first cracks in the specimens without fibre was visible and the number of blows to cause the first crack was lower compared to specimens with fibres. However, the number of blow to cause first crack was not much different due to low fibre content. Though the effect of OPS content to cause first crack in the specimens without fibre is not significant due to increase of OPS content from 0.6 to 0.8. The addition of steel fibres, however, there is slight improvement in the number of blows to cause first crack. The effect of steel fibre in both the impact energy and the first crack is quite significant due to brittle nature of lightweight concrete (LWC). Generally LWC is brittle (Chen & Liu, 2005), but OPS concrete (OPSC) has ductility characteristic (Alengaram et al., 2008a).

Table 4.18: Impact test results tested on OPSGC with and without steel fibre

Mix	Blow number to cause first crack	Impact energy (first crack), $E_{impact, 1st, cr} (J)$	Blow number to cause specimen failure	Impact energy (specimen failure), $E_{impact, fail} (J)$	Impact ductile index, μ_i
OPSGC4-NF-UC	2	58.86	13	382.59	6.5
OPSGC4-F- UC	4	117.72	164	4826.52	41.0
OPSGC6-NF- UC	2	58.86	33	971.19	16.5
OPSGC6-F- UC	7	206.01	202	5944.86	28.9
OPSGC8-NF- UC	3	88.29	41	1206.63	13.7
OPSGC8-F- UC	6	176.58	110	3237.30	18.3
OPSGC4-NF-C	2	58.86	8	235.44	4.0
OPSGC4-F-C	3	88.29	65	1912.95	21.7
OPSGC6-NF-C	2	58.86	17	500.31	8.5
OPSGC6-F-C	5	147.15	195	5738.85	39.0
OPSGC8-NF-C	2	58.86	31	912.33	15.5
OPSGC8-F-C	3	88.29	95	2795.85	31.7

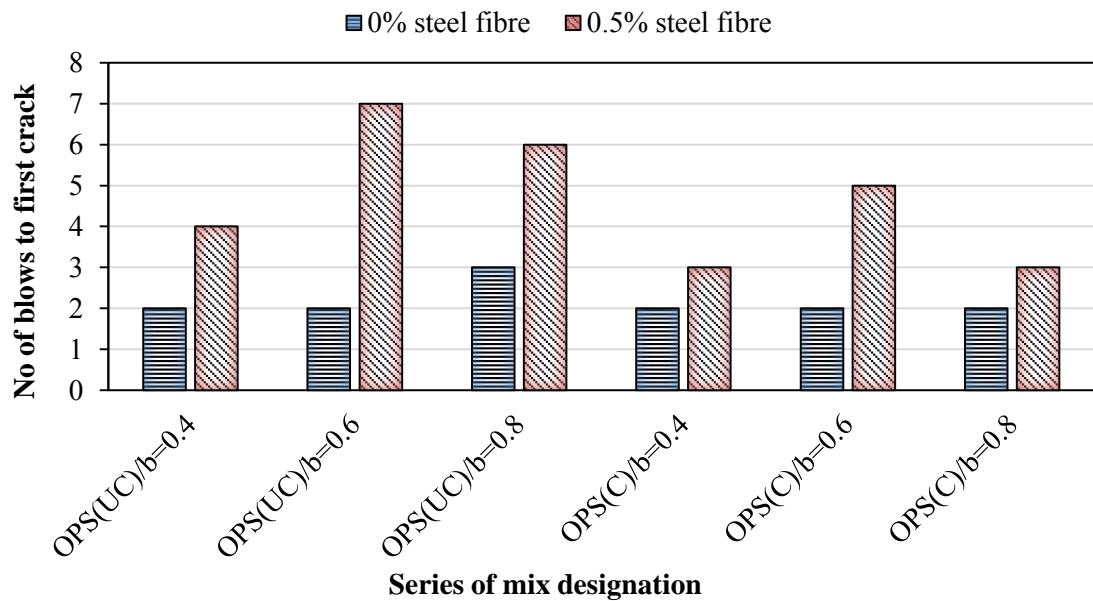


Figure 4.28: Relationship between OPS content and blow number to cause first crack under impact test

The effect of steel fibre to the first crack impact resistance of fibre reinforced oil palm shell geopolymer concrete (FROPSGC) on the addition of steel fibres was observed.

Table 4.18 shows, after adding 0.5% steel fibre, the first crack strength of the geopolymer concrete increases by 1.5 – 3.5 times compared to the corresponding mixes of OPSGC without fibre. The steel fibres were found highly effective in preventing the growth of micro-cracks and diminishing the propagation of these cracks before the cracks joined up to form macro-cracks. The first crack impact strength of uncrushed OPS mixes were found higher than that of the crushed OPS mixes. This could be attributed to the low AIV of uncrushed OPS as these aggregates resist impact due to their shape and orientation of the aggregate during the impact test (Mo et al., 2014b).

4.10.2 Ultimate impact energy

Table 4.18 and Figure 4.29 show the number of blows and impact energy to cause specimen failure under impact test. The impact ductile index (μ_i), is defined as the ratio of the ultimate and initial impact energies. This ratio offers a good indication to the ductility of the concrete subjected to impact load. It was found that the ultimate impact energy of OPSGC and FROPSGC was significantly higher than the first crack impact energy. The mixes without fibre (OPSGC4-NF-UC, OPSGC6-NF-UC, OPSGC8-NF-UC, OPSGC4-NF-C, OPSGC6-NF-C, OPSGC8-NF-C) show the increase in the ultimate impact energy as the OPS content increases (Table 4.18). But in the case of FROPSGC, the optimum OPS to binder (OPS/b) ratio was found 0.6 (OPSGC6-F-UC, OPSGC6-F-C). After the formation of the first cracks, the FROPSGC was able to sustain large amount of impact load before it failed. This could be attributed to the hooked-ends steel fibres has high tensile strength and also better cohesion due to their hooked-ends (Nia et al., 2012).

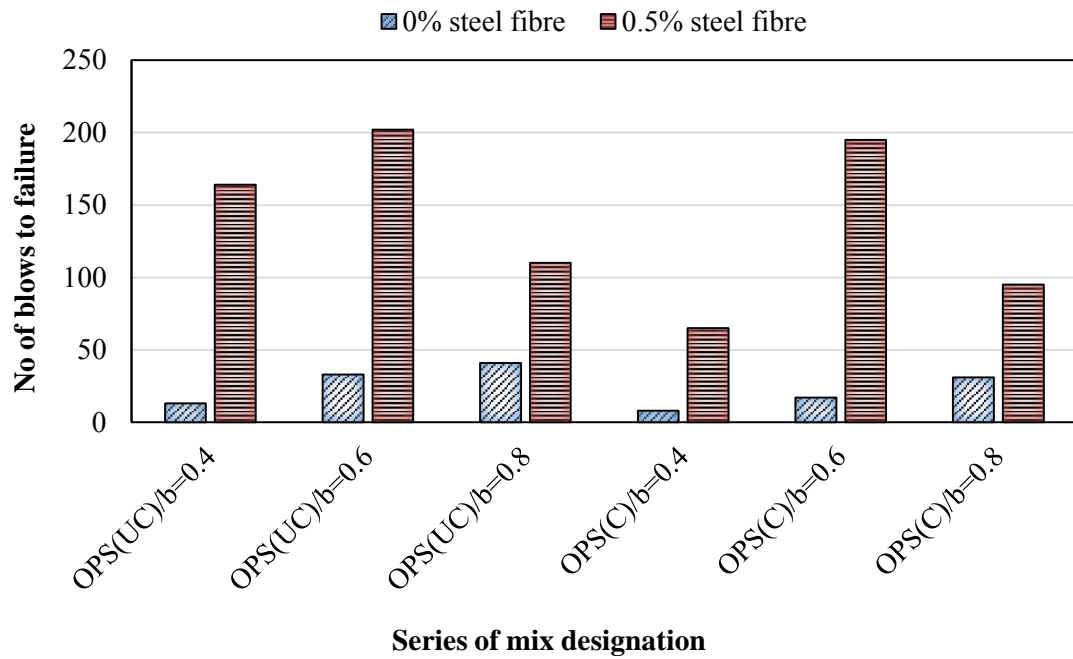


Figure 4.29: Relationship between OPS content and blow number to cause specimen failure under impact test

The effect of uncrushed OPS aggregate became more significant during the post-crack stage when subjected to impact load. Table 4.18 represents that the impact ductile index (μ_i) of all uncrushed OPS mixes were significantly higher compared to the corresponding crushed OPS mixes. The ultimate impact energy of most of the OPSGC and FROPSGC with uncrushed OPS was 15–152% higher compared to the corresponding mixes with the crushed OPS aggregate. The uncrushed OPS with lower aggregate impact value (approx. AIV = 2.63) compared to the crushed OPS (approx. AIV = 3.13). When the cracks originated and encountered with the uncrushed OPS aggregates, more energy is required to force the cracks through the aggregates (Figure 4.30) compared to the crushed aggregates.

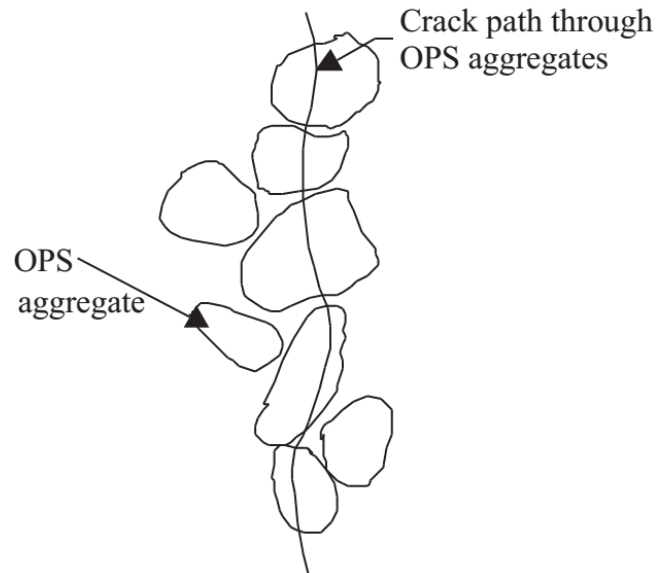


Figure 4.30. Origination process of crack through OPS aggregates at late age (Teo et al., 2006)

The ductility index (μ_i) of FROPSGC was higher than the corresponding mixes without fibres by 1.3 – 6.3 times (

Table 4.18). The highest final impact energy of 5945 J was obtained for FROPSGC (mixes OPSGC6-F-UC) with the combination of the OPS to binder weight ratio of 0.6 and 0.5% steel fibres.

4.10.3 Failure mode

Failure pattern of the OPSGC is shown in Figure 4.31. Two different types of failure pattern were found in the OPSGC panel specimens. For the plain non-fibrous OPSGC, the concrete panel broke into four pieces upon failure (Figure 4.31a). The OPSGC lost its structural integrity and geometry upon reaching the impact energy capacity. Nevertheless the failure of the FROPSGC was due to perforation of the panels by the drop weight hammer and the specimen was not broken into pieces, unlike plane OPSGC panels (Figure 4.31b). This behaviour indicated that the FROPSGC panels remained structurally integral, and also ductile. The failure pattern of FROPSGC also shows with a significant number of secondary cracks.

4.10.4 Crack development resistance

Table 4.19 shows the crack width and number of secondary cracks prior to failure of geopolymer concrete panel. The initial crack width was used as a comparative study to determine the effectiveness of the steel fibre in bridging micro-cracks in the geopolymer concrete. Initial crack widths of the control mixes OPSGC4-NF-UC and OPSGC4-NF-C were found to be around 0.240 and 0.252 mm, respectively. OPS was found to be effective in diminishing the propagation of micro-crack. By increasing OPS content as OPS to binder weight ratio from 0.4 to 0.8, reduction in the initial crack width was found to be about 16 – 20%, in both specimens with uncrushed and crushed OPS aggregates. The reduction in the initial crack width in the FROPSGC specimens was found to be about 54 – 39% and 55 – 40% in the uncrushed and crushed OPS specimens, respectively, compared to the corresponding plain OPSGC. The lowest crack widths of 0.095 mm was found in the specimens with 0.5% of steel fibre of mix OPSGC8-F- UC.

Table 4.19: Crack widths and number of secondary cracks prior to failure of all mixes

Mix	Crack width (mm)		Number of secondary cracks
	First crack	Final crack	
OPSGC4-NF-UC	0.240	1.037	0
OPSGC4-F- UC	0.110	0.470	6
OPSGC6-NF- UC	0.190	0.730	3
OPSGC6-F- UC	0.099	0.440	9
OPSGC8-NF- UC	0.155	0.860	5
OPSGC8-F- UC	0.095	0.930	17
OPSGC4-NF-C	0.252	1.212	0
OPSGC4-F-C	0.112	0.509	5
OPSGC6-NF-C	0.211	0.790	4
OPSGC6-F-C	0.105	0.428	8
OPSGC8-NF-C	0.169	0.968	5
OPSGC8-F-C	0.100	1.010	15

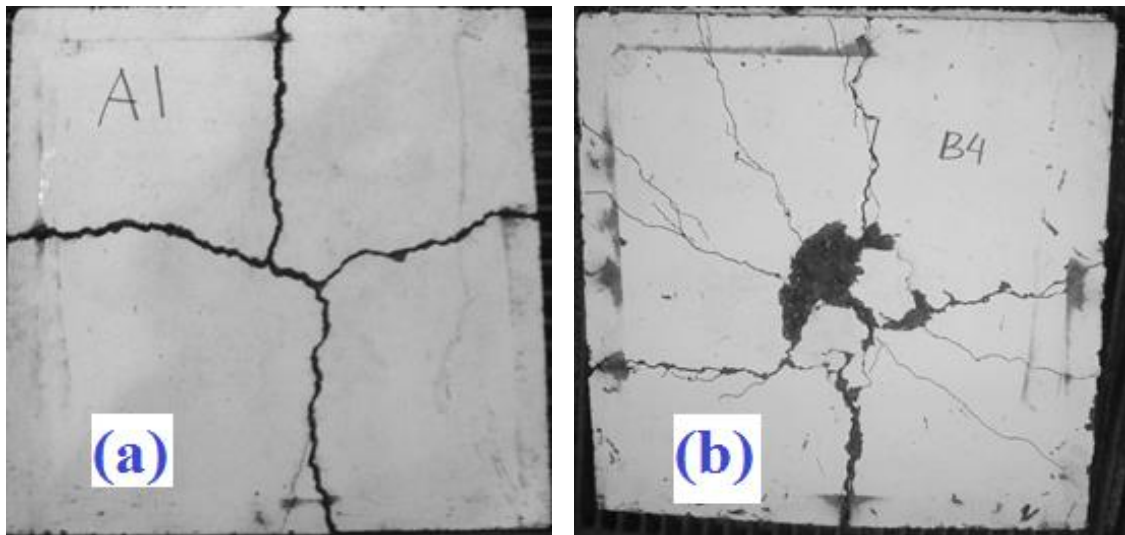


Figure 4.31: (a) Primary cracks in OPSGC panel; and (b) primary and secondary cracks in FROPSGC panel

The secondary cracks initiated to visible just before to the failure in the FROPSGC specimens as shown in Figure 4.31b. The plain OPSGC specimens had no secondary cracks upon failure (Figure 4.31a). The formation of the secondary cracks is an indication of the effect of fibres in arresting and preventing the crack growth.

CHAPTER 5 : CONCLUSIONS AND RECOMMENDATIONS

5.1 Introduction

This chapter presents a summary of the present study, the major conclusions and some recommendations for future research. The main aim of the study was to develop appropriate mixture design for mortar and to utilize it for further mixes in concrete; the mechanical properties of the GGBS-POFA based OPS geopolymer concrete was investigated. In addition, the effects of three different types of fine aggregate – conventional mining sand (NS), manufactured sand (MS) and quarry dust (QD), were studied in two different environment, namely, oven-dry and ambient curing conditions. Another salient feature of the research was the use of fibres in the OPS geopolymer concrete (OPSGC) and its effect on mechanical properties and impact resistance. Based on the experimental investigations, many conclusions could be drawn. The following sub-sections summarize the conclusions based on the objectives of the research.

5.2 Summary of Conclusions

Based on the experimental work reported in this study, the following conclusions are drawn:

Objective 1: To develop appropriate mixture design for geopolymer mortar using ground granulated blastfurnace slag (GGBS), palm oil fuel ash (POFA) and fly ash (FA) as binder.

- The compressive strength of geopolymer mortar increases as the GGBS content is increased up to 70%. Further increase in GGBS content did not produce desired effect.

- The addition of POFA up to 30% with GGBS produced the highest strength and hence it is recommended for strength beyond 60 MPa.
- In most of the specimens 90% of compressive strength of geopolymer mortar was achieved at 7 days.
- The finer particles of GGBS produce dense mix and hence the density of mortar produced using GGBS resulted in about 8% of density increase.
- The use of locally available waste materials such as GGBS, POFA, FA and MS could be used for development of sustainable construction material.

Objective 2: To study the effect of crushed and uncrushed oil palm shell (OPS) as a coarse aggregate and three types of sand (mining sand, manufactured sand and quarry dust) in the geopolymer structural concrete.

- The oven-dry densities of all the OPSGC specimens fell within the range of 1900–1935 kg/m³ and hence fulfilled the requirement for LWC as stipulated in EN206–1.
- The use of manufactured sand as an ideal replacement for the conventional sand is recommended.
- The mixture contained quarry dust produced slightly lower strength compared to natural sand and manufactured sand.
- The OPSGC specimens prepared using crushed OPS aggregate produced lower slump values compared to those specimens prepared using uncrushed OPS aggregate due to the high mortar demand.
- The OPSGC prepared using crushed OPS aggregate produced slightly higher compressive strength of about 7–14% and 3–7% cured in OD and AD, respectively, compared to the corresponding mixes prepared using uncrushed OPS aggregate.

- The splitting tensile and flexural strength of POFA-GGBS based geopolymer concrete is about 6–9% and 9–11% of the compressive strength, respectively.
- The E-value of POFA-GGBS based OPSGC using conventional mining sand was found 11.12 GPa for cube compressive strength of 32 MPa.
- The Poisson's ratio of OPSGC was found about 0.15 to 0.17.

Objective 3: To investigate the effect of curing on the mechanical properties of geopolymer concrete.

- Most of the specimens of geopolymer concrete reached 90% of the 28-day compressive strength at 3-day for OD curing, while AD curing specimens reached 57–82%; however, the final strength of AD curing specimens found slightly higher than the corresponding OD cured specimens at 28-day.
- The early strength development of 92–100% and 81–97% of 28-day compressive strength, respectively, for OD and AD curing at 7 days for both the OPSGC and NWGC, which points to geopolymerization at an early age. The rate of increase in compressive strength in the oven-cured specimens after 7 days is not significant.
- As air curing achieved adequate strength in calcium-based geopolymer concrete, which reduces the energy usage.
- POFA-based geopolymer modified with GGBS is found to be a suitable binder for low to moderate strength or structural grade concrete production at ambient curing as it eliminates the necessity of heat curing.

Objective 4: To investigate the effect of variation in OPS contents and steel fibre on the mechanical properties of geopolymer concrete.

- The density of OPSGC decreases as the OPS content increases.
- The compressive strength of OPSGC decreases as the OPS content increases.
- The addition of 0.5% of steel fibre on volume of concrete increases the density of OPSGC about 2–3%. The rate of reduction in density for OPSGC with crushed OPS is similar to that of uncrushed OPS.
- When fibres were added, the OPSGC with crushed OPS produced the compressive strength close to that of uncrushed OPS. In general, the addition of fibres slightly improves the compressive strength of concrete.
- The rate of early strength (3- and 7-day) of OPSGC is higher compared to NWGC, both in fibrous and non-fibrous specimens.
- The splitting tensile and flexural strength of geopolymer concrete increases with the increases of compressive strength.
- The splitting tensile strength OPSGC prepared using uncrushed OPS aggregate produced about 6–12% higher compared to the corresponding mixes prepared using crushed OPS aggregate at 28-day.
- The flexural strength is about 33–35% higher than splitting tensile strength.
- The compressive strength of FROPSGC is close to the non-fibrous plane OPSGC.
- The addition of 0.5% steel fibres enhanced the splitting tensile and flexural strength of POFA-GGBS based OPSGC by about 19–38% and 13–44%, respectively compared to the non-fibrous OPSGC.
- The addition of 0.5% steel fibres in OPSGC does not have a significant effect on the (E) value.

Objective 5: To study the impact behaviour of the fibre reinforced geopolymer concrete panels with crushed and uncrushed OPS and varying OPS contents.

- The effect of steel fibre in both the impact energy and the first crack is quite significant due to brittle nature of LWC.
- Though the OPSGC specimens with crushed OPS aggregates produced higher compressive strength, its impact resistance was lower compared to the corresponding mixes of the uncrushed OPS aggregates. This could be attributed to the low AIV of uncrushed OPS as these aggregates resist impact due to their shape and orientation of the aggregate during the impact test.
- All the FROPSGC had higher first crack impact energy compared to the plane OPSGC due to the micro-crack bridging of the fibres.
- All the FROPSGC specimens resisted high impact loads before failure and produced smaller crack widths, compared to the OPSGC.
- The uncrushed OPS aggregate produced higher final impact energy due to its energy absorption capability compared to the corresponding crushed OPS specimens. The impact energy distribution in the FROPSGC specimens was clearly evident due to the formation of more number of secondary cracks in the specimens.

5.3 Recommendations for the future works

In addition to the ongoing pursuit of the goal of developing cost effective with superior performance of geopolymer concrete, there is a need for further research in the following areas:

- Further study to increase the concrete setting time to mitigate early setting problem is to be carried out.
- The effect of super-plasticizers to improve early setting of POFA-GGBS based geopolymer concrete has to be investigated.
- The mixing procedure to reduce pores in concrete has to be studied.
- Since geopolymer concrete is sticky, further study is required to improve uniform mixing of fibre.
- Study on the effectiveness of fibres in reducing shrinkage could be investigated.
- Structural behaviour of the GGBS-POFA based concrete has to be investigated.
- Composite applications and design parameters using conventional reinforcement in FROPSGC for structural applications could be investigated.
- Fire resistant properties of fibre reinforced composites needs to be studied.
- Further investigation on using FESEM, XRD, TGA, DTA and DSC techniques is suggested to study the microstructure in a more elaborate way.
- Long term properties such as fatigue, creep and shrinkage tests on POFA-GGBS based OPSGC have to be done.
- Further study to for housing applications have to be done.
- Study on thermal capacity of the GGBS-POFA based concrete has to be investigated.

REFERENCES

- ACI 363R-92. (1992). State-of-the-art report on high-strength concrete. ACI committee report 363 (Vol. 363R1–363R55): American Concrete Institute, Detroit, 363R1–363R55.
- Aldahdooh, M. A. A., Muhamad Bunnori, N., & Megat Johari, M. A. (2013). Development of green ultra-high performance fiber reinforced concrete containing ultrafine palm oil fuel ash. *Construction and Building Materials*, 48(0), 379-389.
- Aldred, J., & Day, J. (2012). *Is geopolymer concrete a suitable alternative to traditional concrete?* Paper presented at the 37th Conference on our world in concrete & structures, Singapore.
- Alengaram, U. J., Al Muhit, B. A., & Jumaat, M. Z. (2013). Utilization of oil palm kernel shell as lightweight aggregate in concrete – A review. *Construction and Building Materials*, 38(0), 161-172.
- Alengaram, U. J., Jumaat, M. Z., & Mahmud, H. (2008a). Ductility behaviour of reinforced palm kernel shell concrete beams. *European Journal of Scientific Research*, 23(3), 406-420.
- Alengaram, U. J., Jumaat, M. Z., & Mahmud, H. (2008b). *Influence of sand content and silica fume on mechanical properties of palm kernel shell concrete*. Paper presented at the International conference on construction and building technology ICCBT.
- Alengaram, U. J., Mahmud, H., & Jumaat, M. Z. (2010a). Comparison of mechanical and bond properties of oil palm kernel shell concrete with normal weight concrete. *International Journal of Physical Sciences*, 5(8), 1231-1239.
- Alengaram, U. J., Mahmud, H., & Jumaat, M. Z. (2011). Enhancement and prediction of modulus of elasticity of palm kernel shell concrete. *Materials & Design*, 32(4), 2143-2148.
- Alengaram, U. J., Mahmud, H., Jumaat, M. Z., & Shirazi, S. M. (2010b). Effect of aggregate size and proportion on strength properties of palm kernel shell concrete. *International Journal of the Physical Sciences*, 5(12)(12), 1848-1856.
- Altwair, N. M., Megat Johari, M. A., & Saiyid Hashim, S. F. (2012). Flexural performance of green engineered cementitious composites containing high volume of palm oil fuel ash. *Construction and Building Materials*, 37(0), 518-525.
- Ariffin, M. A. M., Bhutta, M. A. R., Hussin, M. W., Mohd Tahir, M., & Aziah, N. (2013). Sulfuric acid resistance of blended ash geopolymer concrete. *Construction and Building Materials*, 43(0), 80-86.
- Ashraf, M. A., Maah, M. J., Yusoff, I., Wajid, A., & Mahmood, K. (2011). Sand mining effects, causes and concerns: a case study from Bestari Jaya, Selangor, Peninsular Malaysia. *Scientific Research and Essays*, 6(6), 1216-1231.

- ASTM:C109/C109M-13. (2013). Standard Test Method for Compressive Strength of Hydraulic Cement Mortars (Using 2-in. or [50-mm] Cube Specimen). USA: ASTM International.
- ASTM:C227-10. (2010). Standard Test Method for Potential Alkali Reactivity of Cement-Aggregate Combinations (Mortar-Bar Method). Philadelphia, USA: ASTM International.
- ASTM:C618-12a. (2008). Standard Specification for Coal Fly Ash and Raw or Calcined Natural Pozzolan for Use as a Mineral Admixture in Concrete. Philadelphia, USA: ASTM International.
- ASTM:C 430. (2009). Standard test method for fineness of hydraulic cement by the 45- μ m (No. 325) sieve. Philadelphia, USA: ASTM International.
- Atiş, C. D., & Bilim, C. (2007). Wet and dry cured compressive strength of concrete containing ground granulated blast-furnace slag. *Building and Environment*, 42(8), 3060-3065.
- Bagheri, A., & Nazari, A. (2014). Compressive strength of high strength class C fly ash-based geopolymers with reactive granulated blast furnace slag aggregates designed by Taguchi method. *Materials & Design*, 54(0), 483-490.
- Bakharev, T. (2005a). Durability of geopolymer materials in sodium and magnesium sulfate solutions. *Cement and Concrete Research*, 35(6), 1233-1246.
- Bakharev, T. (2005b). Geopolymeric materials prepared using Class F fly ash and elevated temperature curing. *Cement and Concrete Research*, 35(6), 1224-1232.
- Bakharev, T. (2005c). Resistance of geopolymer materials to acid attack. *Cement and Concrete Research*, 35(4), 658-670.
- Bakharev, T. (2006). Thermal behaviour of geopolymers prepared using Class F fly ash and elevated temperature curing. *Cement and Concrete Research*, 36(6), 1134-1147.
- Bakharev, T., Sanjayan, J. G., & Cheng, Y. B. (1999). Alkali activation of Australian slag cements. *Cement and Concrete Research*, 29(1), 113-120. doi: Doi 10.1016/S0008-8846(98)00170-7
- Basri, H. B., Mannan, M. A., & Zain, M. F. M. (1999). Concrete using waste oil palm shells as aggregate. *Cement and Concrete Research*, 29(4), 619-622.
- Bernal, S., De Gutierrez, R., Delvasto, S., & Rodriguez, E. (2010). Performance of an alkali-activated slag concrete reinforced with steel fibers. *Construction and Building Materials*, 24(2), 208-214.
- Bogas, J. A., Gomes, M. G., & Gomes, A. (2013). Compressive strength evaluation of structural lightweight concrete by non-destructive ultrasonic pulse velocity method. *Ultrasonics*, 53(5), 962-972.
- BS 146. (1996). Specification for Portland blastfurnace cements (9 ed.). London, UK: BSI.

- BS 1881-116. (1983). Testing concrete —Part 116: Method for determination of compressive strength of concrete cubes. London: BSI.
- BS 6699. (1992). Ground granulated blastfurnace slag for use with Portland cement (2 ed.). London, UK: BSI.
- BS 8110-2. (1985). Structural use of concrete- Part 2: Code of practice for special circumstances. London: BSI.
- BS EN 12350-2. (2009). Testing fresh concrete Slump-test. London, UK: BSI.
- BS EN 12390-3. (2009). Testing hardened concrete. Part 3: Compressive strength of test specimens. London, UK: BSI.
- BS EN 12390-7. (2009). Testing hardened concrete Density of hardened concrete: BSI.
- BS EN 12504-4. (2004). Testing concrete Determination of ultrasonic pulse velocity. London, UK: BSI.
- CEB-FIP. (1993). Model code 1990 (Design Code). London, UK: Thomas Telford.
- Celik, T., & Marar, K. (1996). Effects of crushed stone dust on some properties of concrete. *Cement and Concrete Research*, 26(7), 1121-1130.
- Chandra, S., & Berntsson, L. (2002). *Lightweight aggregate concrete*. Norwich, New York: William Andrew Publishing.
- Chen, B., & Liu, J. (2005). Contribution of hybrid fibers on the properties of the high-strength lightweight concrete having good workability. *Cement and Concrete Research*, 35(5), 913-917.
- Clarke, J. L., editor. (2005). *Structural lightweight aggregate concrete* (J. L. Clarke Ed.): Taylor & Francis e-Library.
- Collins, F. (2010). Inclusion of carbonation during the life cycle of built and recycled concrete: influence on their carbon footprint. *The International Journal of Life Cycle Assessment*, 15(6), 549-556.
- Davidovits, J. (1994). Geopolymers: Man-made rock geosynthesis and the resulting development of very early high strength cement. *Journal of Materials education*, 16, 91-139.
- Davidovits, J. (2002). *30 Years of successes and failures in geopolymer applications. Market trends and potential breakthroughs*. Paper presented at the Geopolymer 2002 conference., Melbourne, Australia.
- Davidovits, J. (2011). *Geopolymer chemistry and applications* (3 ed.). France: Geopolymer Institute.
- EN 206-1. (2000). Concrete - Part 1: Specification, performance, production and conformity: European Committee for Standardization CEN.
- ENV 1992-1-1: Part 1. (1991). Design of concrete structures, Part 1 General rules and rules for buildings, Final draft, European Committee for Standardization (*Part*

IC, The use of lightweight concrete with closed structures, to be issued as ENV 1992-1-4.) Brussels.

- Ernst Worrell, Lynn Price, Nathan Martin, Chris Hendriks, & Leticia Ozawa Meida. (2001). Carbondioxide Emissions from the Global Cement Industry (E. Environ., Trans.) (Vol. 26, pp. 303-329). Annu. Rev. Energy Environ., US: Lawrence Berkeley National Laboratory, Berkeley, California 94720.
- FIP Manual. (1983). FIP Manual of Lightweight aggregate concrete (2nd ed.). London, UK: Surrey University Press.
- Gesoğlu, M., Özturan, T., & Güneyisi, E. (2004). Shrinkage cracking of lightweight concrete made with cold-bonded fly ash aggregates. *Cement and Concrete Research*, 34(7), 1121-1130.
- Haque, M. N., Al-Khaiat, H., & Kayali, O. (2004). Strength and durability of lightweight concrete. *Cement and Concrete Composites*, 26(4), 307-314.
- Hardjito, D., & Rangan, B. V. (2005). Development and Properties of Low-Calcium Fly Ash-Based Geopolymer Concrete: Curtin University, Perth, Australia.
- Hardjito, D., Wallah, S. E., Sumajouw, D. M., & Rangan, B. V. (2004). On the development of fly ash-based geopolymer concrete. *ACI Materials Journal-American Concrete Institute*, 101(6), 467-472.
- Huntzinger, D. N., & Eatmon, T. D. (2009). A life-cycle assessment of Portland cement manufacturing: comparing the traditional process with alternative technologies. *Journal of Cleaner Production*, 17(7), 668-675.
- Islam, A., Alengaram, U. J., Jumaat, M. Z., & Bashar, I. I. (2014). The development of compressive strength of ground granulated blast furnace slag-palm oil fuel ash-fly ash based geopolymer mortar. *Materials & Design*, 56(0), 833-841.
- Johari, M. A. M., Zeyad, A. M., Bunnori, N. M., & Ariffin, K. S. (2012). Engineering and transport properties of high-strength green concrete containing high volume of ultrafine palm oil fuel ash. *Construction and Building Materials*, 30(0), 281-288.
- Kanadasan, J., & Razak, H. A. (2014). Mix design for self-compacting palm oil clinker concrete based on particle packing. *Materials & Design*, 56(0), 9-19.
- Khale, D., & Chaudhary, R. (2007). Mechanism of geopolymerization and factors influencing its development: a review. *Journal of Materials Science*, 42(3), 729-746.
- Kosmatka, S. H., Kerkhoff, B., & Panarese, W. C. (2002). *Design and control of concrete mixtures* (14 ed.). USA: Portland Cement Association.
- Kou, S.-C., & Poon, C.-S. (2013). Effects of different kinds of recycled fine aggregate on properties of rendering mortar. *Journal of Sustainable Cement-Based Materials*, UK, 2(1), 43-57. doi: 10.1080/21650373.2013.766400

- Kroehong, W., Sinsiri, T., Jaturapitakkul, C., & Chindapasirt, P. (2011). Effect of palm oil fuel ash fineness on the microstructure of blended cement paste. *Construction and Building Materials*, 25(11), 4095-4104.
- Kupaei, R. H., Alengaram, U. J., Jumaat, M. Z., & Nikraz, H. (2013). Mix design for fly ash based oil palm shell geopolymer lightweight concrete. *Construction and Building Materials*, 43(0), 490-496.
- Li, C., Sun, H., & Li, L. (2010). A review: The comparison between alkali-activated slag (Si+Ca) and metakaolin (Si+Al) cements. *Cement and Concrete Research*, 40(9), 1341-1349.
- Lim, S. K., Tan, C. S., Lim, O. Y., & Lee, Y. L. (2013). Fresh and hardened properties of lightweight foamed concrete with palm oil fuel ash as filler. *Construction and Building Materials*, 46(0), 39-47.
- Lloyd, N., & Rangan, B. V. (2010). *Geopolymer Concrete with Fly Ash*. Paper presented at the Second International Conference on Sustainable Construction Materials and Technologies, Ancona, Italy. http://espace.library.curtin.edu.au/R/?func=dbin-jump-full&object_id=148638&local_base=GEN01-ERA02
- Lo, T. Y., Cui, H. Z., & Li, Z. G. (2004). Influence of aggregate pre-wetting and fly ash on mechanical properties of lightweight concrete. *Waste Manag*, 24(4), 333-338.
- Lohani, T., Padhi, M., Dash, K., & Jena, S. (2012). Optimum utilization of Quarry dust as partial replacement of sand in concrete. *International Journal of Applied Science and Engineering Research*, 1(2), 391-404.
- Malhotra, V. (1999). Making concrete" greener" with fly ash. *CONCRETE INTERNATIONAL-DETROIT*, 21, 61-66.
- Malhotra, V. (2002). High-performance high-volume fly ash concrete. *CONCRETE INTERNATIONAL-DETROIT*, 24(7), 30-34.
- Mannan, M. A., Alexander, J., Ganapathy, C., & Teo, D. C. L. (2006). Quality improvement of oil palm shell (OPS) as coarse aggregate in lightweight concrete. *Building and Environment*, 41(9), 1239-1242.
- Mannan, M. A., & Ganapathy, C. (2002). Engineering properties of concrete with oil palm shell as coarse aggregate. *Construction and Building Materials*, 16(1), 29-34.
- Mehta, P. K., & Monteiro, P. J. (2006). *Concrete: microstructure, properties, and materials* (Vol. 3): McGraw-Hill New York.
- Meyer, C. (2009). The greening of the concrete industry. *Cement and Concrete Composites*, 31(8), 601-605.
- Mijarsh, M. J. A., Megat Johari, M. A., & Ahmad, Z. A. (2014). Synthesis of geopolymer from large amounts of treated palm oil fuel ash: Application of the Taguchi method in investigating the main parameters affecting compressive strength. *Construction and Building Materials*, 52(0), 473-481.

- Mo, K. H., Alengaram, U. J., & Jumaat, M. Z. (2014a). Utilization of ground granulated blast furnace slag as partial cement replacement in lightweight oil palm shell concrete. *Materials and Structures*, 1-12. doi: 10.1617/s11527-014-0336-1
- Mo, K. H., Yap, S. P., Alengaram, U. J., Jumaat, M. Z., & Bu, C. H. (2014b). Impact resistance of hybrid fibre-reinforced oil palm shell concrete. *Construction and Building Materials*, 50(0), 499-507.
- Mohammed, B. S., Al-Ganad, M. A., & Abdullahi, M. (2011). Analytical and experimental studies on composite slabs utilising palm oil clinker concrete. *Construction and Building Materials*, 25(8), 3550-3560.
- Mohammed, B. S., Foo, W. L., & Abdullahi, M. (2014). Flexural strength of palm oil clinker concrete beams. *Materials & Design*, 53(0), 325-331.
- Mohammed, B. S., Foo, W. L., Hossain, K. M. A., & Abdullahi, M. (2013). Shear strength of palm oil clinker concrete beams. *Materials & Design*, 46(0), 270-276.
- Mohammed, M. H., Al-Gburi, M., Al-Ansari, N., Jonasson, J. E., Pusch, R., & Knutsson, S. (2012). Design of concrete mixes by systematic steps and ANN. *Journal of Advanced Science and Engineering Research Vol*, 2(4September), 232-251.
- Mosley, W. H., & Bungey, J. H. (1990). *Reinforced concrete design* (4 ed.). London, UK: Macmillan.
- MPOB. (2012). Overview of the Malaysian Oil Palm Industry.
- Naidu, P. G., Prasad, A. S. S. N., Adishesu, S., & Satayanarayana, P. V. V. (2012). A study on strength properties of geopolymers concrete with addition of G.G.B.S. *International Journal of Engineering Research and Development*, 2(4), 19-28.
- Nazari, A., & Khalaj, G. (2012). Prediction compressive strength of lightweight geopolymers by ANFIS. *Ceramics International*, 38(6), 4501-4510.
- Neville, A. M. (1995). *Properties of concrete* (Vol. 4): Longman London.
- Newman, J., & Choo, B. S., editors. (2003). *Advanced concrete technology constituent materials*: Elsevier Ltd.
- Nia, A. A., Hedayatian, M., Nili, M., & Sabet, V. A. (2012). An experimental and numerical study on how steel and polypropylene fibers affect the impact resistance in fiber-reinforced concrete. *International journal of impact engineering*, 46(0), 62-73.
- Okafor, F. O. (1988). Palm kernel shell as a lightweight aggregate for concrete. *Cement and Concrete Research*, 18(6), 901-910.
- Pakiam, R. (2013, 04/01/2013). Palm Oil Advances as Malaysia's Export Tax May Boost Shipments. *Bloomberg*. Retrieved from <http://www.bloomberg.com/news/2013-01-04/palm-oil-advances-as-malaysia-s-export-tax-may-boost-shipments.html>
- Pangdaeng, S., Phoo-ngernkham, T., Sata, V., & Chindaprasirt, P. (2014). Influence of curing conditions on properties of high calcium fly ash geopolymer containing Portland cement as additive. *Materials & Design*, 53(0), 269-274.

- Phoo-ngernkham, T., Chindaprasirt, P., Sata, V., Hanjitsuwan, S., & Hatanaka, S. (2014). The effect of adding nano-SiO₂ and nano-Al₂O₃ on properties of high calcium fly ash geopolymer cured at ambient temperature. *Materials & Design*, 55(0), 58-65.
- Puertas, F., Amat, T., Fernández-Jiménez, A., & Vázquez, T. (2003). Mechanical and durable behaviour of alkaline cement mortars reinforced with polypropylene fibres. *Cement and Concrete Research*, 33(12), 2031-2036.
- Puligilla, S., & Mondal, P. (2013). Role of slag in microstructural development and hardening of fly ash-slag geopolymer. *Cement and Concrete Research*, 43(0), 70-80.
- Raman, S. N., Ngo, T., Mendis, P., & Mahmud, H. B. (2011). High-strength rice husk ash concrete incorporating quarry dust as a partial substitute for sand. *Construction and Building Materials*, 25(7), 3123-3130.
- Rao, M. C., Bhattacharyya, S. K., & Barai, S. V. (2011). Behaviour of recycled aggregate concrete under drop weight impact load. *Construction and Building Materials*, 25(1), 69-80.
- Razak, H. A., & Sajedi, F. (2011). The effect of heat treatment on the compressive strength of cement-slag mortars. *Materials & Design*, 32(8-9), 4618-4628.
- Reddy, B. V. V. (2012). *Suitability of Manufacture Sand (M-Sand) as fine aggregate in mortars and concrete*. (CSIC project: CP 6597/0505/11-330). India: Indian Institute of Science.
- Ryu, G. S., Lee, Y. B., Koh, K. T., & Chung, Y. S. (2013). The mechanical properties of fly ash-based geopolymer concrete with alkaline activators. *Construction and Building Materials*, 47(0), 409-418.
- Safiuddin, M., Abdus Salam, M., & Jumaat, M. Z. (2011). Utilization of palm oil fuel ash in concrete: a review. *Journal of Civil Engineering and Management, UK*, 17(2), 234-247.
- Sata, V., Jaturapitakkul, C., & Kiattikomol, K. (2004). Utilization of palm oil fuel ash in high-strength concrete. *Journal of materials in civil engineering*, 16(6), 623-628.
- Sata, V., Jaturapitakkul, C., & Rattanashotinunt, C. (2010). Compressive strength and heat evolution of concretes containing palm oil fuel ash. *Journal of Materials in Civil Engineering @ ASCE, USA*, 22(10), 1033-1038.
- Shafigh, P., Alengaram, U. J., Mahmud, H., & Jumaat, M. Z. (2013a). Engineering properties of oil palm shell lightweight concrete containing fly ash. *Materials & Design*, 49, 613-621.
- Shafigh, P., Jumaat, M. Z., & Mahmud, H. (2010). Mix design and mechanical properties of oil palm shell lightweight aggregate concrete: A review. *International Journal of the Physical Sciences*, 5(14), 2127-2134.
- Shafigh, P., Jumaat, M. Z., & Mahmud, H. (2011a). Oil palm shell as a lightweight aggregate for production high strength lightweight concrete. *Construction and Building Materials*, 25(4), 1848-1853.

- Shafigh, P., Jumaat, M. Z., Mahmud, H., & Alengaram, U. J. (2013b). Oil palm shell lightweight concrete containing high volume ground granulated blast furnace slag. *Construction and Building Materials*, 40(0), 231-238.
- Shafigh, P., Jumaat, M. Z., Mahmud, H. B., & Alengaram, U. J. (2011b). A new method of producing high strength oil palm shell lightweight concrete. *Materials & Design*, 32(10), 4839-4843.
- Shafigh, P., Jumaat, M. Z., Mahmud, H. B., & Hamid, N. A. A. (2012). Lightweight concrete made from crushed oil palm shell: Tensile strength and effect of initial curing on compressive strength. *Construction and Building Materials*, 27(1), 252-258.
- Shafigh, P., Mahmud, H., & Jumaat, M. Z. (2011c). Effect of steel fiber on the mechanical properties of oil palm shell lightweight concrete. *Materials & Design*, 32(7), 3926-3932.
- Shetty, M. (2005). *Concrete technology: theory and practice*. New Delhi, India: S. Chand & Company Ltd.
- Short, A., & Kinniburgh, W. (1978). *Lightweight concrete* (3rd ed.). London: Applied Science Publishers.
- Smadi, M., & Migdady, E. (1991). Properties of high strength tuff lightweight aggregate concrete. *Cement and Concrete Composites*, 13(2), 129-135.
- Solís-Carcaño, R., & Moreno, E. I. (2008). Evaluation of concrete made with crushed limestone aggregate based on ultrasonic pulse velocity. *Construction and Building Materials*, 22(6), 1225-1231.
- Sreenivasa, G. (2012). Use of manufactured sand in concrete and construction an alternate to river sand. NBMCW, India.
- Tangchirapat, W., Jaturapitakkul, C., & Chindapasirt, P. (2009). Use of palm oil fuel ash as a supplementary cementitious material for producing high-strength concrete. *Construction and Building Materials*, 23(7), 2641-2646.
- Tangchirapat, W., Khamklai, S., & Jaturapitakkul, C. (2012). Use of ground palm oil fuel ash to improve strength, sulfate resistance, and water permeability of concrete containing high amount of recycled concrete aggregates. *Materials & Design*, 41(0), 150-157.
- Teo, D. C. L., Mannan, M. A., & Kurian, V. J. (2006). Structural concrete using oil palm shell (OPS) as lightweight aggregate. *Turkish Journal of Engineering and Environmental Sciences*, 30(4), 251-257.
- Tho-in, T., Sata, V., Chindapasirt, P., & Jaturapitakkul, C. (2012). Pervious high-calcium fly ash geopolymer concrete. *Construction and Building Materials*, 30(0), 366-371.
- Turner, L. K., & Collins, F. G. (2013). Carbon dioxide equivalent (CO₂-e) emissions: A comparison between geopolymer and OPC cement concrete. *Construction and Building Materials*, 43(0), 125-130.

- UNEP. (2012). 21 issues for the 21st Century: results of the UNEP Foresight Process on Emerging Environmental issues (pp. 56). Nairobi, Kenya.
- Wallah, S. E., & Rangan, B. V. (2006). Low-Calcium Fly Ash-Based Geopolymer Concrete: Long-Term Properties. Perth, Australia: Curtin University of Technology.
- Wong, H. D. (2013, 18 April 2013). *Cylinder Strength versus Cube Strength*. Paper presented at the Standing Committee on Concrete Technology Annual Concrete Seminar, Hong Kong.
- Wongpa, J., Kiattikomol, K., Jaturapitakkul, C., & Chindaprasirt, P. (2010). Compressive strength, modulus of elasticity, and water permeability of inorganic polymer concrete. *Materials & Design*, 31(10), 4748-4754.
- Woolard, C., Petrus, K., & Van der Horst, M. (2000). The use of a modified fly ash as an adsorbent for lead.
- Xu, H., & Van Deventer, J. S. J. (2002). Geopolymerisation of multiple minerals. *Minerals Engineering*, 15(12), 1131-1139.
- Yip, C. K., Lukey, G. C., & van Deventer, J. S. J. (2005). The coexistence of geopolymeric gel and calcium silicate hydrate at the early stage of alkaline activation. *Cement and Concrete Research*, 35(9), 1688-1697.
- Yusuf, M. O., Megat Johari, M. A., Ahmad, Z. A., & Maslehuddin, M. (2014a). Evolution of alkaline activated ground blast furnace slag-ultrafine palm oil fuel ash based concrete. *Materials & Design*, 55(0), 387-393.
- Yusuf, M. O., Megat Johari, M. A., Ahmad, Z. A., & Maslehuddin, M. (2014b). Strength and microstructure of alkali-activated binary blended binder containing palm oil fuel ash and ground blast-furnace slag. *Construction and Building Materials*, 52(0), 504-510.
- Zain, M. F. M., Mahmud, H. B., Ilham, A., & Faizal, M. (2002). Prediction of splitting tensile strength of high-performance concrete. *Cement and Concrete Research*, 32(8), 1251-1258.
- Zhang, Z.-h., Yao, X., Zhu, H.-j., Hua, S.-d., & Chen, Y. (2009). Preparation and mechanical properties of polypropylene fiber reinforced calcined kaolin-fly ash based geopolymer. *Journal of Central South University of Technology*, 16, 49-52.
- Zheng, W., Kwan, A., & Lee, P. (2001). Direct tension test of concrete. *ACI materials journal*, 98(1), 63-71.

LIST OF PUBLICATIONS AND PAPERS PRESENTED

Journal Papers

Islam, A., Alengaram, U. J., Jumaat, M. Z., & Bashar, I. I. (2014). The development of compressive strength of ground granulated blast furnace slag-palm oil fuel ash-fly ash based geopolymer mortar. *Materials & Design*, 56(0), 833-841. (*Published*)

Bashar, I. I., Alengaram, U. J., Jumaat, M. Z., & **Islam, A.** (2014). The Effect of Variation of Molarity of Alkali Activator and Fine Aggregate Content on the Compressive Strength of the Fly Ash: Palm Oil Fuel Ash Based Geopolymer Mortar. *Advances in Materials Science and Engineering*, 2014, 13. (*Published*)

Conference Papers

Islam, A., Alengaram, U. J., Jumaat, M. Z., & Bashar, I. I. (2014, 24th - 26th November). Development of geopolymer mortar using palm oil fuel ash-blast furnace slag-fly ash-as binders. Paper will be presented at the International Conference on Construction Materials and Structures (ICCMATS), Johannesburg, South Africa. (*Accepted*)

Bashar, I. I., Alengaram, U. J., Jumaat, M. Z., & **Islam, A.** (2014, 24th - 26th November). The development of sustainable geopolymer mortar from fly ash-palm oil fuel ash based binder and manufactured sand. Paper will be presented at the International Conference on Construction Materials and Structures (ICCMATS), Johannesburg, South Africa. (*Accepted*)

Bashar, I. I., **Islam, A.**, Alengaram, U. J., & Jumaat, M. Z. (2014, 4th-5th November). Development of sustainable geopolymer mortar using industrial waste materials. Paper will be presented at the Conference for Civil Engineering Research Networks (ConCERN), Bandung, Indonesia. (*Abstract accepted*)

APPENDICES

APPENDIX A (Material Estimation)

Table: Volume of concrete for One (1) mixture

Tests name	Specimens	Nos.	Size (mm)			Vol. (m ³)
Compressive strength test	Cube	12	100	100	100	0.0120
Flexural strength test	Prism	3	100	100	500	0.0150
Splitting tensile strength test	Cylinder (s)	6	100	200 Ø		0.0094
Young's modulus test	Cylinder (b)	2	150	300 Ø		0.0106
Impact test	Panel	2	600	600	50	0.0360
Sub-Total						0.0830
5%	Extra					0.0042
					Total	0.0872

APPENDIX B (Mix Design)

Group (Binder/OPS)	Mix designation	Mix Proportion Binder:MS:OPS	Binder				Fine Aggregate		Coarse Aggregate				Activator		Added water		Steel fibre
			GGBS		POFA		MS		OPS (UC)		OPS (C)						Volume
			kg/m ³	kg	kg/m ³	kg	kg/m ³	kg	kg/m ³	kg	kg/m ³	kg	kg/m ³	kg	kg/m ³	kg	kg/m ³
0.4	OPSGC4-NF-UC	1 : 2.5 : 0.4	227	22.35	227	22.35	1134	111.77	181	17.88	-	-	204	20.118	114	11.18	0
	OPSGC4-F- UC	1 : 2.5 : 0.4	227	22.35	227	22.35	1134	111.77	181	17.88	-	-	204	20.118	114	11.18	0.5
	OPSGC4-NF-C	1 : 2.5 : 0.4	227	22.35	227	22.35	1134	111.77	-	-	181	17.88	204	20.118	114	11.18	0
	OPSGC4-F-C	1 : 2.5 : 0.4	227	22.35	227	22.35	1134	111.77	-	-	181	17.88	204	20.118	114	11.18	0.5
0.6	OPSGC6-NF- UC	1 : 2.5 : 0.6	212	21.26	212	21.26	1061	106.32	255	25.52	-	-	191	19.137	106	10.63	0
	OPSGC6-F- UC	1 : 2.5 : 0.6	212	21.26	212	21.26	1061	106.32	255	25.52	-	-	191	19.137	106	10.63	0.5
	OPSGC6-NF-C	1 : 2.5 : 0.6	212	21.26	212	21.26	1061	106.32	-	-	255	25.52	191	19.137	106	10.63	0
	OPSGC6-F-C	1 : 2.5 : 0.6	212	21.26	212	21.26	1061	106.32	-	-	255	25.52	191	19.137	106	10.63	0.5
0.8	OPSGC8-NF- UC	1 : 2.5 : 0.8	200	20.27	200	20.27	998	101.37	319	32.44	-	-	180	18.25	100	10.14	0
	OPSGC8-F- UC	1 : 2.5 : 0.8	200	20.27	200	20.27	998	101.37	319	32.44	-	-	180	18.25	100	10.14	0.5
	OPSGC8-NF-C	1 : 2.5 : 0.8	200	20.27	200	20.27	998	101.37	-	-	319	32.44	180	18.25	100	10.14	0
	OPSGC8-F-C	1 : 2.5 : 0.8	200	20.27	200	20.27	998	101.37	-	-	319	32.44	180	18.25	100	10.14	0.5

APPENDIX C

Carbon Footprint

The total carbon footprint cannot be calculated because of the large amount of data required and the fact that carbon dioxide can be produced by natural occurrences. The calculation on the amount of CO₂ emission (CO₂-e) for a particular component of concrete was based on 1 m³ of concrete. In this investigation the estimation of CO₂ emission for the manufactured sand (MS) and quarry dust (QD) have been taken the same as that of crushed granite aggregate. This could be justified due to the fact that the MS/QD is the by-product of crushed granite aggregate and needs electricity for further processing (Mo et al., 2014a). As the POFA and OPS are also an industrial by-product, the CO₂ emission was not considered in the calculation of the carbon foot print for OPSGC.

Table: CO₂ emission factors evolved from manufacturing of concrete producing materials and construction activities (Collins, 2010; Turner & Collins, 2013)

Concrete producing material	Emission factors (<i>t CO₂-e/tonne</i>)
OPC	0.82
GGBS	0.143
POFA	0
Crushed granite / MS / QD	0.0459
Mining sand	0.0139
NaOH manufacture	1.915
Na ₂ SiO ₃ manufacture	1.514
OPS	0

APPENDIX C (Cont.)

Table 3.9 shows the utilisation of NaOH (12 M) and Na₂SiO₃ solutions are 25 and 63 kg/m³ for NWGC; 49 and 122 kg/m³ for OPSGC. The quantity of solid form of NaOH and Na₂SiO₃ in the NWGC and OPSGC are as follows:

NWGC: NaOH 25x0.361=9.025 kg/m³, Na₂SiO₃ 63x0.43=27.09 kg/m³

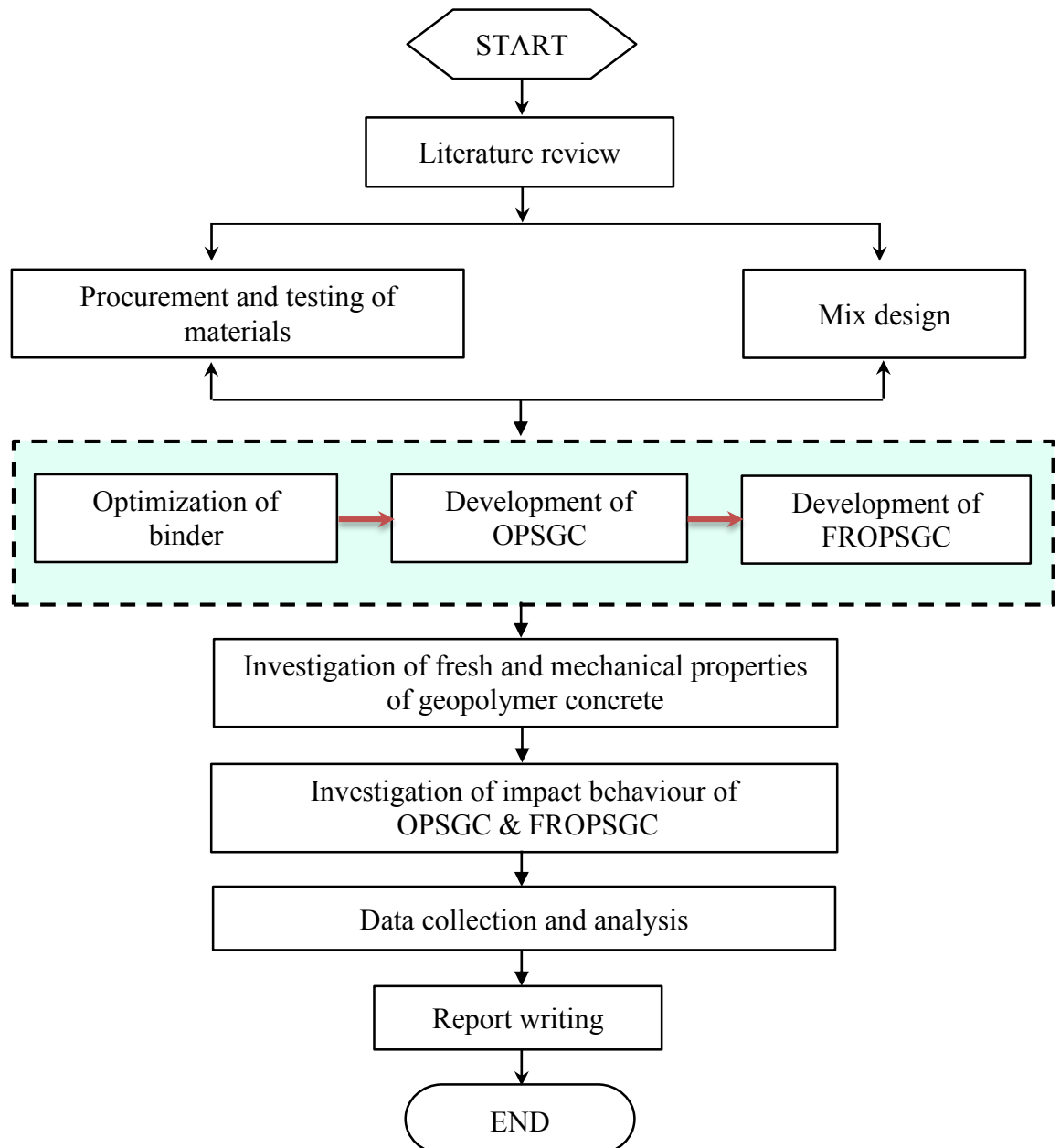
OPSGC: NaOH 49x0.361=17.689 kg/m³, Na₂SiO₃ 122x0.43=52.46 kg/m³

Table: Estimated carbon dioxide emission for NWC (Mohammed et al., 2012), NWGC and OPSGC of grade 30 concrete mixes

Label	Binder content (kg/m ³)			CO ₂ -e/t from binder	Crushed granite (kg/m ³)	OPS (kg/m ³)	CO ₂ -e/t from coarse aggregate	Fine aggregate (kg/m ³)		CO ₂ -e/t from fine aggregate	Alkali activator (solid) (kg/m ³)		CO ₂ -e/t from Alkali activator	Total CO ₂ -e/m ³ of concrete
	OPC	GGBS	POFA					NS	MS, QD		NaOH	Na ₂ SiO ₃		
NWC	335	0	0	0.2747	1303	0	0.0598	560	0	0.0078	0	0	0	0.3423
NWGC														
NWGC-NS	0	132	88	0.0189	994	0	0.0456	884	0	0.0123	9.025	27.09	0.0583	0.1351
NWGC-MS NWGC-QD	0	132	88	0.0189	994	0	0.0456	0	884	0.0406	9.025	27.09	0.0583	0.1634
OPSGC														
OPSGC-NS-C OPSGC-NS-UC	0	255	170	0.0365	0	255	0	1064	0	0.0148	17.689	52.46	0.1133	0.1646
OPSGC-MS-C OPSGC-QD-C OPSGC-MS-UC OPSGC-QD-UC	0	255	170	0.0365	0	255	0	0	1064	0.0488	17.689	52.46	0.1133	0.1986

APPENDIX D

Methodology (Flowchart)



APPENDIX E



POFA collection



OPS



Palm Fruit



Palm Fruit



Manufactured sand



Quarry dust



Concrete specimens



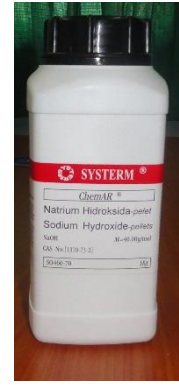
Ambient curing



Oven-curing chamber



Sodium silicate



Sodium hydroxide



**Alkaline activators solution
($\text{Na}_2\text{SiO}_3 + \text{NaOH}$)**



NaOH solution



Pan mixer



Drum mixer



Impact testing arrangement



Young's modulus testing